# AN EXPERIMENTAL STUDY OF CONFORMANCE TREATMENTS USING CROSSLINKED POLYACRYLAMIDE POLYMER

by

JENN-TAI LIANG, B.S.,M.S.

DISSERTATION

Presented to the Faculty of the Graduate School of

The University of Texas at Austin

in Partial Fulfillment

of the Requirements

for the Degree of

DOCTOR OF PHILOSOPHY

THE UNIVERSITY OF TEXAS AT AUSTIN

December, 1988

To my mother and the memory of my father

# AN EXPERIMENTAL STUDY OF CONFORMANCE TREATMENTS USING CROSSLINKED POLYACRYLAMIDE POLYMER

APPROVED BY
SUPERVISORY COMMITTEE:

L. W. Lake

K. Sepehrnoori

Gary A. Pope

James Hutchison

G. P. Thurston

# Acknowledgments

I would like to thank my supervising professors, Dr. A. D. Hill and Dr. K. Sepehrnoori for their guidance and encouragement during the course of this study. Without them this dissertation could not have been written, so I owe them a special debt of gratitude. I would also like to extend my appreciation to my supervisory committee members, Dr. D. V. Hinkley, Dr. G. A. Pope and Dr. G. B. Thurston, for their valuable comments and suggestions and to Dr. Bruce Rouse, for his technical assistance.

Financial support from the Department of Petroleum Engineering and the Center for Enhanced Oil and Gas Recovery Research at The University of Texas are gratefully acknowledged.

Special appreciation is extended to my wife Chi for her love and sacrifice.

# Table of Contents

# List of Tables

# List of Figures

# Chapter 1

# Introduction

In various secondary and tertiary recovery processes, it is a common practice to inject water or chemical solutions into reservoirs to increase oil recovery. However, reservoirs having high permeability contrasts between distinct horizontal layers often exhibit poor vertical conformance. The poor vertical conformance allows the injected fluid to sweep preferentially into the higher permeability zones, thereby causing early breakthrough of the injected fluid. Consequently, when the process reaches its economic limit, significant amounts of oil in low permeability zones remain poorly swept or even unswept.

The low sweep efficiency of a reservoir having poor vertical conformance can be improved by reducing the permeability contrasts between distinct horizontal layers. The improved vertical conformance as the result of permeability contrast reduction causes the redistribution of the injection fluid into the low permeability zones which have not been efficiently swept. Hence, improved vertical conformance results in more efficient use of the injected fluid and more economically recoverable reserves.

Many vertical conformance improvement techniques have been developed and implemented by the oil industry. The objective is to increase oil

recovery by redirecting the injected fluid into the poorly swept low permeability zones. This can be accomplished by putting mechanical device in the wellbore to isolate the high permeability thief zones [1,2,3], plugging the near wellbore area of the thief zones with solid plugging materials [1,2,3,4,5], stimulating the low permeability zones rather than plugging their high permeability counterparts [1,6,7,8], and using polymer gels for in-depth treatment [9,10,11,12,13,14,15,16]. These treatments can be applied at either injection or production wells [12]. However, every treatment technique has its limitations and disadvantages with the success of the treatment depending heavily on the reservoir characteristics of each individual case.

Results of several reservoir modeling studies indicate that crossflow is a vital factor affecting the outcome of a treatment. Silva et al. [17] studied the effectiveness of a near wellbore treatment using a two-phase, three-dimensional reservoir simulator. They simulated the treatment in a normal waterflood process by plugging off the near wellbore portions of the high permeability zones. Their results indicated that crossflow between horizontal layers had a detrimental effect on the treatment. Abdo et al. [15] employed a two-dimensional, incompressible flow model to study the effects of the in-depth treatment of a thief zone using complexed biopolymer. They learned that crossflow would cause a delay in oil production increase and the magnitude of the increase would be much less than that for the case without crossflow. They also indicated that the effects of crossflow can be minimized by more efficient vertical conformance treatment and more in-depth treatment using polymers. Tsau [18] modified the DOE BOAST black oil simulator in order to determine the reservoir characteristics that lead to successful vertical

conformance treatments. He performed a simulation of a vertical conformance treatment in an actual field case. His results indicated that little or no incremental recovery could be observed after treatment when crossflow existed between horizontal layers. However, the amount of injected water needed to recover a given amount of oil for the treated case was found to be less than that for the untreated case.

In order to minimize the negative effect caused by the crossflow between horizontal layers, it is obvious that an in-depth treatment using polymer or crosslinked polymer is the most promising method among existing vertical conformance treatment techniques. Many polymeric systems including polyacryamides, polysaccharides, lignosulfonate gels, furfuryl alcohol polymer, acrylic/epoxy emulsion gels, silica gels, and polyisocyanurate salts have been examined for vertical conformance treatments. Among these, polyacrylamides received the most attention because of their relatively low cost and their ability at times to greatly reduce the permeability to water while not significantly affecting the permeability to oil [14,19,20].

The commonly used partially hydrolyzed polyacrylamide polymer is believed to reduce the permeability of the porous media by adsorption and physical entrapment [21,22]. Although the polyacrylamide is susceptible to shear degradation during the injection process, the shear doesn't affect its permeability reducing ability appreciably [23]. Some researchers [24,25] showed that when equal amount of polymer solution was flowed through two cores with different permeabilities, the resulting permeability reducing effect is greater in the lower permeability core than in the higher permeability one.

Crosslinked polymer is often employed in cases where greater and more persistent permeability reduction is required. The polyacrylamides are usually crosslinked with multivalent cations such as aluminum and chromium to form a three dimensional gel structure [14]. In-depth treatments using polyacrylamide gels can be accomplished by employing a technique called delayed gelation. The gelation reaction between polyacrylamide and trivalent chromium cations can be delayed by mixing the polymer with a redox system consisting of hexavalent chromium cations and a reducing agent [26]. The rate of the gelation reaction can be controlled by varying the concentration of the polymer and that of the redox system [28]. Hence, the gelation reaction can be delayed until the gelling solution is placed at the desired location in the reservoir. The gel is then set in-situ.

However, results of the field treatments varied widely while often no obvious reason can be attributed to the success and failure of the treatments. Although extensive efforts have been made to study the mechanism of gelation reactions [28,29,30,31,32,33,34] and the behavior of polymer gels in porous media [26,27,35,36], a lot of details still remain to be worked out before a comprehensive model for polymer gel treatment design and optimization can be developed.

The objective of this research was to identify the correlation among the gel strength, the redox concentration, the permeability of the porous medium before treatment and the extent of permeability reduction after treatment. In order to simulate in-depth treatment, a technique which delays the gelation reaction until the gelling solution is placed at the desired position of the reservoir was employed. The gelling solution employed consisted of partially

hydrolyzed polyacrylamide polymer, sodium dichromate as the source of hexavalent chromium cations, and a reducing agent. A series of gelation tests and rheological measurements were first performed to identify the gelation time and gel strength of different gelling solutions. In the subsequent in-situ gelation studies, the gelling solutions were first thoroughly mixed and then injected into unconsolidated sandpacks. After a shut-in period, the extent of permeability reduction was determined by comparing the residual permeability of the sandpack after treatment with the permeability of the sandpack before treatment. All experiments were conducted at 50°C and the sandpacks were conditioned to residual oil saturation prior to the start of treatment. The study of in-situ gelation reaction using sandpacks at residual oil saturation and at the temperature of 50°C to simulate the reservoir condition as well as the shut-in strategy employed to allow the three dimensional gel structure to be fully developed are unique features of this study which have not been found in any published literature.

The literatures pertaining to the gelling solutions employed in this study are summarized in Chapter 2. The gelling solution rheology and the gelation time and gel strength measurements are discussed in Chapter 3. The detailed procedures of in-situ gelation sandpack flood experiments as well as that of the yield stress measurements of the fully developed gels are described in Chapter 4. Chapter 5 presents the discussion of results. The conclusions drawn from the results of this study and the recommendations for future work are summarized in Chapter 6.

# Chapter 2

# Literature Review

The delayed gelation technique employed in this research involved the reduction of the hexavalent chromium cations into its trivalent form which then crosslinked with HPAM polymer to form a stiff gel. The hexavalent chromium compound, sodium dichromate dihydrate, and a reducing agent constituted the redox system used in this study. Sodium bisulfite, sodium thiosulfate, and thiourea were used as the reducing agents and the rate of reduction decreased in the respective order.

The detailed mechanism of the gelation reaction between partially hydrolyzed polyacrylamide polymer and the redox system is still unknown. However, it is believed that the gel is formed by the crosslinking of the trivalent chromium cations with polymer molecules [52] and the formation of the three dimensional gel structure can be divided into the following steps.

1. The reduction of Cr(VI) to Cr(III).
2. The crosslinking of Cr(III) with a polymer molecule.
3. The crosslinking of another polymer molecule with the crosslinked product from Step 2.

The gelation reaction is initiated by the reduction of the hexavalent chromium

cations into trivalent chromium cations. A huge three dimensional gel network is then formed through the continued reaction between crosslinked polymer molecules and Cr(III).

## 2.1 Redox Reaction

Terry et al. [28] suggested that the redox reaction was the rate controlling step of the gelation reaction. Hence, for those applications requiring short gelation time such as near wellbore treatments, sodium bisulfite was always selected as the reducing agent for its fast reaction rate with hexavalent chromium cations. For the applications that required longer gelation time, sodium thiosulfate or thiourea was employed depending on the length of the gelation time needed.

Aslam et al. [34] proposed the the reaction between bisulfite and dichromate followed a stoichiometry of three moles of bisulfite per mole of dichromate. In the case of no other interference, the reaction is shown as follow:

$$Cr_2O_7^{2-} + 3HSO_3^- + 5H^+ \rightarrow 3SO_4^{2-} + 2Cr^{3+} + 4H_2O \qquad (2.1)$$

The following is the redox reaction between dichromate and sodium thiosulfate

$$2Cr_2O_7^{2-} + 3S_2O_3^{2-} + 22H^+ \rightarrow 4Cr^{3+} + 6H_2SO_3 + 5H_2O. \qquad (2.2)$$

The stoichiometry of this redox reaction is three moles of sodium thiosulfate per two moles of dichromate. Olatunji et al. [51] reported that the thiourea was oxidized to the dimer by reacting with dichromate

$$Cr_2O_7^{2-} + 3NH_2CSNH_2 + 8H^+ \rightarrow 2Cr^{3+} + 3N_2H_3CSCSN_2H_3 + 7H_2O. \quad (2.3)$$

Southard et al. [29] assumed in their study that no further oxidization of the thiourea dimer occurred in the redox reaction. The stoichiometry of this reaction is three moles of thiourea per mole of dichromate.

## 2.2 Kinetics of Gelation Reaction

Kinetics of a chemical reaction is concerned with the rate of reaction and the mechanisms by which reactions occur. Important information may be obtained by studying the effect of changing the temperature, electrolyte concentration, and reactant concentration on the rate of reaction.

Terry et al. [28] studied the relationship between process parameters and gelation time. The process parameters included polymer type and concentration, dichromate concentration, and reducing agent type and concentration. The viscosity of the gelling solutions were monitored throughout the gelation process by Brookfield viscometers and the temperature of the reactions was controlled at $25 \pm 0.2$°C. The gelation time was defined as the time

required for the viscosity of the gelling solution to reached an arbitrary value. They reported that the gelation time of a gelling solution decreased with the increasing polymer and redox system concentrations and a linear relationship existed between the reciprocal of the gelation time and the reciprocal of the initial polymer concentration. Their results also indicated that for the polyacrylamide polymers having higher degree of hydrolysis the gelation time was more sensitive to changes in polymer concentration. For the two different reducing agents studied, the gelation time of the gelling solution using thiourea as reducing agent were found to be much longer than the comparable gelling solutions using sodium bisulfite as reducing agent.

The effect of temperature on gelation reaction was investigated by Jordan et al. [31] in an attempt to determine the correlation between temperature and gelation time. The gelling solutions involved in their studies consisted of polyacrylamide polymer, sodium dichromate as the source of hexavalent chromium cation, and sodium bisulfite as reducing agent. The temperature range of 25 to 80°C was chosen to simulate the temperatures commonly encountered in reservoirs. For all the gelling solutions they studied, the gelation time was found to decrease with increasing temperature. The correlation between gelation time and temperature was found to follow an Arrhenius type equation in which the logarithm of the gelation time was proportional to the reciprocal of the absolute reaction temperature. They also reported that the gelation time was function of sodium chloride concentration. For sodium chloride concentration up to approximately 5,000 to 10,000 ppm it was found that the gelation time decreased with the increasing salt concentration, and then increased as salt concentration was increased above 10,000 ppm level.

Aslam et al. [34] examined the effect of shear rate on gelation time and gel properties of polyacrylamide/chromium gel. A Weissenberg Rheogoniometer was used to monitor the progress of gelation and viscometric properties of the gels. In order to obtain short gelation time, sodium bisulfite was selected as the reducing agent. They found that the rate of gelation reaction was accelerated by the applied shear field. Their results also indicated that gels formed at higher shear rate exhibited lower gel strength and were more resistant to subsequent shear degradation than gels formed at lower shear rate.

Huang et al. [26] performed an experimental study of the in-situ gelation of the polyacrylamide/chromium gel in unconsolidated sandpacks to identify the relationship between in-situ gelation time and the gelation time obtained from beaker tests. The gelling solutions consisting of polyacrylamide polymer, sodium dichromate, and thiourea were injected continuously into unconsolidated sandpacks and the pressure drops along the flow direction were recorded to monitor the progress of gelation in porous media. Their results indicated that in-situ gelation occurred much earlier than gelation in beaker tests and higher flow rate and smaller grain size shortened the in-situ gelation time. The higher rate of in-situ gelation was attributed to the shear field imposed on the gelling solution during the injection period and agreed with the results of Aslam et al. [34] that the rate of gelation increased with the increasing shear rate. The shear history was also found to affect the in-situ gelation and the longer the gelling solution was exposed to the shear field, the faster the gelation reaction was.

The monitoring of shear viscosity increase during the buildup of three

dimensional gel structure has been proven effective in identifying the gelation time of different gelling solutions [28,31,34]. However, the breakdown of the gel structure caused by the shear stress imposed on the gelling solution during the measurement process prohibits the use of shear viscosity changes to study the fundamental kinetics of gel formation. Prud'homme et al. [32] proposed the use of dynamic mechanical rheological measurement to follow the progress of gelation. Since the gelling solution was only subjected to small sinusoidal shear deformation, the gel structure remained intact during the gelation process. The time dependence of the storage modulus increase on the buildup of the gel structure was utilized to study the kinetics of the gelation process. The measured value of the storage modulus was correlated to the crosslinking density in the gel by the modified theory of rubber elasticity [53,54]. After studying the effect of polymer concentration on the rate change of storage modulus, $G'$, with respect to time at a constant redox concentration and the effect of redox concentration on the rate change of storage modulus, $G'$, with respect to time at a constant polymer concentration, the overall kinetics of the gelation was found to be second order in both polyacrylamide polymer and chromium.

The addition of salt ions into the gelling solution was found to increase the rate of gelation reaction for anionic polyacrylamide solutions, while no change in reaction rate was observed for nonionic polyacrylamide solutions [30]. It was believed that the screening effect provided by the addition of salt ions allowed the long chain polymer molecules to approach each other more closely, thereby increasing the rate of gelation reaction.

Southard et al. [29] studied the reaction kinetics of the redox reaction

between dichromate and thiourea. In their studies, the solution color change during the reduction of hexavalent chromium cations into trivalent chromium cations was monitored spectrophotometrically in the visible spectrum. The results indicated that the kinetics of the redox reaction was first order in dichromate, thiourea, and hydrogen ion. They also reported that regardless of the initial concentration of the dichromate, only a constant amount of dichromate was consumed, indicating that the redox reaction may be the rate determining step.

## 2.3 Summary

For the delayed gelation technique employed in this study, the redox reaction involving the reduction of the hexavalent chromium cations to its trivalent form is believed to be the rate controlling step of the gelation reaction. The gelation time of a gelling solution decreases with the increasing polymer and redox system concentrations where a linear relationship exists between the reciprocal of the gelation time and the reciprocal of the initial polymer concentration.

The increasing salt content of the gelling solution increases the rate of gelation reaction for anionic polyacrylamide solutions, while no change in reaction can be observed for nonionic polyacrylamide solutions.

The effect of temperature on gelation reaction can be described by an Arrhenius type equation in which the logarithm of the gelation time is proportional to the reciprocal of the reaction temperature.

The applied shear field and shear history both affect the rate of gelation. The gelation time decreases with the increasing shear rate and the higher rate of in-situ gelation reaction can be attributed the shear field imposed on the gelling solution during the injection period. The shear history affects the gelation reaction in a way that the longer the gelling solution is exposed to the shear field, the shorter the gelation time is.

Dynamic oscillatory reheological measurement is an effective tool in studying the kinetics of the gelation reaction. The time dependence of the storage modulus increase on the buildup of the gel structure can be used to investigate the kinetic models of different gelling solutions.

# Chapter 3

# Gelation and Rheological Studies

The gelation time and gel strength are two important characteristics which have to be determined before a gelling solution can be selected for in-situ gelation studies. The goal of the gelation and rheological studies was to identify the gelling solutions having appropriate gelation time and gel strength for subsequent in-situ gelation studies.

## 3.1 Gelling Solution System

The gelling solution system employed in this study consisted of American Cyanamid CYANAGEL 100, a partially hydrolyzed polyacrylamide polymer(HPAM), sodium dichromate(S.D.) as the source of hexavalent chromium cations, and a reducing agent. The hexavalent chromium cations were first reduced to the trivalent state by the reducing agent and then crosslinked with polyacrylamide polymer to form a stiff gel. Sodium bisulfite(S.B.), sodium thiosulfate(S.T.), and thiourea(T.) have all been used as reducing agents in this study. Throughout this dissertation, HPAM denotes CYANAGEL 100 polymer, S.B., S.D., S.T, and T. denote sodium bisulfite, sodium dichromate, sodium thiosulfate, and thiourea repectively.

### 3.1.1 Characteristics of the Chemicals Involved

The polyacrylamide polymer, CYANAGEL 100, used in this study was obtained as small laboratory samples from American Cyanamid Company. It is an anionic polyacrylamide polymer with an average molecular weight of nine hundred thousand. The activity of the stock solution provided by the manufacturer was 22% polymer and the degree of hydrolysis was about 10%. Typical molecular structures of polyacrylamide polymers are shown in Figure 3.1. The important physical properties of CYANAGEL 100 are listed in Table 3.1.

The stock polymer solution provided by the manufacturer was in concentrated aqueous form which could be readily diluted to the desired concentration by simply mixing it with distilled water. A magnetic stirrer was used in the mixing process and a consistent shear environment was achieved by using the same rotation speed for every sample preparation job. All polymer solutions were forced through a five micron membrane filter paper by 40 psi compressed air to remove solid particles and undissolved microgels.

The other chemicals used in this study such as sodium dichromate, sodium bisulfite, sodium thiosulfate, thiourea, and sodium chloride were all reagent grade chemicals and these chemicals were used as obtained.

### 3.1.2 Gelling Solution Preparation

In order to obtain reproducible results in gelation studies, a consistent way of preparing the gelling solution was established and carefully followed. The procedure of preparing gelling solution followed in this study is outlined

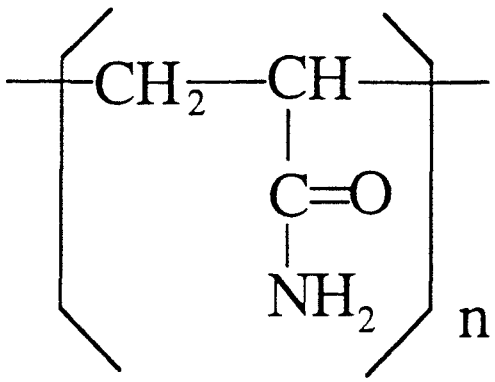

Polyacrylamide Polymer

(PAM)

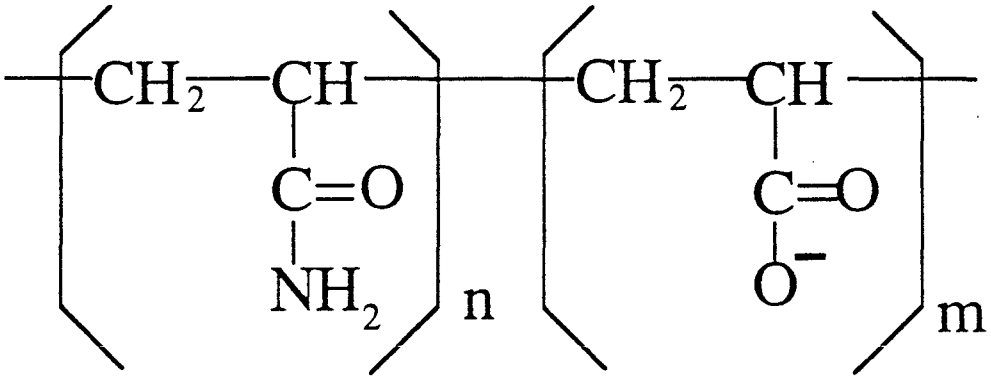

Partially Hydrolyzed Polyacrylamide Polymer

(HPAM)

Figure 3.1: Molecular structure for PAM and HPAM

Table 3.1: Physical properties of CYANAGEL 100 polyacrylamide polymer [American Cyanamid Company]

| | |
|---|---|
| **Appearance and Odor:** | Colorless liquid; Odorless |
| **Boiling Point:** | $\sim 212°F$ ($\sim 100°C$) |
| **Average Molecular Weight:** | $9.0 \times 10^5$ |
| **Activity:** | 22% solid |
| **Degree of Hydrolysis:** | $\sim 10\%$ |
| **Specific Gravity:** | 1.07 |
| **pH:** | 4.5–5.5 |
| **Vapor Pressure:** | Similar to water |
| **Vapor Density:** | Similar to water |
| **Evaporation Rate:** | Similar to water |
| **Solubility in Water:** | Complete |

below.

1. The polymer solution was diluted to the appropriate concentration by mixing the predetermined amount of stock solution and sodium chloride with distilled water to the desired volume. The solution was then placed on a magnetic stirrer and kept stirring for 10 minutes to ensure complete mixing.

2. The sodium dichromate solution with predetermined concentration was introduced into the polymer solution prepared in Step 1 and stirred for another 30 seconds.

3. The solution of reducing agent with predetermined concentration was introduced into the gelling solution and the time of mixing was recorded. The gelling solution was stirred continuously for 3 minutes before commencing the measurement process. The time of mixing was used as the reference point in measuring gelation time of the gelling solution.

## 3.2 Gelling Solution Rheology

*Rheology* is generally defined as the science of the deformation and flow of a material [55]. Only a limited amount of data has been published on the rheological properties of polymeric gels [30,32,34,56]. The results of these studies indicate that the polymeric gel type material exhibits unusual deformation and flow behavior. Unlike the purely viscous and elastic materials, Newton's law and Hooke's law are not reasonable approximations for polymeric gel type materials. This type of material demonstrates a viscoelastic

response which is neither viscous nor elastic but a combination of both, and the relative magnitudes of which depend on the strength of the individual gel. Since during the buildup of a three dimensional gel structure the relative magnitudes of viscous and elastic behavior of the gelling solution shift from the more viscous toward the more elastic, the progress of gelation can be followed by monitoring the change of the rheological properties of the gelling solution with time. Steady shear measurements and dynamic oscillatory testing are the two most commonly used techniques for gelling solution rheology studies. However, under the steady shear environment, only the viscous behavior of the gelling solution can be measured while the dynamic oscillatory testing is effective in studying the viscoelastic behavior of the gelling solution.

### 3.2.1 Behavior of Gelling Solution under Steady Shear Environment

We begin our discussion of steady shear measurement from the definition of viscosity. The viscosity of a material is the measure of its resistance to flow under a mechanical stress. Consider a layer of fluid of thickness $dy$ contained between two parallel plates as shown in Figure 3.2. The top plate, under a mechanical force $F$, moves with a velocity $u = dx/dt$ in the $x$ direction, while the bottom plate remains stationary. The shear strain, $\gamma$, is defined as the ratio of the displacement of the fluid in the $x$ direction to the thickness of the fluid layer.

$$\gamma = \frac{dx}{dy} \tag{3.1}$$

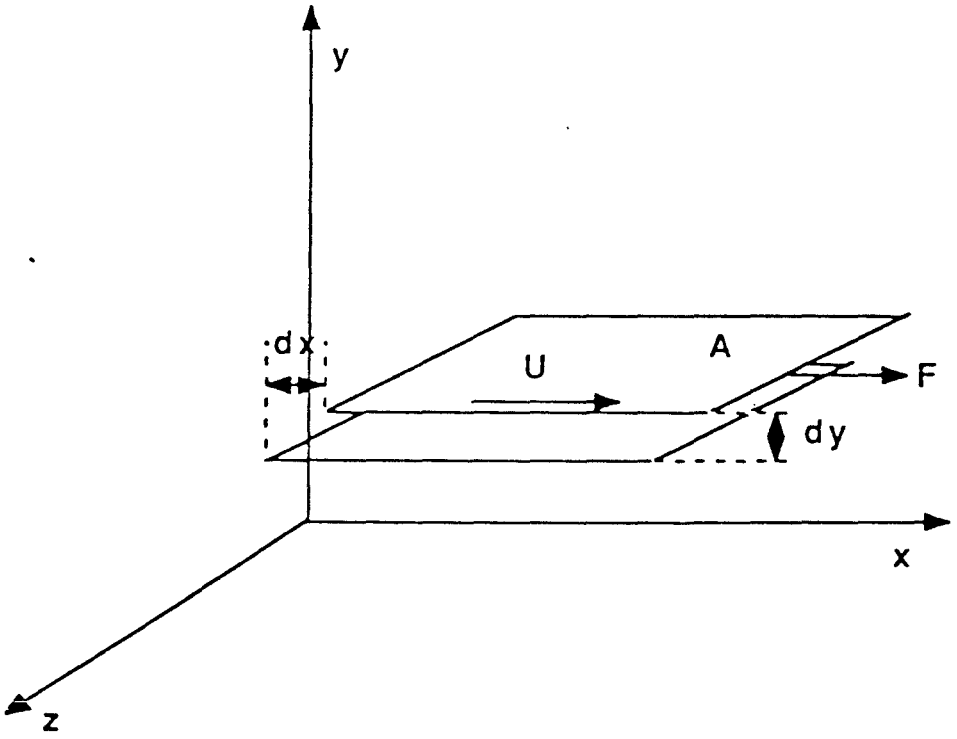


Figure 3.2: Parallel plate model for fluid viscosity definition

The shear rate, $\dot{\gamma}$, is the time rate of change of shear strain, which can be expressed as the derivative of shear strain with respect to time.

$$\dot{\gamma} = \frac{d}{dt}(\gamma) = \frac{d}{dt}(\frac{dx}{dy}) = \frac{d}{dy}(\frac{dx}{dt}) = \frac{du}{dy} \tag{3.2}$$

After applying the chain rule to the derivative, it is obvious that the shear rate is also equivalent to the velocity gradient.

The shear stress is the force per unit area normal to the $x$ direction.

$$\tau = \frac{F}{A} \tag{3.3}$$

Quantitatively, the viscosity of a material, $\mu$, is defined as the ratio of shear stress to shear rate:

$$\mu \equiv \frac{\tau}{\dot{\gamma}} \tag{3.4}$$

For a Newtonian fluid, the shear stress is linearly proportional to the shear rate and the proportionality constant is the viscosity of the fluid.

$$\tau = \mu\dot{\gamma} \tag{3.5}$$

Therefore, a plot of shear stress $\tau$ versus shear rate $\dot{\gamma}$ creates a straight line through the origin with a slope $\mu$ for a Newtonian fluid.

For non-Newtonian fluids, since shear stress is not linearly proportional to shear rate, the viscosity is no longer a constant. Polymer solutions, for example, exhibit non-Newtonian behavior where the shear stress and shear rate relationship can be approximated mathematically by the power law model

$$\mu = K\dot{\gamma}^{n-1} \tag{3.6}$$

Where K and n are the power-law coefficient and exponent respectively. However, the behavior of gelling solution after the onset of gelation is not only non-Newtonian but also time dependent, so no simple mathematical relationship can be found to describe the correlation between shear stress and shear rate . The ratio of shear stress to shear rate varies with the changing of shear rate, and it doesn't represent the true viscosity of the fluid. Consequently, the reading we get from a viscometer at a specific shear rate can only be called the apparent viscosity $\mu_{app}$ of the gelling solution at that shear

rate. The continuous crosslinking between the polymer molecules and the metal cations during the gelation process causes the apparent viscosity of the gelling solution to increase and it can be used as an indicator of the progress of the gelation reaction.

### 3.2.2 Behavior of Gelling Solution under Dynamic Oscillatory Shear Environment

It has long been realized that the shear stress shear rate relationship of a purely viscous fluid follows Newton's law of viscosity as shown in equation (3.5). Hooke's law

$$\tau = G\gamma \tag{3.7}$$

describes the stress strain relationship of a purely elastic solid, where the constant $G$ is the shear modulus. Hence, if a purely elastic material is sheared sinusoidally according to

$$\gamma = \gamma' \sin \omega t \tag{3.8}$$

where $\gamma'$ is the maximum strain, $\omega$ is the angular velocity (radians/second), and t is time, the resulting shear stress is given by

$$\tau = G\gamma' \sin \omega t \tag{3.9}$$

and the shear stress is in phase with the strain. For a purely viscous fluid, according to equation (3.5) the shear stress $\tau$ is proportional to the shear rate $\dot{\gamma}$ rather than the strain $\gamma$, where

$$\dot{\gamma} = \omega\gamma' \cos \omega t. \tag{3.10}$$

Thus, the resulting shear stress is given by

$$\tau = \mu\omega\gamma' \cos \omega t \tag{3.11}$$

and the shear stress is 90° out of phase with the strain.

However, viscoelastic materials, such as polymeric gels, exhibit an intermediate response with the stress strain phase angle falling between 0° and 90°. This relationship can also be viewed as the projection of two vectors, $\tau^*$ and $\gamma^*$ rotating in the complex plane as shown in Figure 3.3. In order to quantify the viscous and elastic elements of the response of a viscoelastic material to the sinusoidal shear environment, the stress vector $\tau^*$ is decomposed into two orthogonal components $\tau'$ and $\tau''$. As illustrated in Figure 3.3, $\tau'$ is

in phase ($\delta = 0°$) with the strain and $\tau''$ is out of phase ($\delta = 90°$) with the strain. Since in this case the strain is the independent variable, $\gamma^* = \gamma'$ and $\gamma'' = 0$. We can now define the storage modulus $G'$ as

$$G' = \frac{\tau'}{\gamma'} \tag{3.12}$$

and the loss modulus $G''$ as

$$G'' = \frac{\tau''}{\gamma'} \tag{3.13}$$

where the storage modulus and the loss modulus represent the elastic and the viscous elements of the response of the viscoelastic material to the sinusoidal varying strain respectively. The magnitudes of the storage modulus and the loss modulus of a gelling solution depend upon the phase angle between the stress and strain.

The frequency dependence of $G'$ and $G''$ provides useful information about the characteristics of a viscoelastic material. If we perform a dynamic oscillatory frequency sweep measurement on a gelling solution which is more viscous than elastic before the onset of gelation, $G''$ is greater than $G'$ at all frequencies and $G'$ decreases more rapidly than $G''$ as frequency decreases. When the gelling solution gradually becomes more elastic than viscous after the onset of gelation, $G'$ increases and $G''$ decreases at low frequencies. After

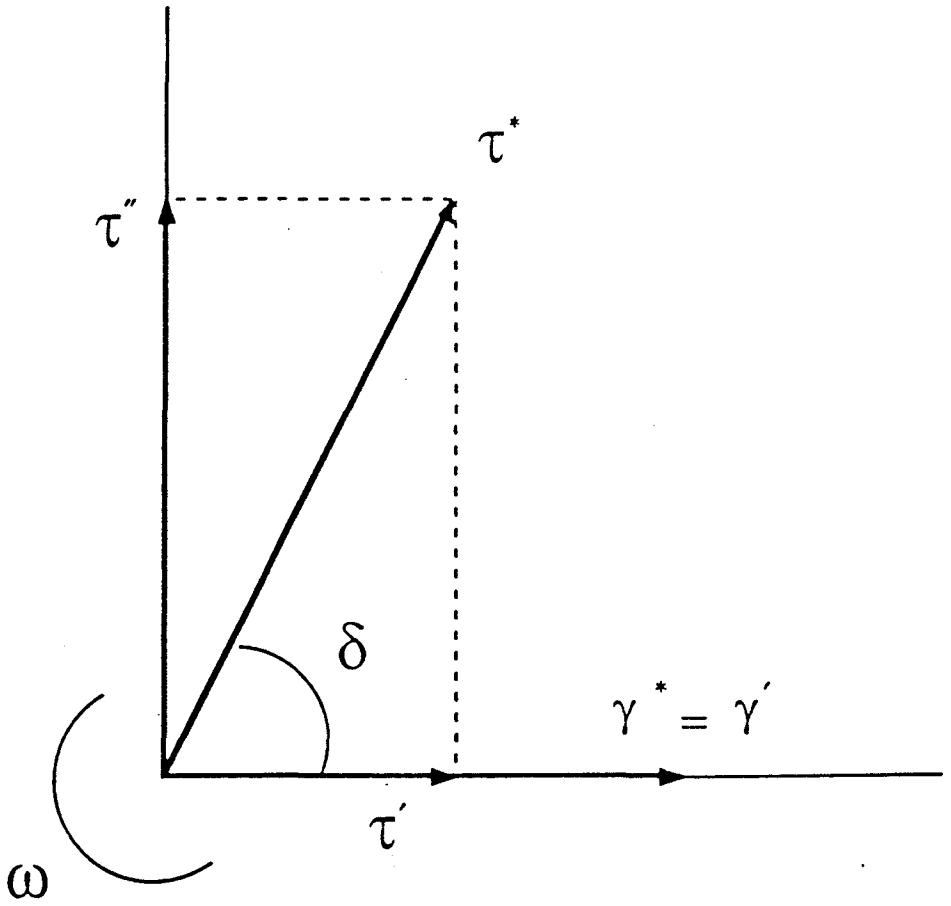


Figure 3.3: Rotating vector diagram of stress strain relationship under dynamic oscillatory shear environment

the three dimensional gel structure is fully developed, $G'$ is substantially larger than $G''$ and for a very strong gel $G'$ is actually independent of frequency.

## 3.3 Steady Shear Measurement and Gelation Time Determination

The increase of apparent viscosity during the build up of the three dimensional gel structure furnishes a way of monitoring the progress of gelation. However, since the steady shear motion imposed on the gelling solution tends to break down the gel structure being formed, the steady shear measurement technique can only be used to determine the gelation time by monitoring the changes of apparent viscosity of the gelling solution.

A series of screening tests was conducted to identify the gelling solutions with appropriate gelation time for subsequent rheological and in-situ gelation studies. A Brookfield Synchro-Lectric Model LVT viscometer with a UL adapter was used to monitor the changes of apparent viscosity during the gelation process. A Colora Ultra Thermostats Model NB water bath was used to maintain the reaction temperature at the desired value. The temperature was controlled at $50 \pm 0.2°C$ throughout the gelation process. The experimental setup is shown schematically in Figure 3.4.

The viscometer was powered by a precision synchronous inductor motor which rotated a cylinder or disc in a fluid. The torque necessary to overcome the viscous resistance to the induced movement was measured by the degree to which a beryllium copper spring was wound. The position of a red pointer on the viscometer's dial which indicated the degree to which the spring was

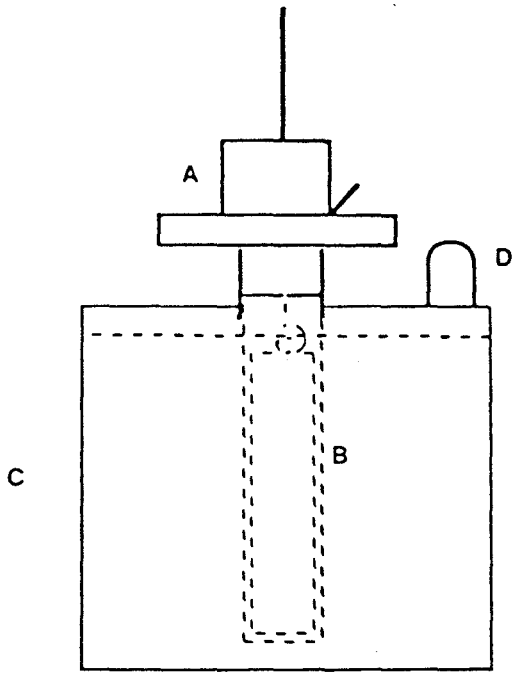


Figure 3.4: Experimental setup of steady shear measurement using Brookfield Viscometer

wound, was proportional to the viscosity of the fluid. The dial reading was then converted to the viscosity through a conversion table. Since the viscometer alone did not have the precision required at the range of viscosity typical for the gelling solution, a UL adapter was used in conjunction with the viscometer to measure low viscosities. This combination changed the range of measurement from $0 - 100$ cps to $0 - 10$ cps. The adapter consisted of a large cylindrical spindle which was rotated within the walls of a tube, the tube being held concentric by a special adapter and pivot housing.

It is customary to use an abrupt change in apparent viscosity of the gelling solution to define the gelation time. Various researchers have proposed different ways to define the gelation time such as, "the point of maximum rate of increase of viscosity," [57] "the point at which the viscosity becomes infinitely large," [58] and "a point on the steeply rising part of the viscosity vs. time curve," [28,58]. In this study, the gelation time of a gelling solution was defined as the time required to reach the point of maximum rate of increase of apparent viscosity.

The gelling solution sample was prepared according to the procedure described in Section 3.1.2 and then transferred into a small glass vial. The glass vial was kept in a water bath at $50 \pm 0.2°C$ throughout the test period. Periodically, the sample was loaded into the UL adapter and the apparent viscosity reading was recorded. The procedure was repeated until the apparent viscosity of the gelling solution was out of the range of the viscometer. After the test was completed, an apparent viscosity vs. elapsed time plot was constructed and the gelation time was determined.

The gelling solutions involved in this study consisted of 3.3% HPAM, 2% NaCl, sodium dichromate ranging from 300 ppm to 1000 ppm, and sodium thiosulfate or thiourea as the reducing agent. The concentrations of the reducing agents were determined according to the stoichiometry of the redox reactions shown in equation 2.2 and equation 2.3.

The apparent viscosity versus elapsed time plots for the gelling solutions involved in this study are presented in Figure 3.5 to Figure 3.10. It is obvious that in the early stage of the gelation process, the apparent viscosity was low and no significant changes could be observed over a period of time. Then the apparent viscosity increased rapidly when the gel piont was reached. As previously indicated, the time required to reach the point of maximum rate of increase of apparent viscosity was defined as the gelation time of the gelling solution involved. The results of the screening tests using Brookfield Viscometer are summarized in Table 3.2.

## 3.4 Dynamic Oscillatory Shear Measurement and Gel Strength Determination

Based upon the fact that the viscous and elastic elements of the polymeric gel type material respond differently to a sinusoidal varying stress or strain, rheological measurements are commonly used as diagnostic tools to study the gelation reaction. Since the gel structure remains intact under small sinusoidal shear motion, the storage modulus $G'$ can be used as the indicator of gel strength. The time dependence of the storage modulus $G'$ and the loss modulus $G''$ during the gelation process makes it possible to

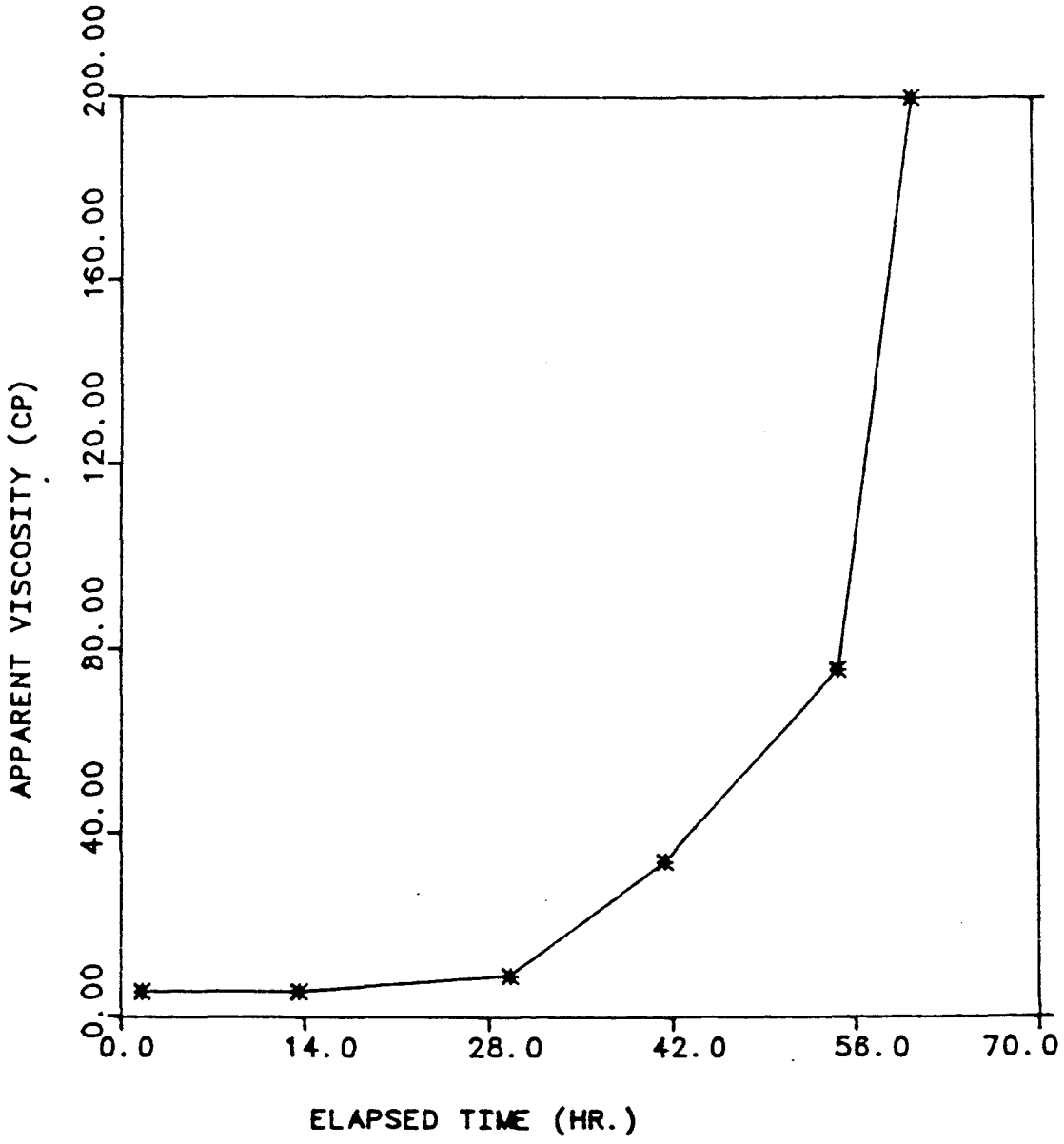


Figure 3.5: Apparent viscosity versus elapsed time plot;
HPAM:3.3%,S.D.:300ppm,S.T.:375ppm,NaCl:2%

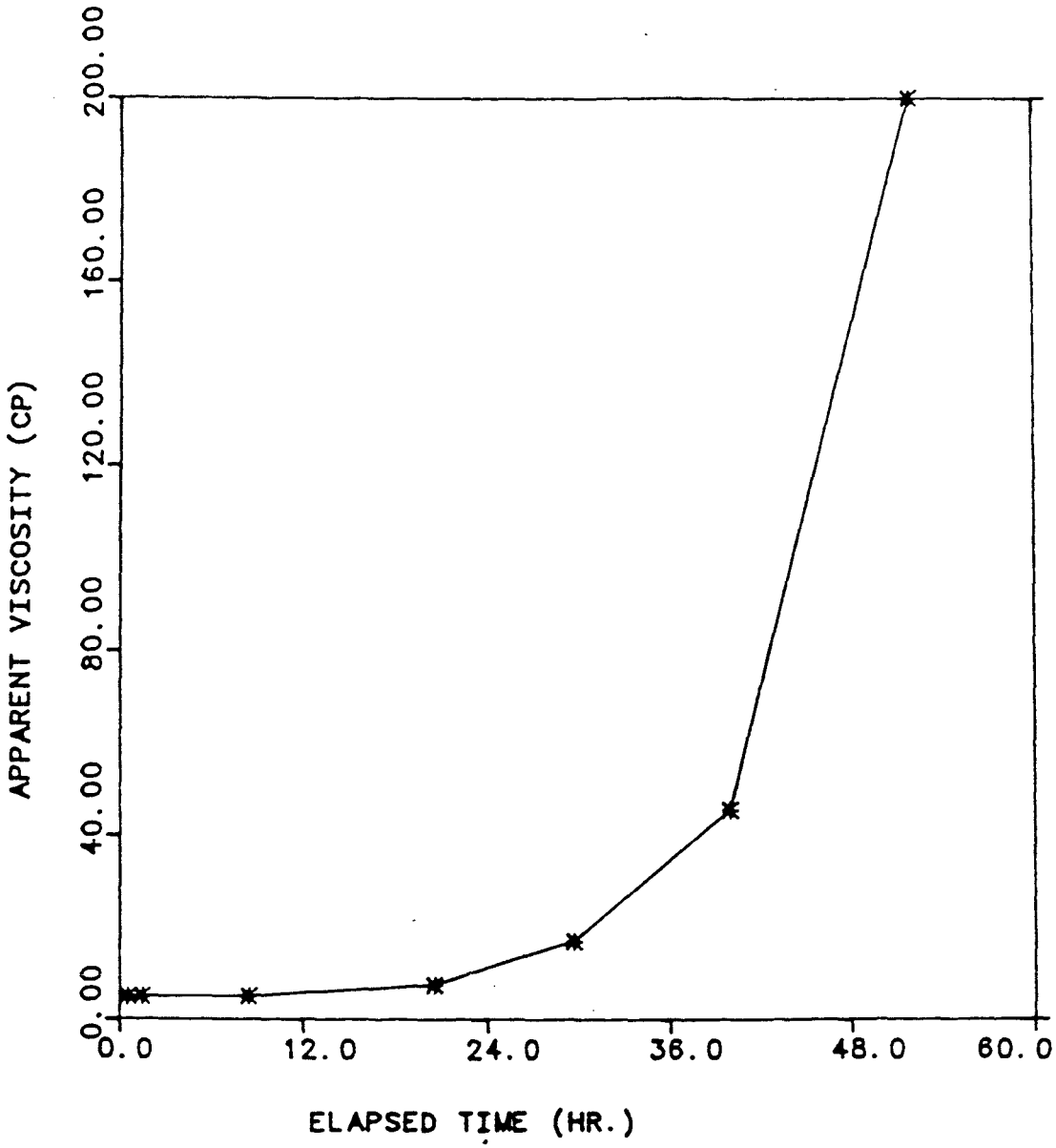


Figure 3.6: Apparent viscosity versus elapsed time plot;
HPAM:3.3%,S.D.:350ppm,S.T.:440ppm,NaCl:2%

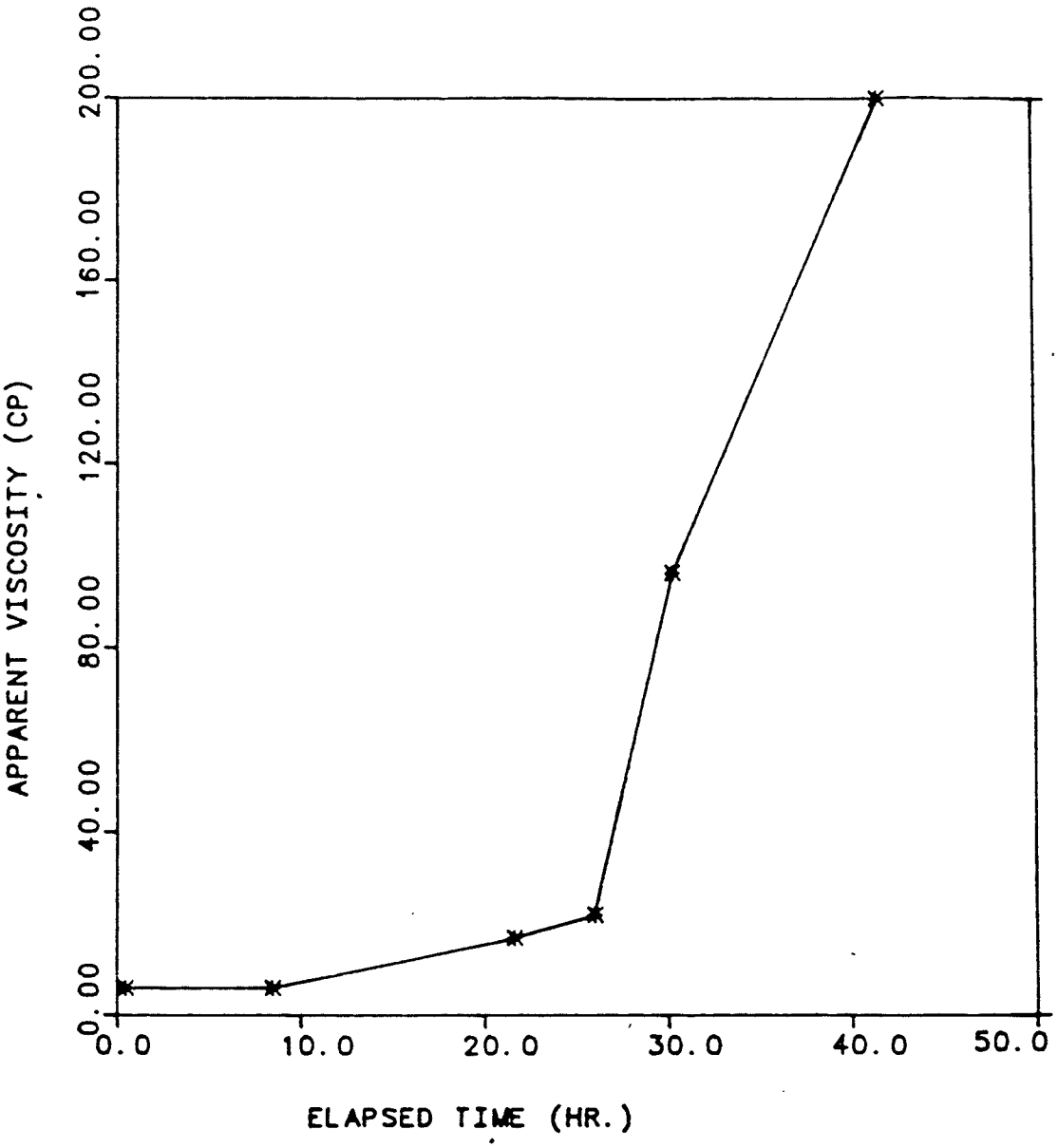


Figure 3.7 : Apparent viscosity versus elapsed time plot;
HPAM:3.3%,S.D.:400ppm,S.T.:500ppm,NaCl:2%

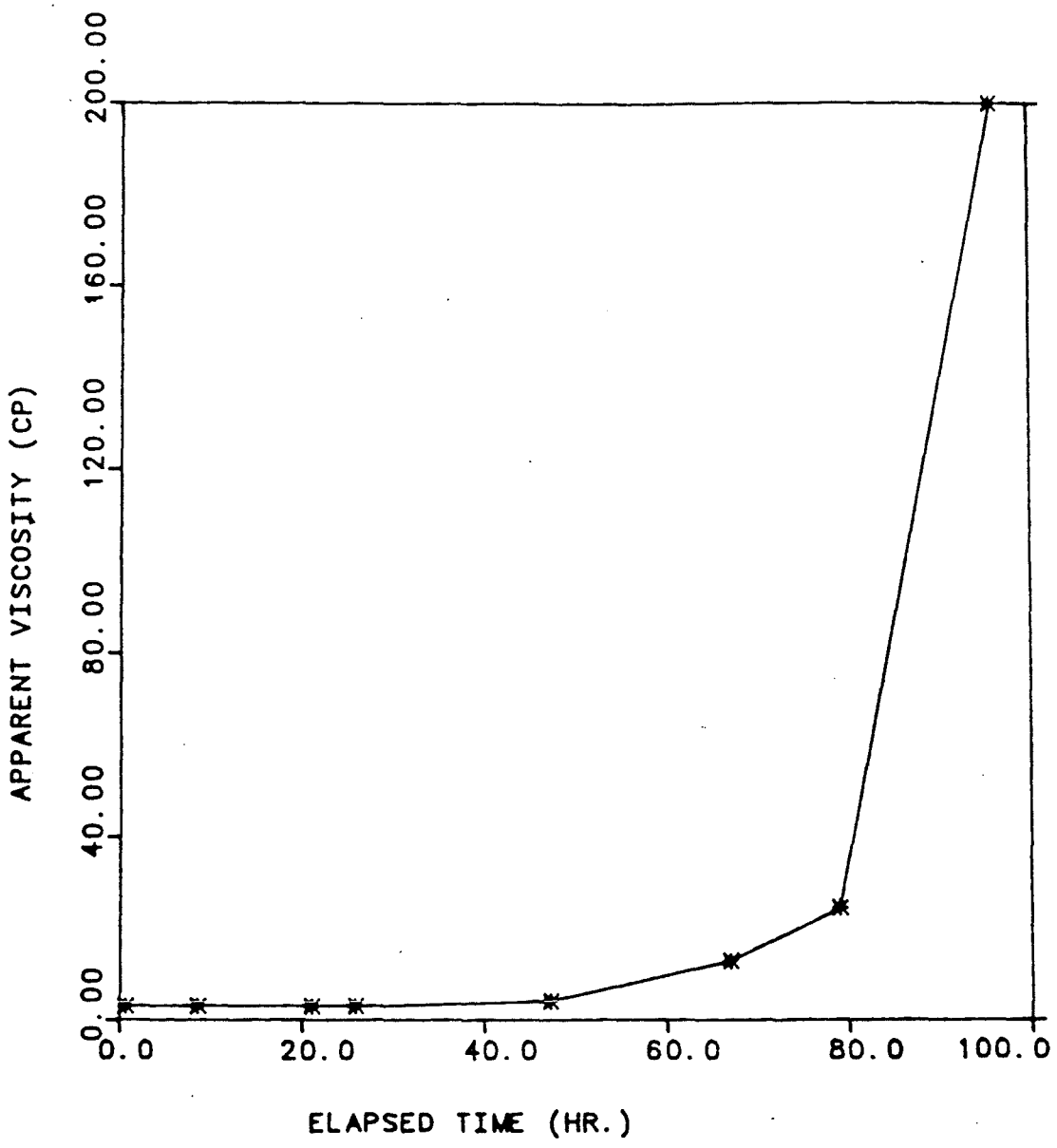


Figure 3.8 : Apparent viscosity versus elapsed time plot;
HPAM:3.3%,S.D.:600ppm,T.:600ppm,NaCl:2%

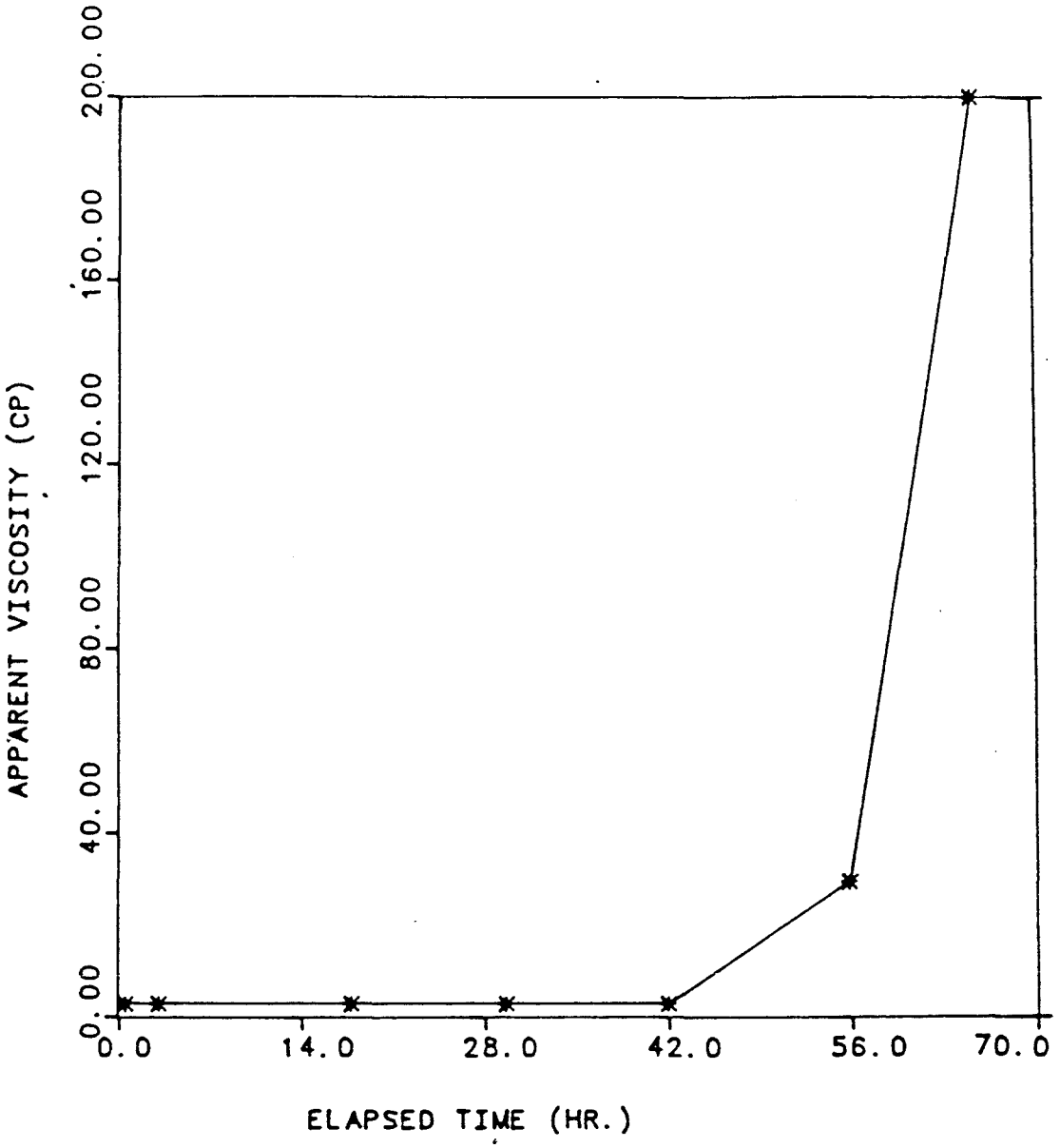


Figure 3.9 : Apparent viscosity versus elapsed time plot;
HPAM:3.3%,S.D.:750ppm,T.:750ppm,NaCl:2%

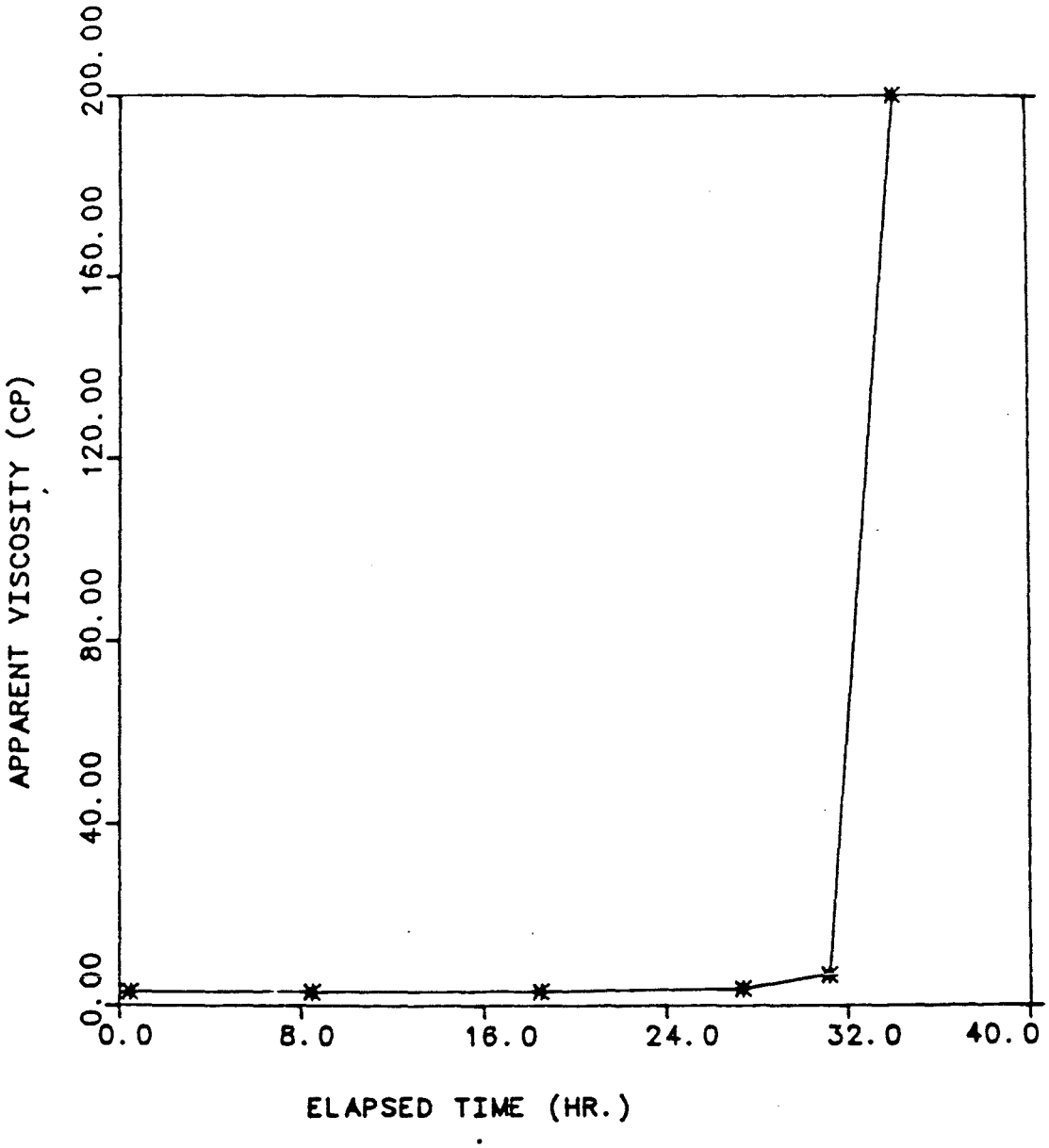


Figure 3.10: Apparent viscosity versus elapsed time plot;
HPAM:3.3%, S.D.:1000ppm,T.:1000ppm,NaCl:2%

Table 3.2: Gelation time of the gelling solutions involved

| Gel System | HPAM | S.D. (ppm) | Reducing Agent (ppm) | Gelation Time (hr.) |
|---|---|---|---|---|
| GS-1 | 3.3% | 300 | S.T.: 375 | 55.0 |
| GS-2 | 3.3% | 350 | S.T.: 440 | 40.0 |
| GS-3 | 3.3% | 400 | S.T.: 500 | 30.0 |
| GS-4 | 3.3% | 500 | S.T.: 625 | 17.0 |
| GS-5 | 3.3% | 600 | S.T.: 750 | 12.0 |
| GS-6 | 3.3% | 600 | T.: 600 | 79.0 |
| GS-7 | 3.3% | 750 | T.: 750 | 56.0 |
| GS-8 | 3.3% | 1000 | T.: 1000 | 32.0 |

**HPAM: Partially Hydrolyzed Polyacrylamide**
**S.D.: Sodium Dichromate**
**S.T.: Sodium Thiosulfate**
**T. : Thiourea**

effectively monitor the buildup of the three dimensional gel structure.

A Rheometric Fluids Spectrometer Model 8400 (RFS-8400) with a cone and plate geometry test fixture was employed to conduct the rheological measurements. The RFS-8400 can be divided into a test station and computer controlled input/output devices. The computer serves as the central nerve system of the whole unit controlling the test sequence, making measurements and processing the results. The test station consists of an environmental chamber, servo motors, transducer and electronics which apply the necessary deformation history to the sample and detect the results. The test fixture is enclosed in the environmental chamber and the temperature is maintained at the desired level by recirculating the temperature controlled silicon oil through the environmental chamber.

In the steady shear mode, the rotating plate imposes a steady shear rate on the sample. The cone is mounted on a precise air bearing which is supported by a torque motor. While the imposed shear stress attempts to rotate the cone, the torque motor generates a restoring torque to return it to the balanced position. The torque generated by the shear is detected by a sensitive transducer and the apparent viscosity is calculated from the resulting shear stress and shear rate by the computer.

In the oscillatory mode, the sample experiences a sinusoidally varying strain imposed by the movement of the bottom flat plate. Comparing the amplitude and phase shift between the strain and stress, the computer makes a digital cross-correlation of strain and torque. The average torque is converted to stress by using the equation appropriate to the geometry under test

and the rheological properties of the sample such as the storage modulus $G'$ and the loss modulus $G''$ can thus be calculated.

Prior to the start of the test, the test fixture enclosed in the environmental chamber was heated to the test temperature of $50 \pm 0.2°C$. The gelling solution was prepared according to the procedure described in Section 3.1.2 and 0.72 cc of the sample was loaded into the test fixture five minutes after the time of mixing. The sample was immediately covered by 3 cc of the mineral oil to prevent evaporation. The repeated dynamic oscillatory measurements were conducted every thirty minutes at a frequency of 10 rad/sec and 50% maximum strain to monitor the progress of gelation. The % strain, $\gamma$, in this case was defined as

$$\gamma = \frac{\theta}{\alpha} \times 100 \tag{3.14}$$

where $\theta$ denotes the angle of rotation of the plate and $\alpha$ denotes the cone and plate angle.

The compositions of the gelling solutions involved are: 3.3% HPAM, 2% NaCl, sodium dichromate ranging from 300 ppm to 1000 ppm, and a reducing agent. Sodium thiosulfate, thiourea were all used as reducing agents where the concentrations of the reducing agents were determined according to the stoichiometry of the redox reactions shown in equation 2.2 and equation 2.3.

The changes of storage modulus $G'$ and loss modulus $G''$ of the gelling solutions tested during the progress of gelation are shown in Figure 3.11 to

Figure 3.17. The discontinuity of the $G'$ and $G''$ curves in Figure 3.15 are caused by the restart of the instrument after the maximum time limit of the software was reached.

These plots reveal that the loss modulus $G''$ remained low throughout the gelation process, while the storage modulus $G'$ was initially low and increased sharply after the onset of gelation, then eventually reached a point where no significant increase of $G'$ was observed. The leveling of the storage modulus $G'$ indicate that the three dimensional gel structure was fully developed. Hence, it seemed logical to use $G'$ as the indicator of the gel strength of a mature gel. However, for gelling solutions having a final $G'$ value greater than 6000 $dyne/cm^2$, which is the limit of the instrument, no leveling of $G'$ could be observed.

Dynamic oscillatory frequency sweep measurement was performed at 50% maximum strain after the gel had developed to its full strength. The value of $G'$ at the frequency of 10 rad/sec was arbitrarily chosen as the quantitative indicator of the gel strength. The results of the dynamic oscillatory frequency sweep measurements are presented in Figure 3.18 to Figure 3.22. The gel strength and gelation time of different gelling solutions are summarized in Table 3.3.

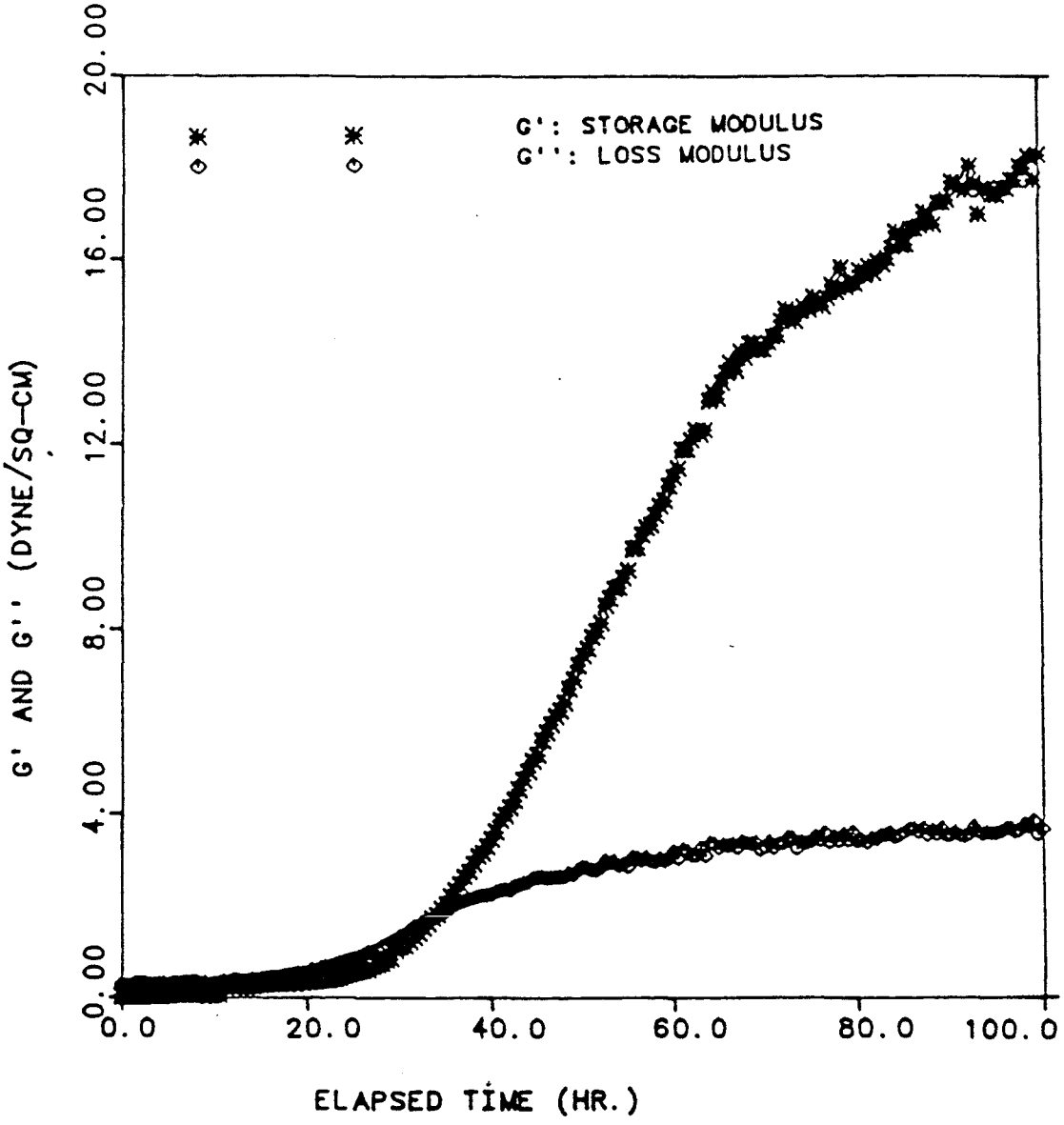


Figure 3.11: Storage modulus versus elapsed time plot;HPAM:3.3%,S.D.:300ppm,S.T.:375ppm,NaCl:2%

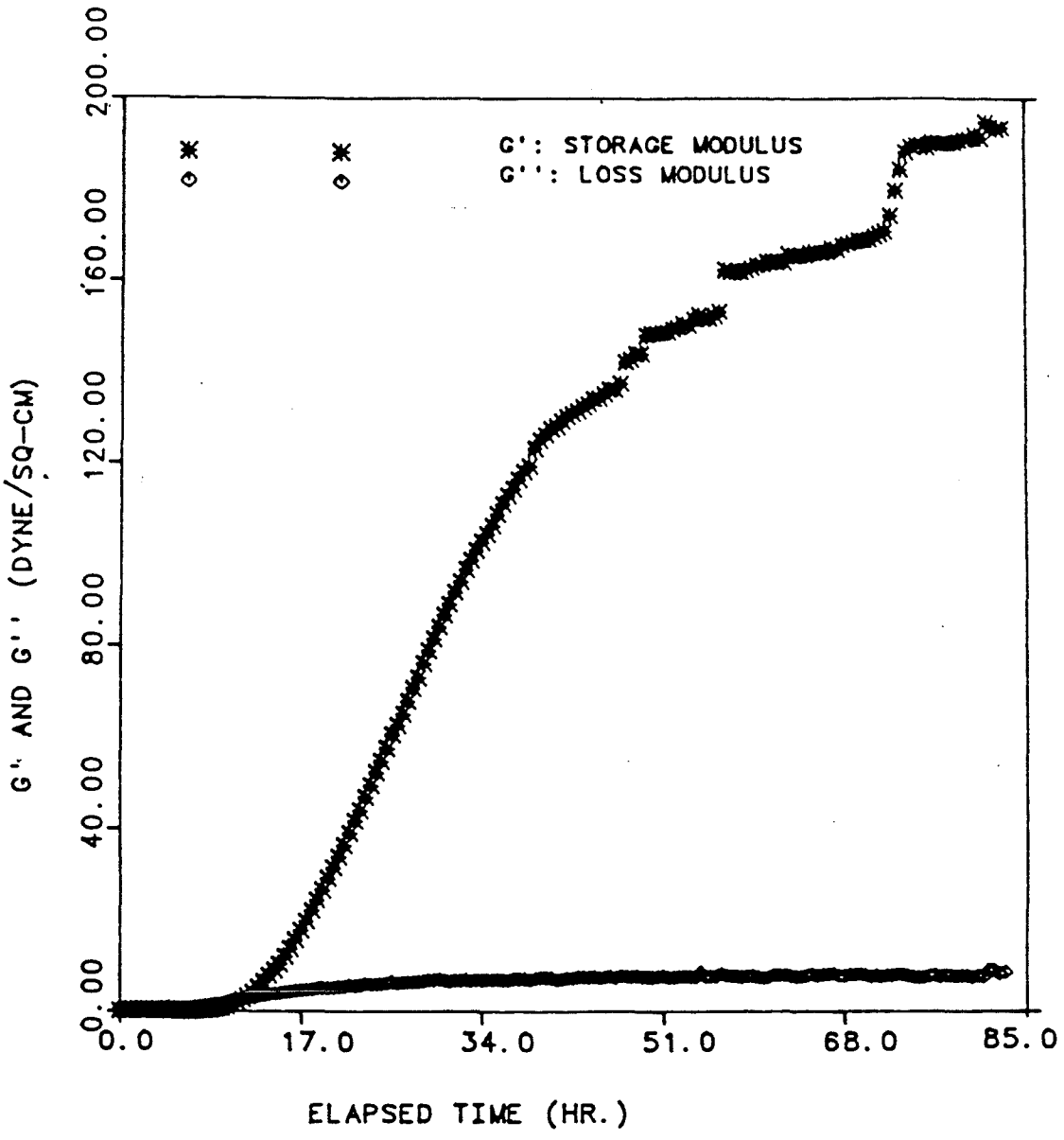


Figure 3.12: Storage modulus versus elapsed time plot;HPAM:3.3%,S.D.:400ppm,S.T.:500ppm,NaCl:2%

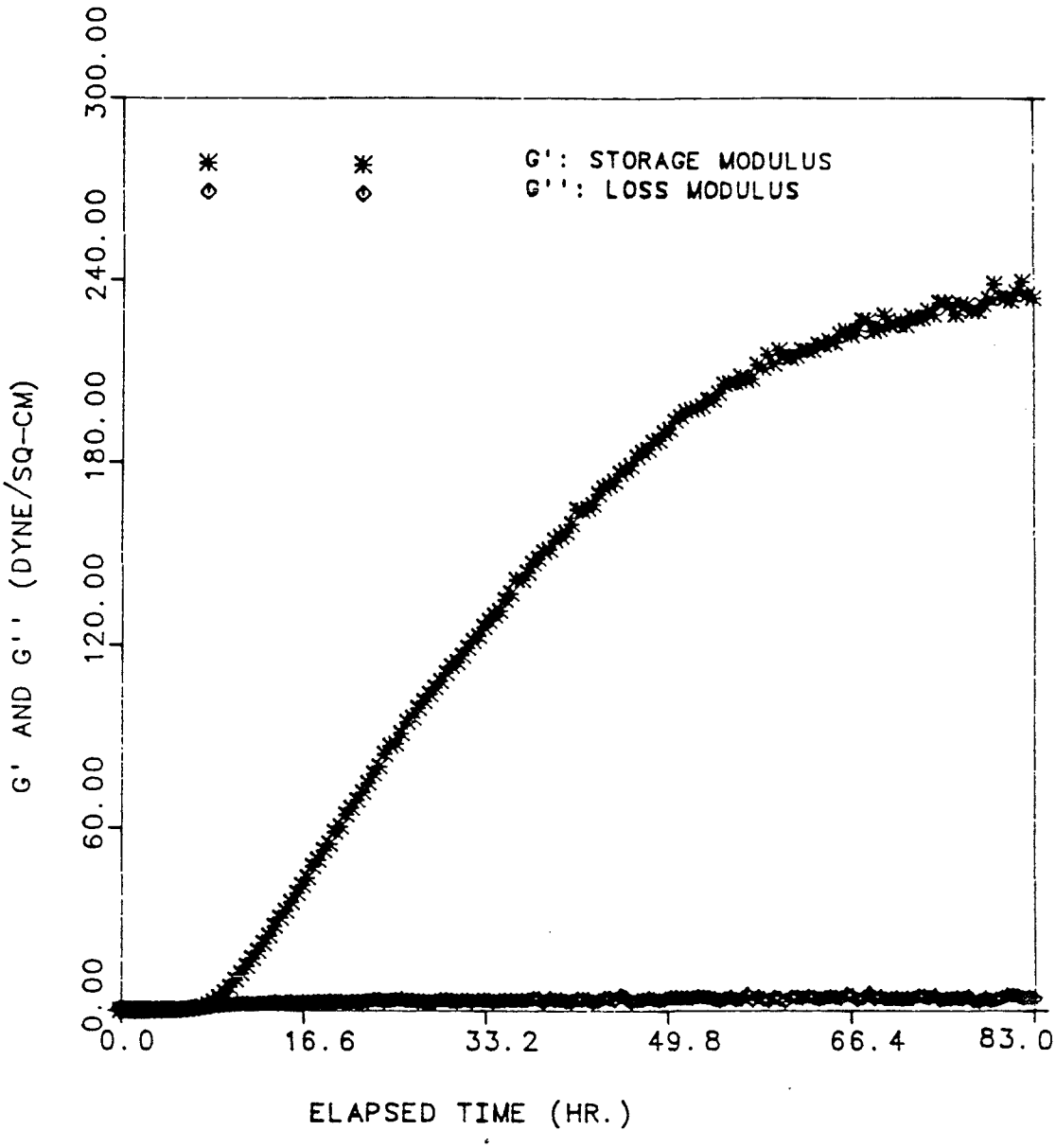


Figure 3.13: Storage modulus versus elapsed time plot;
HPAM:3.3%,S.D.:500ppm,S.T.:625ppm,NaCl:2%

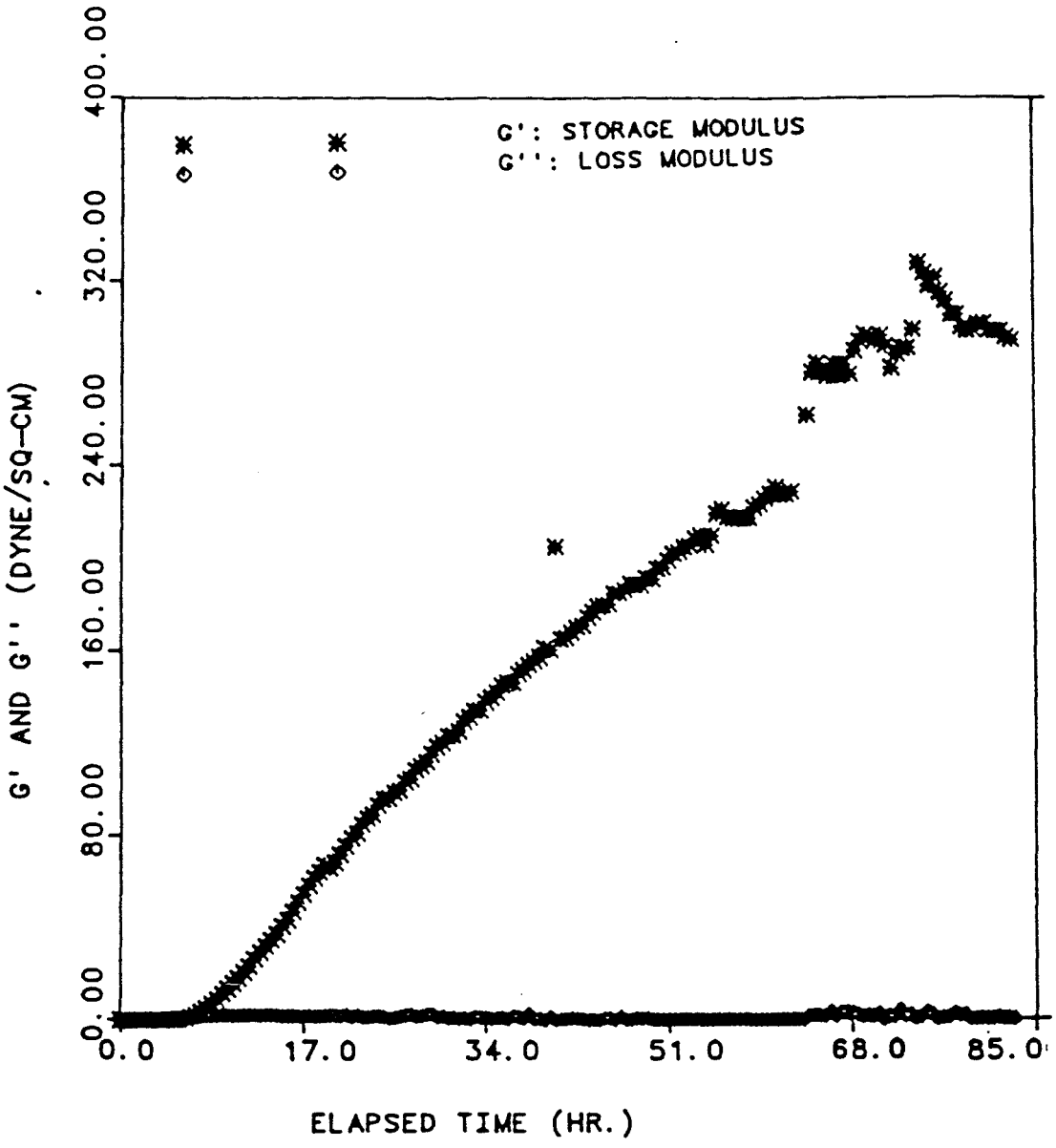


Figure 3.14: Storage modulus versus elapsed time plot;
HPAM:3.3%,S.D.:600ppm,S.T.:750ppm,NaCl:2%

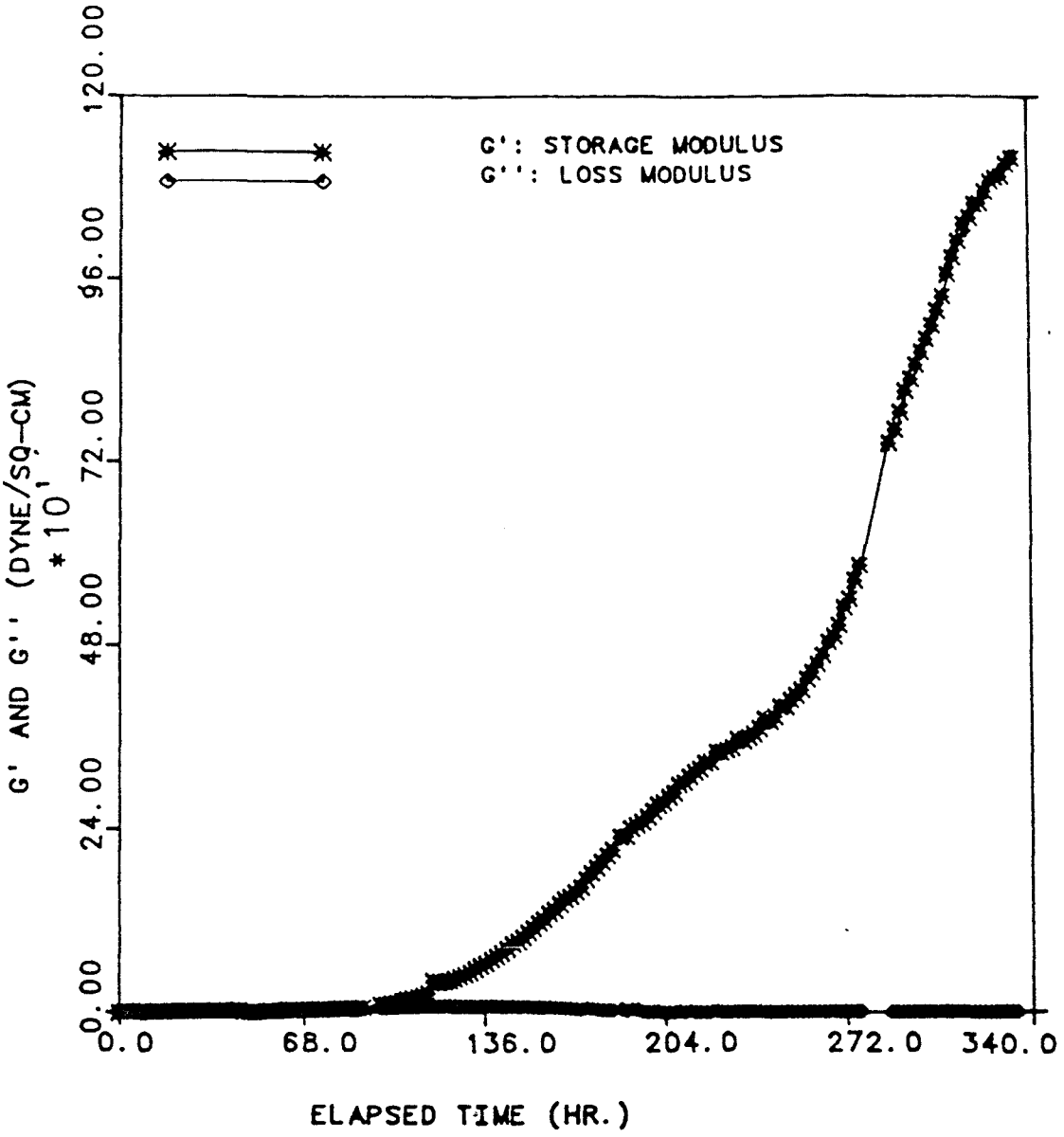


Figure 3.15: Storage modulus versus elapsed time plot;
HPAM:3.3%,S.D.:600ppm,T.:600ppm,NaCl:2%

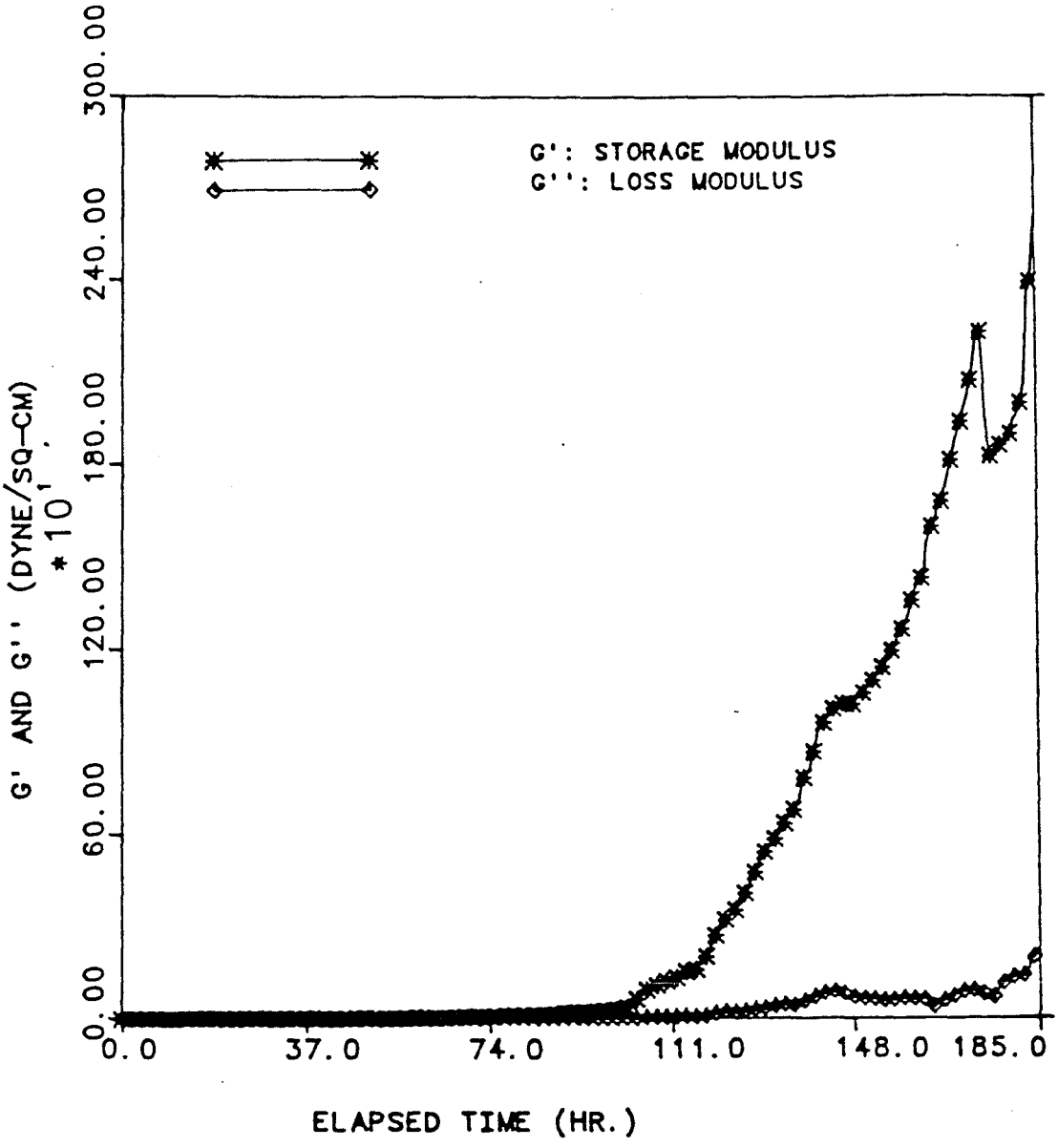


Figure 3.16: Storage modulus versus elapsed time plot;
HPAM:3.3%, S.D.:750ppm, T.:750ppm, NaCl:2%

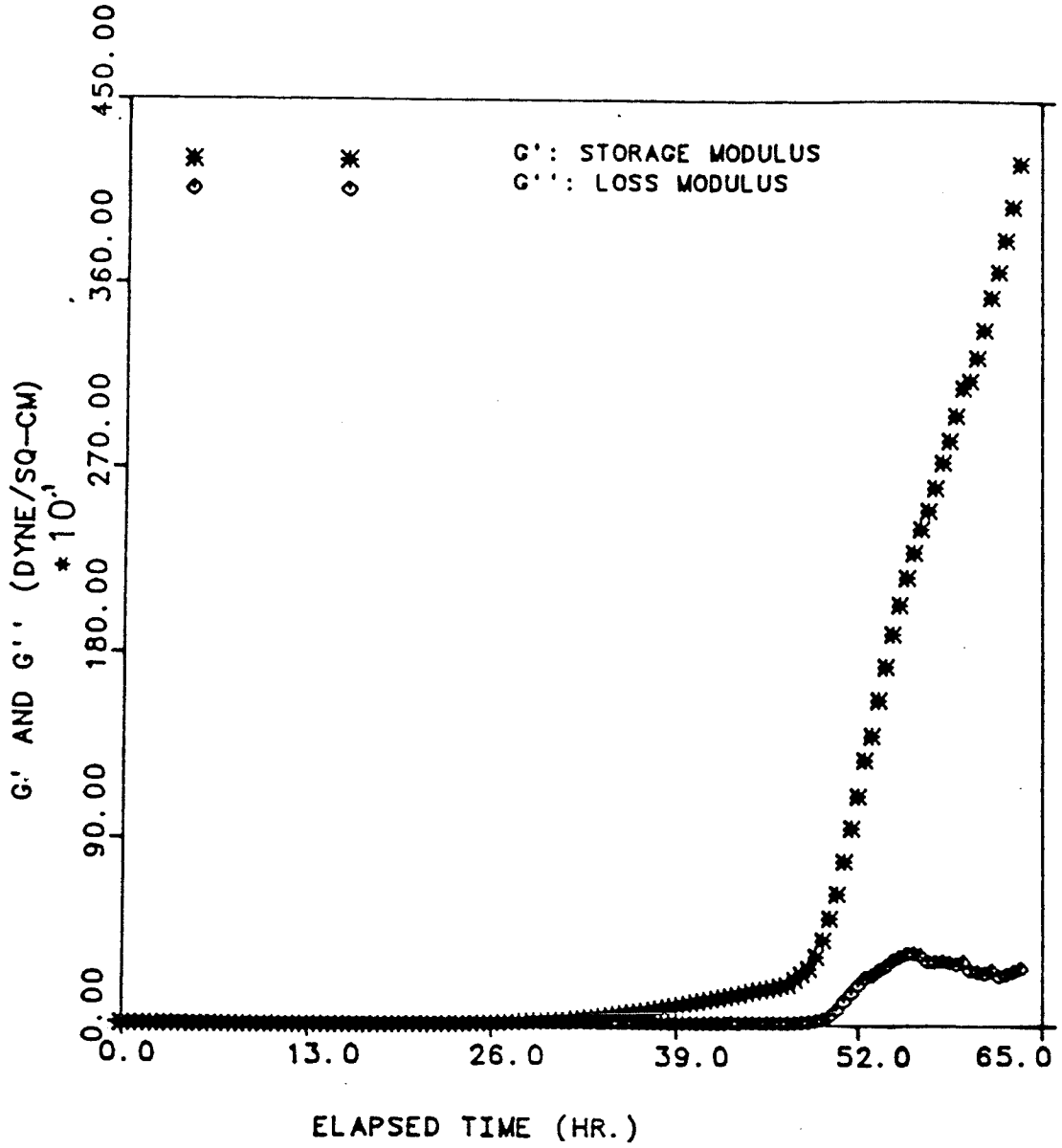


Figure 3.17: Storage modulus versus elapsed time plot;
HPAM:3.3%,S.D.:1000ppm,T.:1000ppm,NaCl:2%

Table 3.3: Gel strength of the gelling solutions involved

| Gel System | HPAM | S.D. (ppm) | Reducing Agent (ppm) | Gelation Time (hr.) | $G'$ $(dyne/cm^2)$ |
|---|---|---|---|---|---|
| GS-1 | 3.3% | 300 | S.T.: 375 | 55.0 | 18.99 |
| GS-3 | 3.3% | 400 | S.T.: 500 | 30.0 | 194.80 |
| GS-4 | 3.3% | 500 | S.T.: 625 | 17.0 | 236.80 |
| GS-5 | 3.3% | 600 | S.T.: 750 | 12.0 | 314.20 |
| GS-6 | 3.3% | 600 | T.: 600 | 79.0 | 1128.00 |
| GS-7 | 3.3% | 750 | T.: 750 | 56.0 | > 6000 |
| GS-8 | 3.3% | 1000 | T.: 1000 | 32.0 | > 6000 |

HPAM: Partially Hydrolyzed Polyacrylamide
S.D.: Sodium Dichromate
S.T.: Sodium Thiosulfate
T. : Thiourea

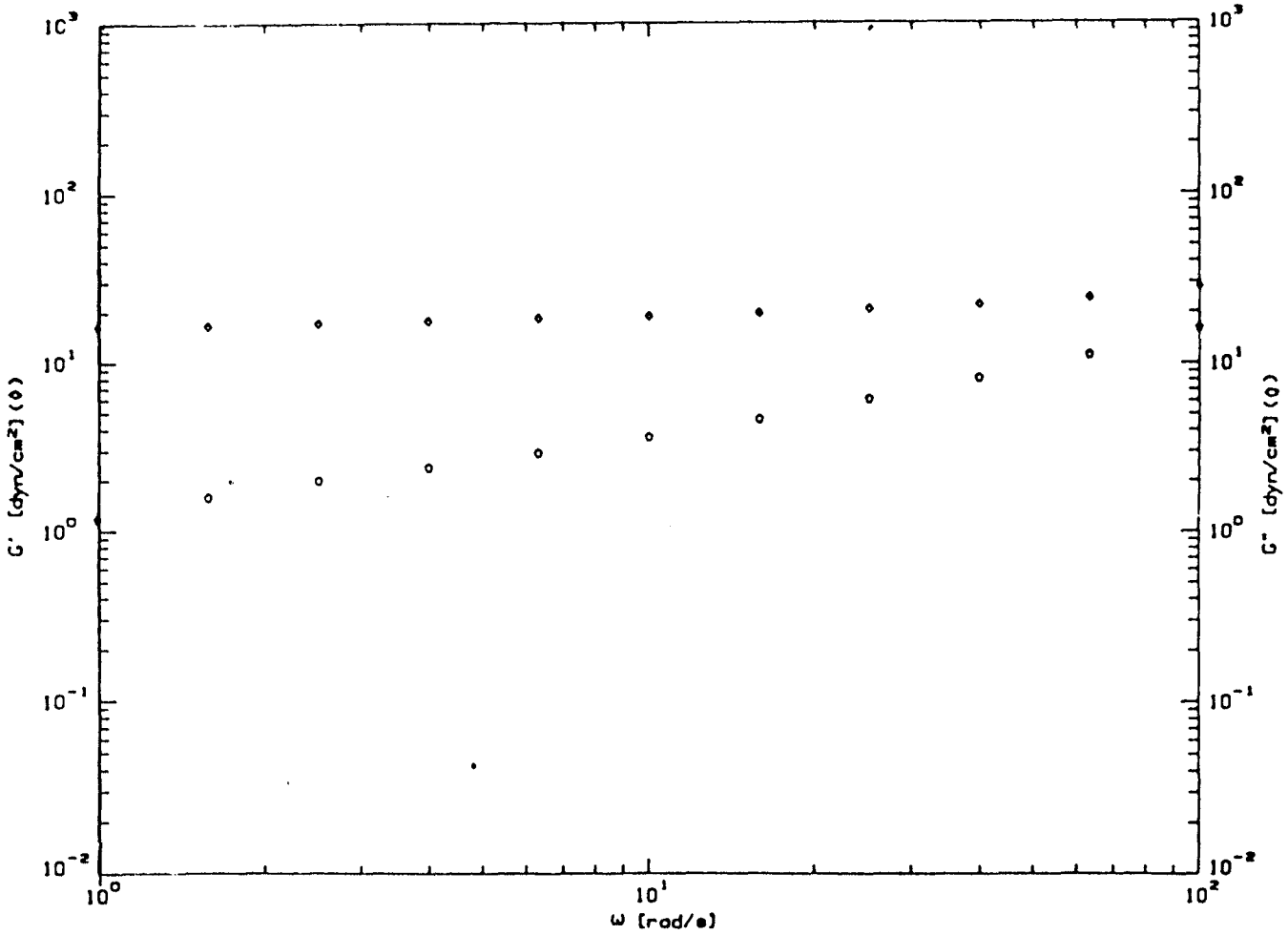


Figure 3.18: Dynamic frequency sweep measurement;
HPAM:3.3%,S.D.:300ppm,S.T.:375ppm,NaCl:2%

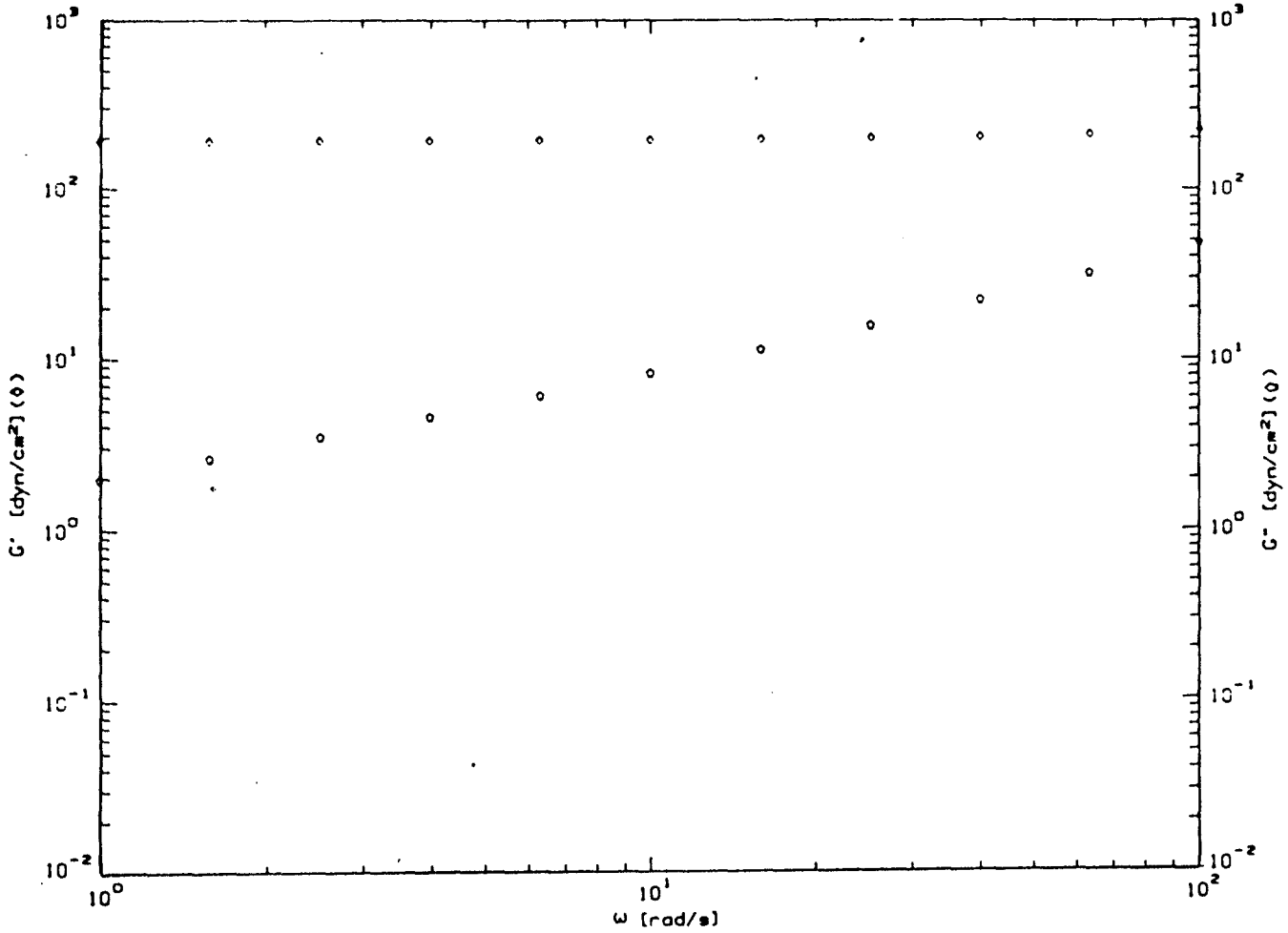


Figure 3.19: Dynamic frequency sweep measurement; HPAM:3.3%, S.D.:400ppm, S.T.:500ppm, NaCl:2%

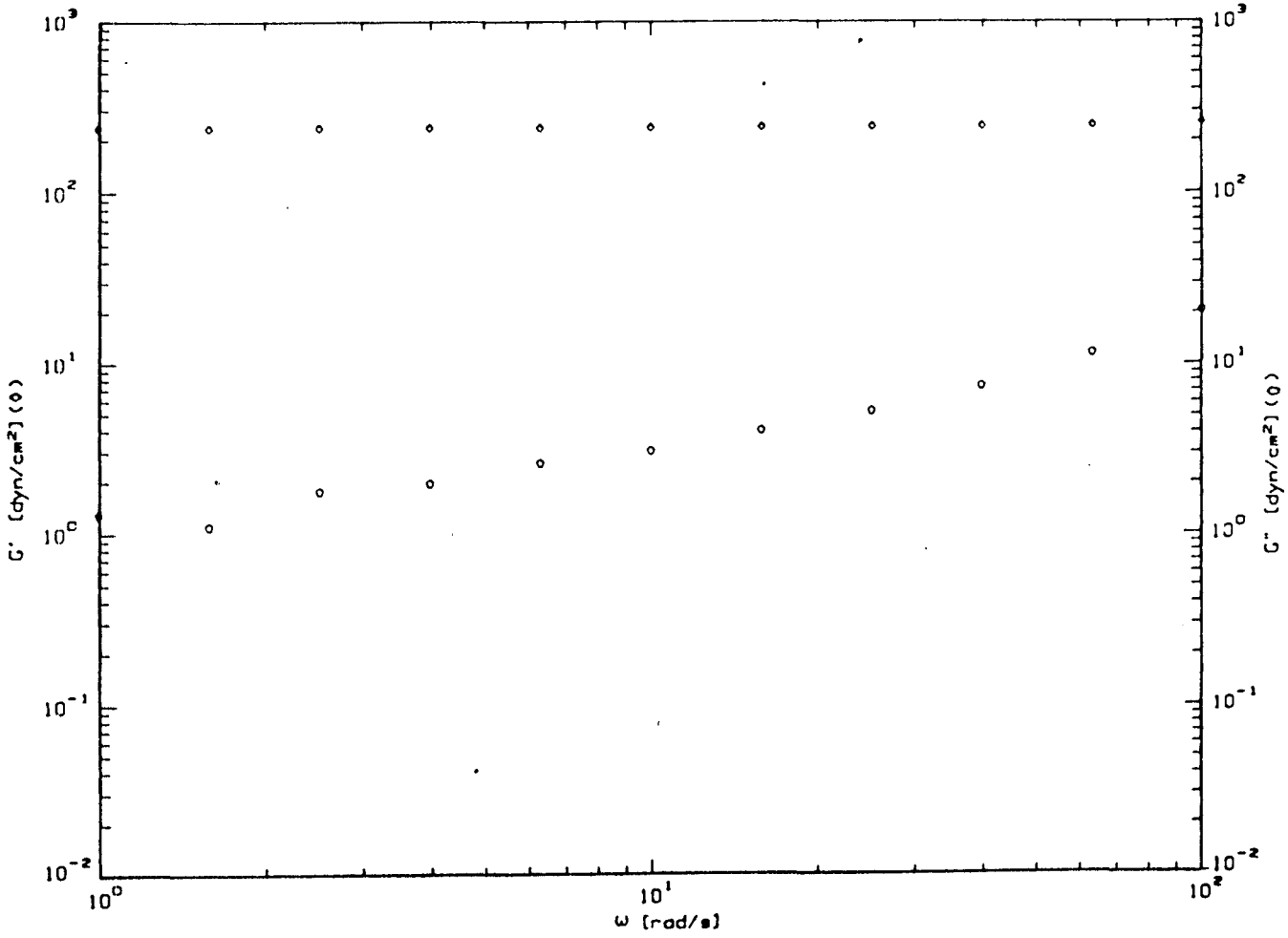


Figure 3.20: Dynamic frequency sweep measurement; HPAM:3.3%, S.D.:500ppm, S.T.:625ppm, NaCl:2%

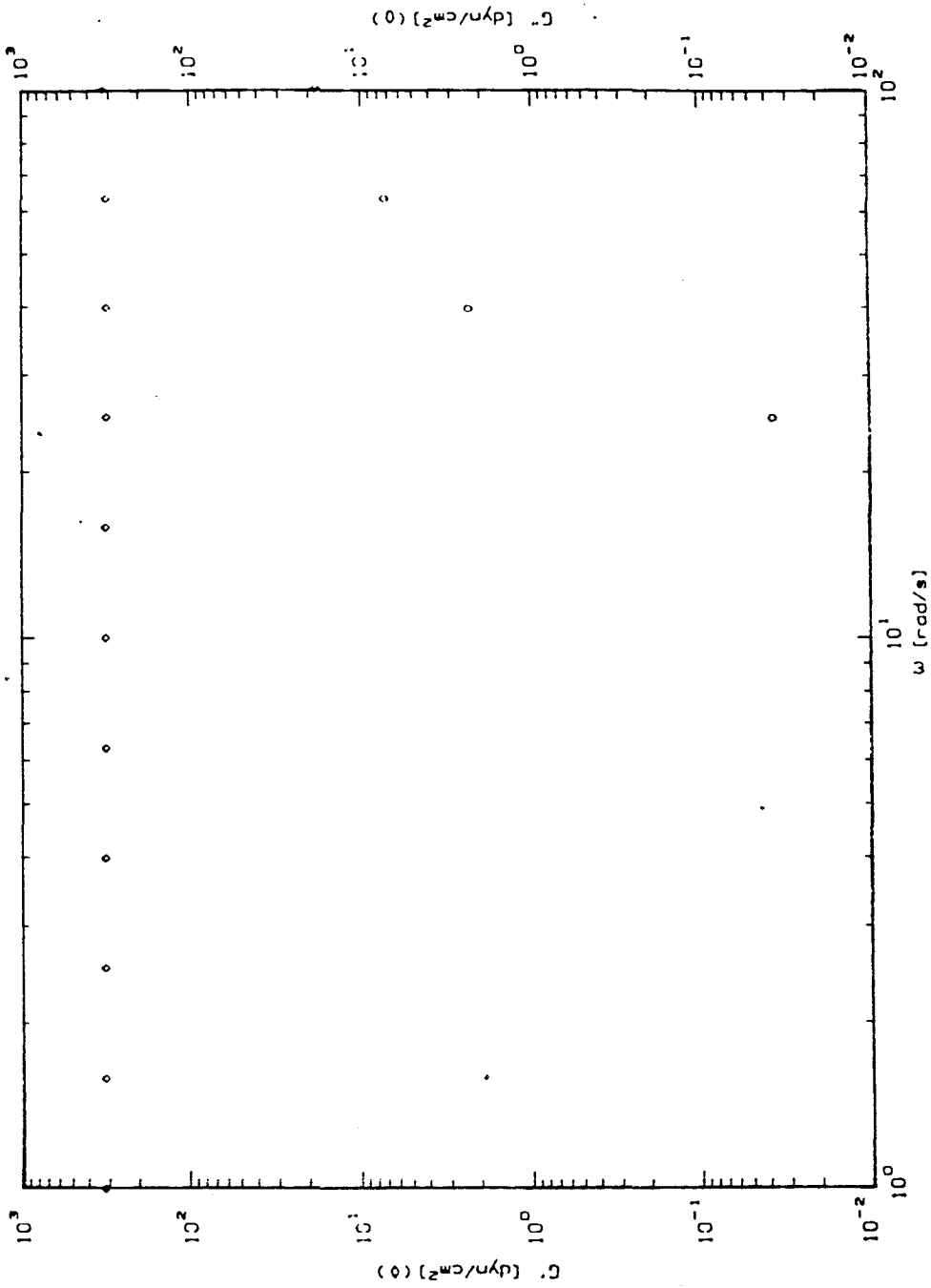


Figure 3.21: Dynamic frequency sweep measurement; HPAM:3.3%, S.D.:600ppm, S.T.:750ppm, NaCl:2%

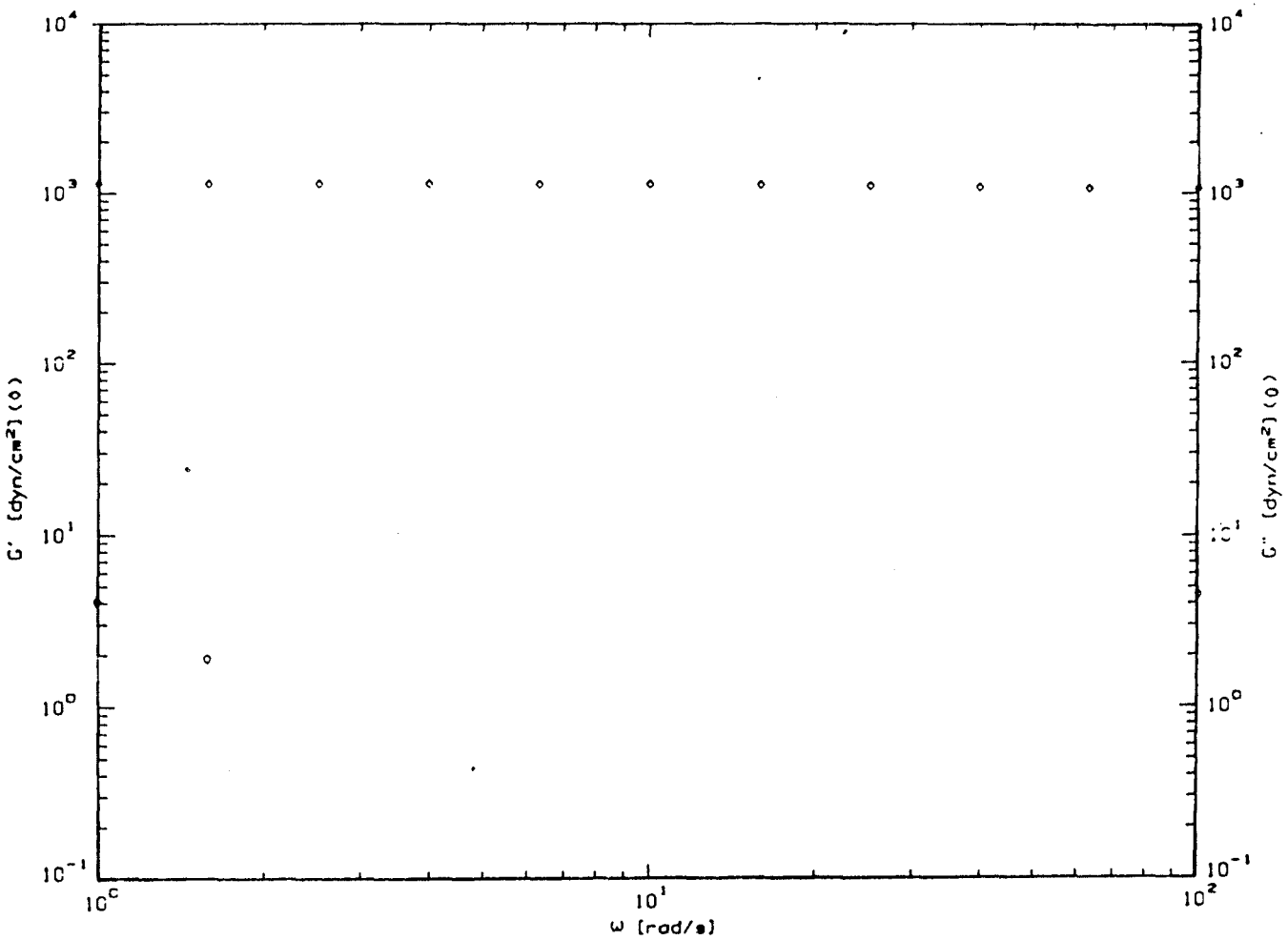


Figure 3.22: Dynamic frequency sweep measurement; HPAM:3.3%, S.D.:600ppm, S.T.:600ppm, NaCl:2%

# Chapter 4

# In-Situ Gelation Studies

## 4.1 Introduction

The objective of the in-situ gelation studies was to correlate the gel strength of polyacrylamide/chromium gels with their permeability reduction characteristics in porous media. Gelling solutions with a wide range of gel strength and appropriate gelation time were selected from the previous gelation and rheological studies for the in-situ gelation studies.

During the in-situ gelation experiments, the gelling solutions were thoroughly mixed and then injected into unconsolidated sandpacks. The sandpacks were preconditioned to residual oil saturation prior to the start of the gelling solution injection. The pressure drop across each section of the sandpack was monitored during the injection process by a pressure sensing and recording system. The pressure distribution across the sandpack could be used to interpret the behavior of gelling solution during the injection process. After a shut-in period, the sandpack was flushed with brine(2% NaCl) until no polymer could be detected in the effluent. The extent of permeability reduction was then determined by comparing the permeability of the sandpack after postflush and the permeability of the sandpack before treatment. The whole experimental setup was placed in a temperature controlled air bath as

shown in Figure 4.1 and the temperature was kept at $50°C$ throughout the experimental process. Effluent samples were collected by a fraction collector and chemical analyses were performed to determine the amount of polymer and chromium retained in the sandpack after treatment.

## 4.2 Experimental Apparatus

### 4.2.1 Porous Media

In-situ gelation studies of the polyacrylamide/chromium gel system were conducted in unconsolidated sandpacks. Oklahoma No. 1 sand was employed to build the sandpack. The screen and chemical analyses for Oklahoma No. 1 sand are listed in Table 4.1 and Table 4.2.

The sand was first sieved to the desired mesh size range and then packed into a $2-in$ ID by $24-in$ long stainless steel holder. The sandpack holder consisted of a stainless steel column and two endcaps. Five equally spaced pressure taps were installed along the sandpack holder with $5-in$ intervals in between. Two butyl rubber O-rings were used to provide the leak-proof seal between the stainless steel column and the endcaps. A schematic diagram of the sandpack holder is shown in Figure 4.2.

The sandpacks were prepared with the help of a electric shaker which provided even and constant vibration throughout the packing process. The sand grains were loaded into a separatory funnel and the flow rate of the sand grains was adjusted by the stop-cock so that the packing could be completed in two hours. A plastic column with seven layers of metal screens was installed atop the sandpack holder during the packing process to insure that the sand

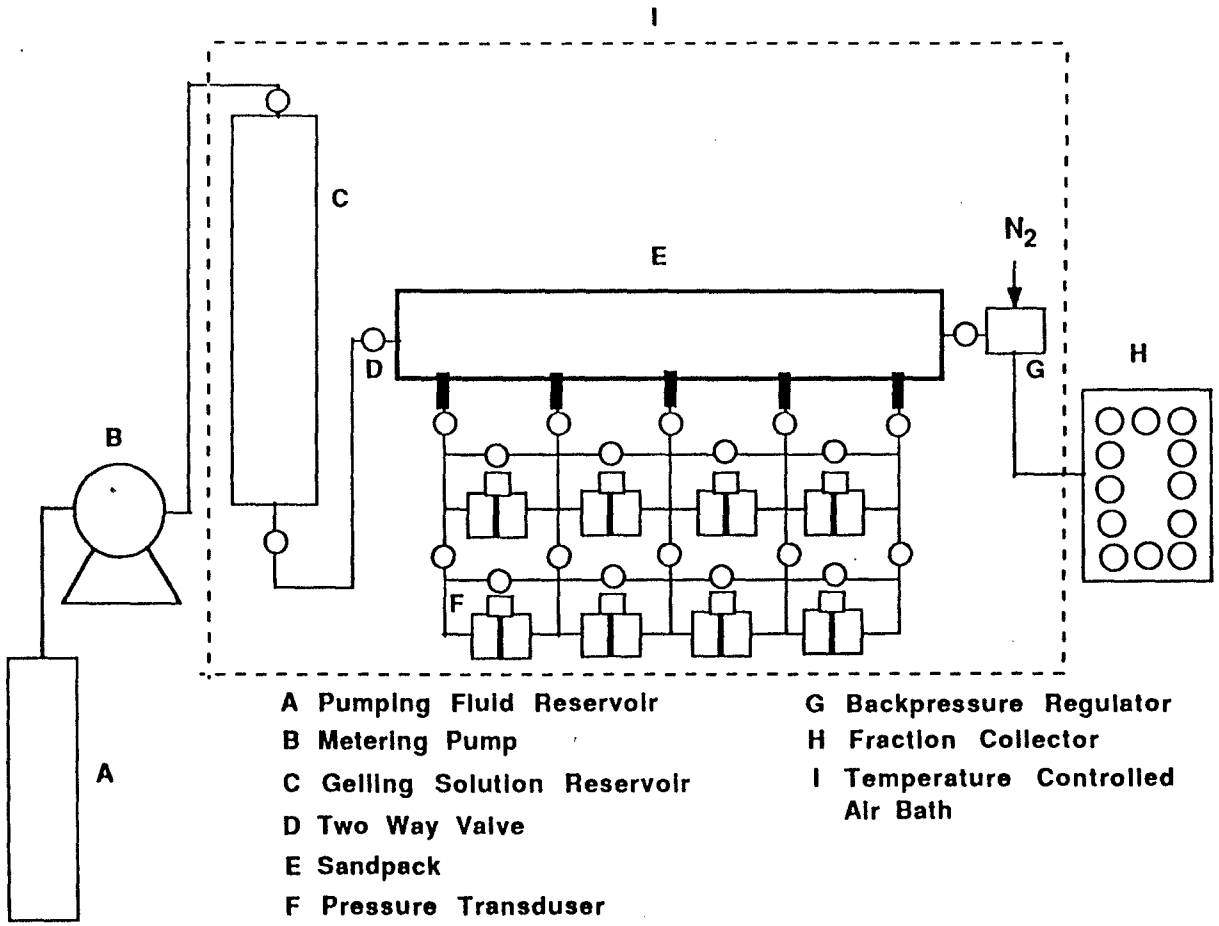


Figure 4.1: A schematic diagram of the experimental setup for in-situ gelation studies

Table 4.1: Screen analysis of Oklahoma No. 1 sand

| Screen Mesh Size | Percent Stopped By Screen | Cum. Percent Stopped By Screen |
|---|---|---|
| 40 | Trace | Trace |
| 50 | 0.5 | 0.5 |
| 70 | 6.6 | 7.1 |
| 100 | 40.0 | 47.1 |
| 140 | 38.2 | 85.3 |
| 200 | 12.8 | 98.1 |
| Thur 200 | 1.9 | 100.0 |

Table 4.2: Chemical analysis of Oklahoma No. 1 sand

| | Total Amount (%) |
|---|---|
| $SiO_2$ | 99.9 |
| $Fe_2O_3$ | 0.018 |
| $Al_2O_3$ | 0.120 |
| $TiO_2$ | 0.007 |
| $CaO$ | 0.010 |
| $MgO$ | Trace |

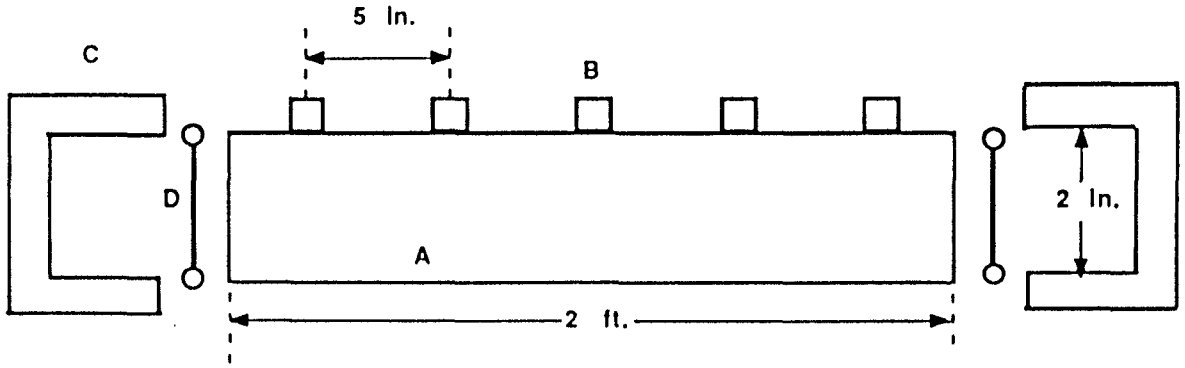


Figure 4.2: Diagram of the stainless steel sandpack holder

grains fell evenly into the holder. After the completion of the packing process, the sandpack was evacuated and saturated with brine(2% NaCl).

### 4.2.2 Pressure Sensing and Recording System

In order to obtain accurate and continuous pressure drop readings during the experiments, a pressure sensing and recording system consisting of pressure transducers, carrier demodulators and a multichannel data acquisition instrument was employed to perform the task. Validyne Model DP-15 diaphragm-type variable reluctance differential pressure transducers were used in this study to monitor the pressure differentials between pressure taps. The diaphragm plates were interchangeable and many selections were available for different full scale pressure measurements. The diaphragm plates used in this study were selected based upon the estimated flow resistance to be encountered during the experiments so that the maximum precision could be obtained.

An applied pressure differential changed the gap between the transducer body and the diaphragm. The accompanied magnetic reluctance change was immediately sensed by an AC bridge circuit and an output voltage signal proportional to the pressure differential was sent to the carrier demodulator. The Validyne Model CD-19A carrier demodulator then converted the output signal from a pressure transducer to a DC voltage.

A Validyne Model MC1-20 module case capable of housing up to twenty separate plug-in signal conditioning modules was used to provide the necessary DC operating voltage and carrier excitation both for the carrier de-

modulators and their associated transducers. The DC voltage output from the carrier demodulator was sent to an Esterline Angus Model MRL multi-point recorder/logger. The MRL is a multiple-microprocessor programmable multichannel data acquisition instrument which can be set up as a ordinary strip chart recorder to produce a hard-copy record, or as a logger to produce tabular digital output at user selected intervals.

The pressure transducer and demodulator as a set must be calibrated against a secondary pressure standard before it can be used for pressure measurements. A MENSOR QUARTZ MANOMETER with interchangeable Quartz Pressure Sensors was used as the pressure standard. The range of the manometer is determined by the particular sensor installed. Heise gauges and a water manometer were used in some cases as well. Figure 4.3 is the sketch of the setup used in this study for pressure transducer calibration. The calibration procedure followed in this study is described as follows:

1. Connect the pressure transducer, the carrier demodulator, and the recorder with the proper cables and connectors.

2. Adjust the R screw on the carrier demodulator until the reading on the recorder shows zero.

3. Apply pressure to the full scale of the particular diaphragm plate involved.

4. Adjust the gain knob on the carrier demodulator until the reading on the recorder shows full scale pressure.

5. Bleed off the pressure in the system.

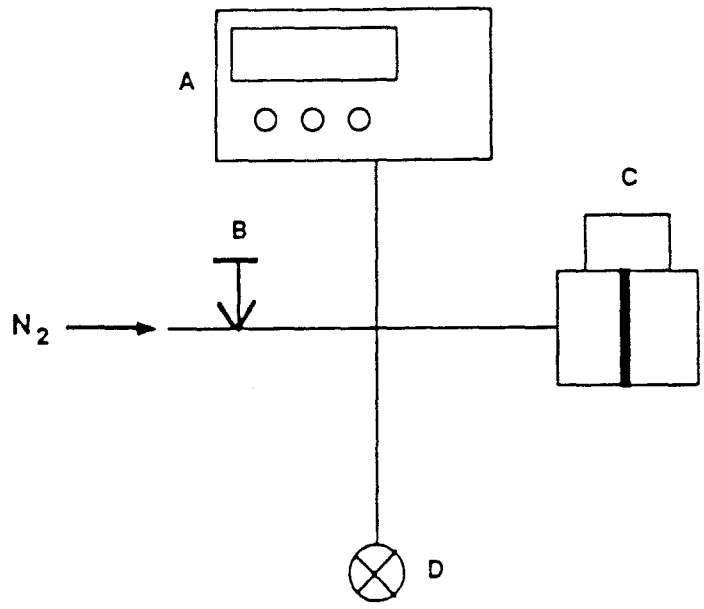


Figure 4.3: Diagram of the setup used in pressure transducer calibration

6. Adjust the R screw on the carrier demodulator until the reading on the recorder shows zero again.

7. Apply pressure to the full scale again and readjust the gain knob on the carrier demodulator so that the output on the recorder shows exactly full scale pressure.

8. Bleed off the pressure in the system and check for zero output again.

9. Repeat Step 2 through Step 8 if necessary.

10. Apply pressure to 20%, 40%, 60%, and 80% of the full scale pressure to check for linearity.

### 4.2.3 Pumping Systems

The Cheminert CMP-2 Metering Pump and constaMetric-III Metering Pump manufactured by LDC/Milton Roy Company were employed in the in-situ gelation studies. The Cheminert CMP-2 Metering Pump is a constant rate pump which has three independent pump chambers each consisting of a Kel-F cylinder, glass piston, and Teflon piston seal. Two of the glass pistons are 180° out of phase and the third pump chamber serves to pressurize the filled chamber just before it is switched to the outlet line. The perfect coordination of the three pump chambers is vital in providing surge-free constant flow rate. The maximum output pressure of the pump is 500 psig and the flow rate range is from 0.2 cc/min to 2 cc/min.

The constaMetric-III Metering Pump is also a constant rate pump capable of delivering selected flow rate ranging from 0.5 cc/min to 10 cc/min at

50 to 6000 psi downstream pressure. The pumping unit consists of a pumping chamber, a single plunger, and a computer-designed cam. The reciprocating movement of the plunger driven by the cam delivers the selected flow rate regardless of the downstream pressure up to 6000 psi. The pump also features an analog display of system pressure and a setting of high/low limits which will shut down the pump if the system pressure exceeds or falls below the selected pressure limits. A strain gauge bridge type pressure transducer serves as the pressure sensing device of the pump.

### 4.2.4 Effluent Collection System

An ISCO Model RETRIVER-II fraction collector was employed in this study to collect effluent samples. Graduated test tubes of 10 and 15 cc in 0.1 cc increment were used in combination with the fraction collector for sample collection. The collection time period for each test tube was preset to suit different kind of test tubes. In addition to the pore volume calculation, the volume reading of each test tube could also be used to verify the flow rate of the pump.

### 4.2.5 Temperature Control System

Since all in-situ gelation experiments were performed at 50° C, the apparatus must be contained in a temperature controlled environment. A fiberglass hood with two heaters and a temperature unit was used in this study to perform the task. The dimension of the hood is 6 ft long by 5 ft high by 3 ft deep and it has a vertically sliding glass door providing the access

to the inside. Two heaters controlled by an Athena Model 4000-f temperature control unit were the heat sources of the air bath. A mercury thermometer was always attached to the sandpack holder during the experiments and the temperature control unit was adjusted according to the reading of thermometer to insure that the temperature at the sandpack holder was at the desired 50° C level.

## 4.3 Sandpack Characterization

### 4.3.1 Dispersion Test

A dispersion test using tritium as radioactive tracer in the brine(2% NaCl) was conducted as a check on sandpack homogeneity before it was used for in-situ gelation experiment.

Perkins et al. [59] described a method of calculating the longitudinal dispersion for one-dimensional single-phase miscible displacement from the experimental data of flowing a non-adsorbing solute tracer through the porous medium. A function $\lambda$ defined as

$$\lambda = \frac{t_D - 1}{\sqrt{t_D}} \tag{4.1}$$

was used by Perkins et al. [59] where $t_D$ = dimensionless time or pore volume. The plot of normalized tracer concentration against the function $\lambda$ on the probability scale yields a straight line and the longitudinal dispersion coefficient $\alpha_l$ can be calculated according to the following equation:

$$\alpha_l = L\left(\frac{\lambda_{90} - \lambda_{10}}{3.625}\right)^2 \tag{4.2}$$

where $L$ is the length of the porous medium, $\lambda_{90}$ and $\lambda_{10}$ are the values of $\lambda$ at 90% and 10% of the full strength tracer concentration respectively.

Typical examples of the breakthrough curves for tritium tracer in 100% brine(2% NaCl) saturated sandpacks and their corresponding $\lambda$ vs. normalized tracer concentration plots are presented in Figure 4.4 and Figure 4.5. The S-shaped tracer breakthrough curves indicate that the sandpacks tested are homogeneous. The results of the dispersion tests are summarized in Table 4.3.

### 4.3.2 Porosity and Permeability Measurements

The porosity and permeability must be determined before a sandpack could be used for in-situ gelation studies. The procedure employed in this study to determine the porosity of the sandpack is outlined as follows:

1. The empty holder with valves and fittings attached was weighed.
2. After the holder was completely packed with sand grains, it was weighed again and the amount of sand packed in the holder was determined by subtracting the weight of empty holder form the weight of packed holder.
3. The sandpack was then saturated with brine(2% NaCl) after being evacuated for 24 hours by a vacuum pump.

Table 4.3: Summary of the resulting $\alpha_l$ on sandpacks having different permeability before treatment

| Exp. No. | Dispersivity (cm) |
|---|---|
| EXP-5 | 0.110 |
| EXP-7 | 0.232 |
| EXP-9 | 0.234 |
| EXP-10 | 0.275 |
| EXP-11 | 0.119 |
| EXP-12 | 0.562 |
| EXP-15 | 2.901 |

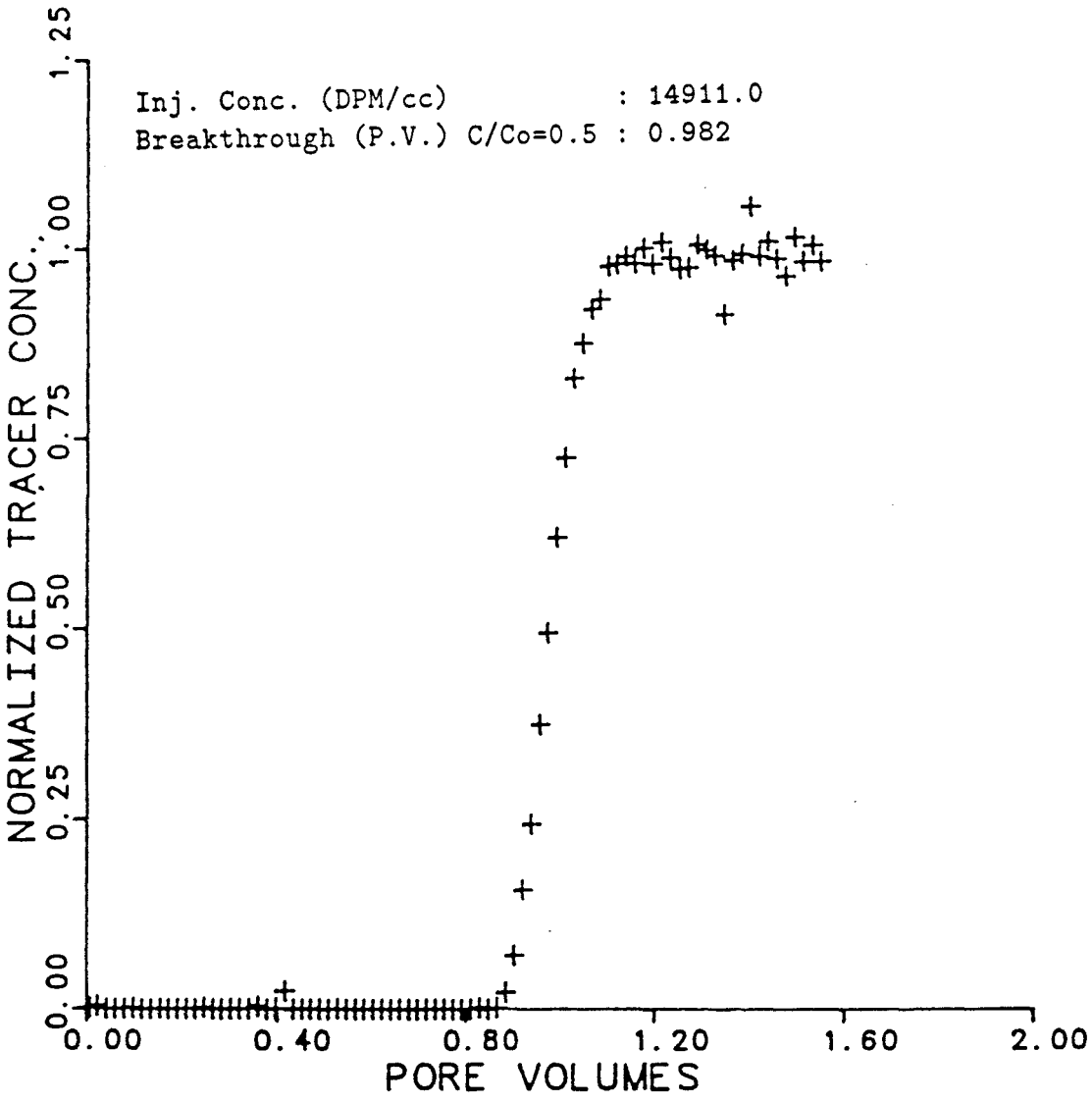


Figure 4.4: Tracer breakthrough curve of the sandpack used in EXP-5

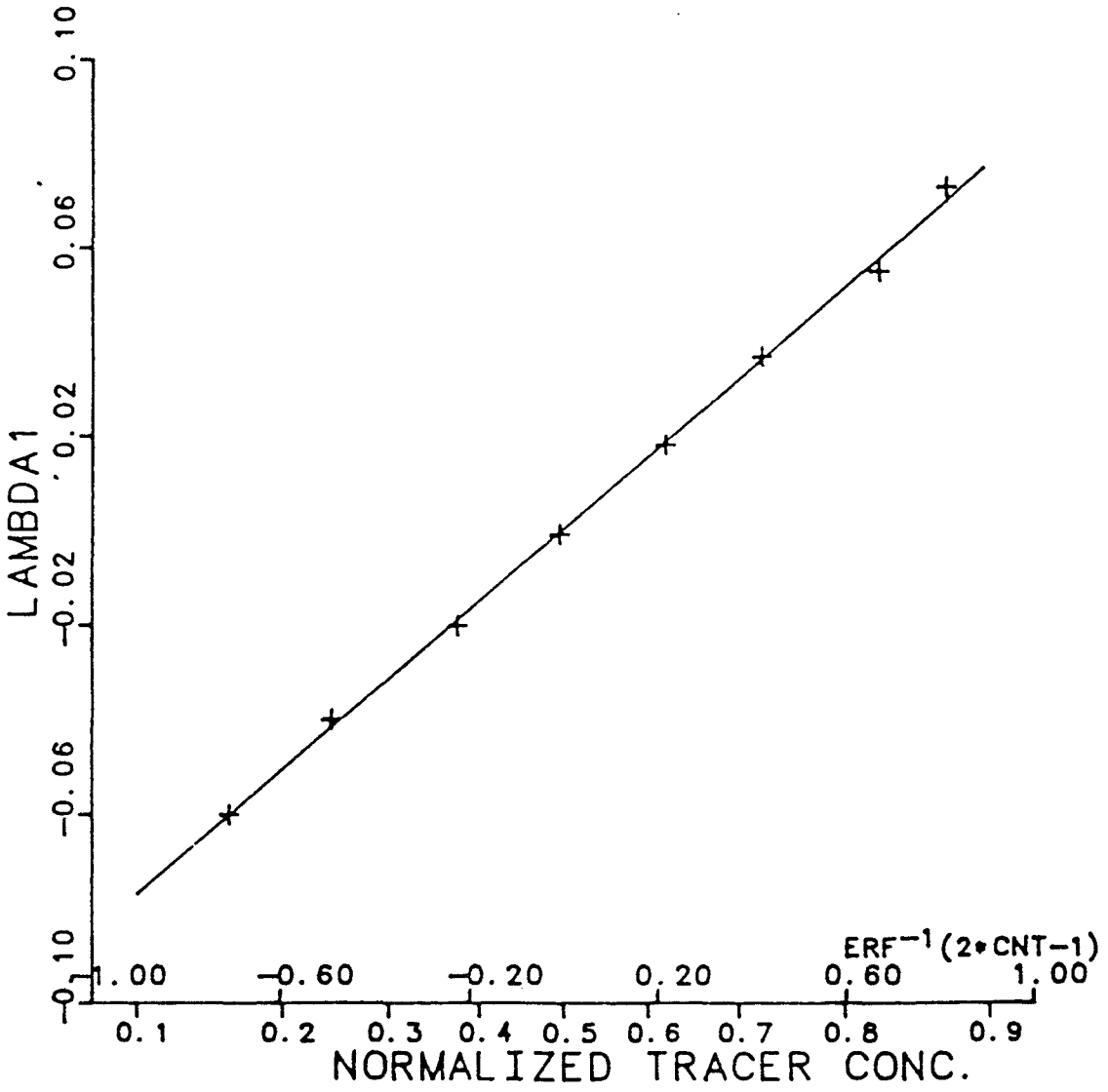


Figure 4.5: $\lambda$ vs. normalized tracer concentration plot of the sandpack used in EXP-5

4. The saturated pack was weighed and the weight of brine in the saturated pack was determined from the difference between the weight of sandpack before and after brine saturation.

5. The pore volume of the sandpack was calculated by subtracting the dead volume of the holder from the quotient of the weight and the density of brine.

6. The net volume occupied by sand grains was calculated by dividing the weight of the sand grains by the sand grain density. The bulk volume could thus be determined from the summation of pore volume and the net volume occupied by sand grains.

7. The porosity of the sandpack was determined from the ratio of pore volume to bulk volume.

The brine permeability of the sandpack was determined by pumping brine(2% NaCl) into the sandpack at a constant flow rate. After reaching steady state, the pressure drop across each section of the sandpack was measured and recorded. Darcy's law was then applied to calculate the permeability. The whole process was repeated at several different flow rates and the average value of the permeabilities estimated from different flow rates was taken as the permeability of the sandpack.

The porosity, permeability and other properties of the sandpacks used in the in-situ gelation studies are summarized in Table B.1 to Table B.7. Sandpacks having different initial permeabilities were used in the in-situ gelation studies to study the effect of permeability of the porous medium before treatment on the permeability reduction characteristic of the gelling solution.

## 4.4 Experimental Procedure

### 4.4.1 Experimental Strategy of Sandpack Flood Experiments

The experimental strategy employed in the in-situ gelation studies was aimed at the identification of the relationship between gel strength and the permeability reduction characteristic of the gelling solution.

The sandpack flood experiment was divided into four stages: preflush, gelling solution injection, shut-in, and postflush. In the first stage, the sandpack was conditioned to simulate the situation of a reservoir after waterflood. SONTEX 55 white mineral oil with the viscosity of 3.8 cps at 50°C was used in preconditioning the sandpack. In the second stage, up to two pore volumes of the gelling solution were injected into the sandpack to simulate the treatment process. In the third stage, the system was shut in to allow the gelling solution in the sandpack to mature. The length of the shut-in period varied depending upon the gelation time of the gelling solution involved. In the last stage, the system was flushed with brine and the residual permeability of the sandpack was measured after no more polymer could be detected in the effluent sample. The detailed procedure in each stage is outlined below:

- Stage One: Preflush

    1. The brine saturated sandpack was flooded with filtered mineral oil until no more brine was observed in the effluent solution.
    2. The sandpack was then flooded by brine solution until no more oil could be observed in the effluent solution.

- Stage Two: Gelling Solution Injection

    1. The gelling solution was prepared according the procedure described in Section 3.1.2.
    2. The gelling solution was introduced into the fluid reservoir and then placed in the temperature controlled air bath.
    3. The gelling solution injection was started one hour after the time of mixing and the pressure distribution along the sandpack was monitored throughout the injection process.
    4. The effluent solution was collected and immediately diluted to prevent it from gelling.
    5. Up to two pore volumes of gelling solution was pumped into the sandpack at an injection rate of 2 cc/min before the system shut-in.

- Stage Three: Shut-In

    1. The system was completely shut in and the system temperature was maintained at 50°C during the shut-in period.

- Stage Four: Postflush

    1. The brine injection was resumed after the conclusion of shut-in period.
    2. The effluent solution was also collected and diluted for effluent analysis.
    3. The brine postflush was continued until the polymer concentration in the effluent solution reached zero.

4. The residual permeability of the sandpack to brine was estimated at different flow rates and the average value was taken as the residual permeability.

### 4.4.2 Permeability Reduction Determination

The primary objective of the polymeric gel treatment is to modify the vertical conformance of a reservoir by selectively plugging the high permeability thief zones. Hence, the permeability reduction is the primary measure of the performance of a polymeric gel treatment.

The residual resistance factor $R_{RF}$ chosen in this study as the quantitative indicator of the permeability reduction effect caused by the polymeric gel treatment is defined as

$$R_{RF} = \frac{\lambda_i}{\lambda_f} \tag{4.3}$$

where $\lambda_i$ is the mobility of the brine before treatment and $\lambda_f$ is the mobility of the brine after treatment. Since the viscosity of the brine remains unchanged before and after treatment, the ratio of $\lambda_i$ to $\lambda_f$ can be reduced to the ratio of the brine permeability before treatment to the brine permeability after treatment. Hence, the extent of permeability reduction can be determined by comparing the permeability of the sandpack to brine after brine postflush with the permeability of the sandpack to brine before treatment.

The results of the in-situ gelation sandpack flood experiments are sum-

marized in Table 4.4. A significant amount of mineral oil was produced during the gelling solution injection period and the postflush period. The mineral oil saturations of the sandpacks at different stages of the experiments are listed in Table 4.5.

## 4.5 Effluent Analysis

In order to determine the amount of polymer and chromium cations retained in the sandpack after treatment, the effluent during the gelling solution injection and the postflush was collected in graduated test tubes for later analytical measurements. Since it is difficult to dissolve the gel after it is well developed, the effluent samples were immediately diluted to one fifth of the original concentration and stored at room temperature to prevent further gelation reaction.

### 4.5.1 Determination of Polyacrylamide Concentration

Foshee et al. [60] developed a general purpose analytical method for the determination of polyacrylamide concentration. The method utilizes the fact that the reaction between polyacrylamide and sodium hypochlorite (bleach) in an acid solution produces an insoluble white colloidal suspension and the turbidity produced by this reaction is a function of polyacrylamide concentration. Their test results also indicate that the turbidity was not sensitive to either the molecular weight or the degree of hydrolysis of the polyacrylamide and was capable of providing high accuracy over a wide concentration range.

The solution turbidity is time dependent as it first increases to a max-

Table 4.4: Summary of the results of the sandpack flood experiments

| Exp. No. | Gel System | Shut-in Time (hr.) | $G'$ $(dyne/cm^2)$ | $k_i$ (Darcy) | $R_{RF}$ |
|---|---|---|---|---|---|
| EXP-5 | GS-8 | 100 | $> 6000$ | 5.5 | $\sim \infty$ |
| EXP-7 | GS-1 | 100 | 18.99 | 4.7 | 1.21 |
| EXP-9 | GS-3 | 100 | 194.80 | 5.2 | 1.38 |
| EXP-10 | GS-7 | 100 | $> 6000$ | 6.2 | $\sim \infty$ |
| EXP-11 | GS-6 | 200 | 1128.00 | 5.5 | $\sim \infty$ |
| EXP-12 | GS-3 | 100 | 194.80 | 3.3 | 1.22 |
| EXP-15 | GS-3 | 100 | 194.80 | 1.4 | 1.52 |

Table 4.5: Summary of the mineral oil saturation of sandpacks at different stages of the in-situ gelation experiments

| Exp. No. | $S_o$ After Waterflood | $S_o$ After Gel Injection | $S_o$ After Postflush |
|---|---|---|---|
| EXP-5 | 0.203 | 0.169 | NA |
| EXP-7 | 0.210 | 0.190 | 0.190 |
| EXP-9 | 0.188 | 0.173 | 0.155 |
| EXP-10 | 0.215 | 0.208 | 0.08 |
| EXP-11 | 0.204 | 0.202 | NA |
| EXP-12 | 0.227 | 0.222 | 0.222 |
| EXP-15 | 0.207 | 0.200 | 0.200 |

imum then starts decreasing. The maximum absorbance was taken in this study as the measure of the polymer concentration. A Varian Cary 2300 UV-Visible-NIR Spectrophotometer was employed to measure the solution turbidity. All spectrophotometric readings were taken at 550 nm instead of 470 nm suggested by Foshee et al. [60] to prevent the interference of other chemicals involved. A calibration curve must be established so that the polyacrylamide concentration in the effluent samples could be determined from the absorbance readings recorded by the spectrophotometer. The procedure of using turbidity method to determine the effluent polyacrylamide concentration is outlined below:

1. Prepare 5N acetic acid and 25% sodium hypochlorite solutions.
2. Establish the calibration curve by measuring the maximum absorbance at 500, 400, 300, 200, and 100 ppm polyacrylamide concentration.
3. Dilute sample until the polymer concentration is within the range of the calibration curve.
4. Pipette 1 cc of polymer solution into a small cell.
5. Add 1 cc of 5N acetic acid solution into the cell and stir.
6. Add 1 cc of 25% sodium hypochlorite solution into the cell and stir gently.
7. Place the cell into the spectrophotometer and start recording until the maximum is reached.

Typical examples of the results of the measurements of polymer concentration in the effluent and postflush samples are presented in Figure 4.6 and Figure 4.7.

### 4.5.2 Determination of Total Chromium Concentration

Sodium dichromate was introduced into the gelling solution as the source of hexavalent chromium cations. During the progress of gelation, the hexavalent chromium cations were first reduced by a reducing agent to the trivalent state then crosslinked with polymer molecules to form the gel. The redox reaction involved the formation of many intermediate products and the detailed mechanism of the reaction was largely unknown. Since our concern was the amount of chromium retained in the porous medium after treatment, it was important to be able to determine the total chromium concentration in the effluent samples.

A Perkin-Elmer ICP/6500 Inductively Coupled Plasma System was used in this study to measure the total chromium concentration in the effluent samples. The system consists of a plasma torch housing, a RF power supply, a Model 5000 Spectrophotometer, and a Perkin-Elmer 7300 Professional Computer. The emission source is an inductively coupled, argon-supported plasma powered by the RF power supply. Liquid sample is introduced into the plasma through a nebulizer and reduced to the atomic state in the hot ionized gas. The resulting spectral transitions at wavelengths characteristic of the elements in the sample are reflected to the Model 5000 monochromator and detected. The PE 7300 Professional Computer together with the software

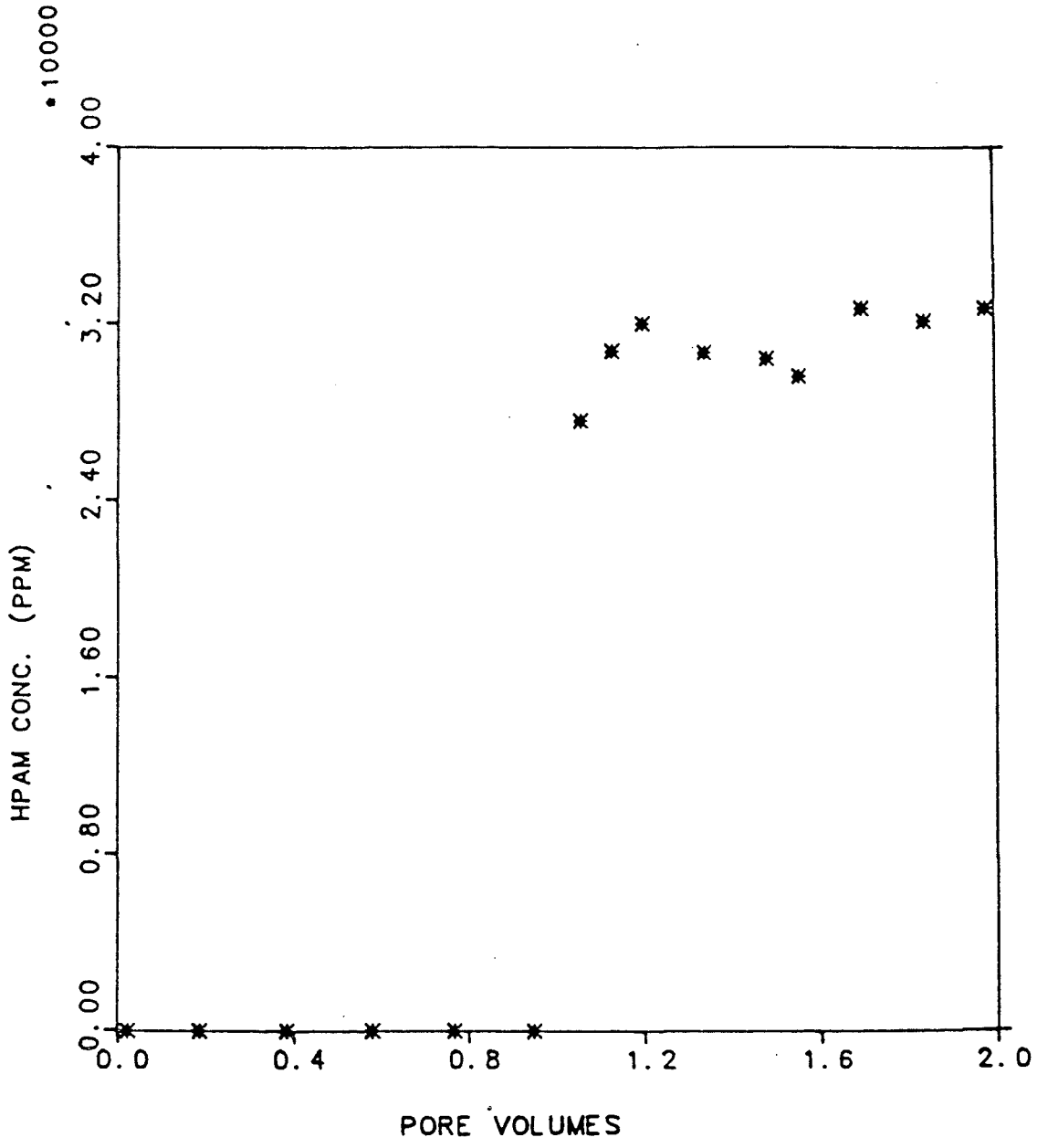


Figure 4.6: EXP-7 HPAM effluent concentration

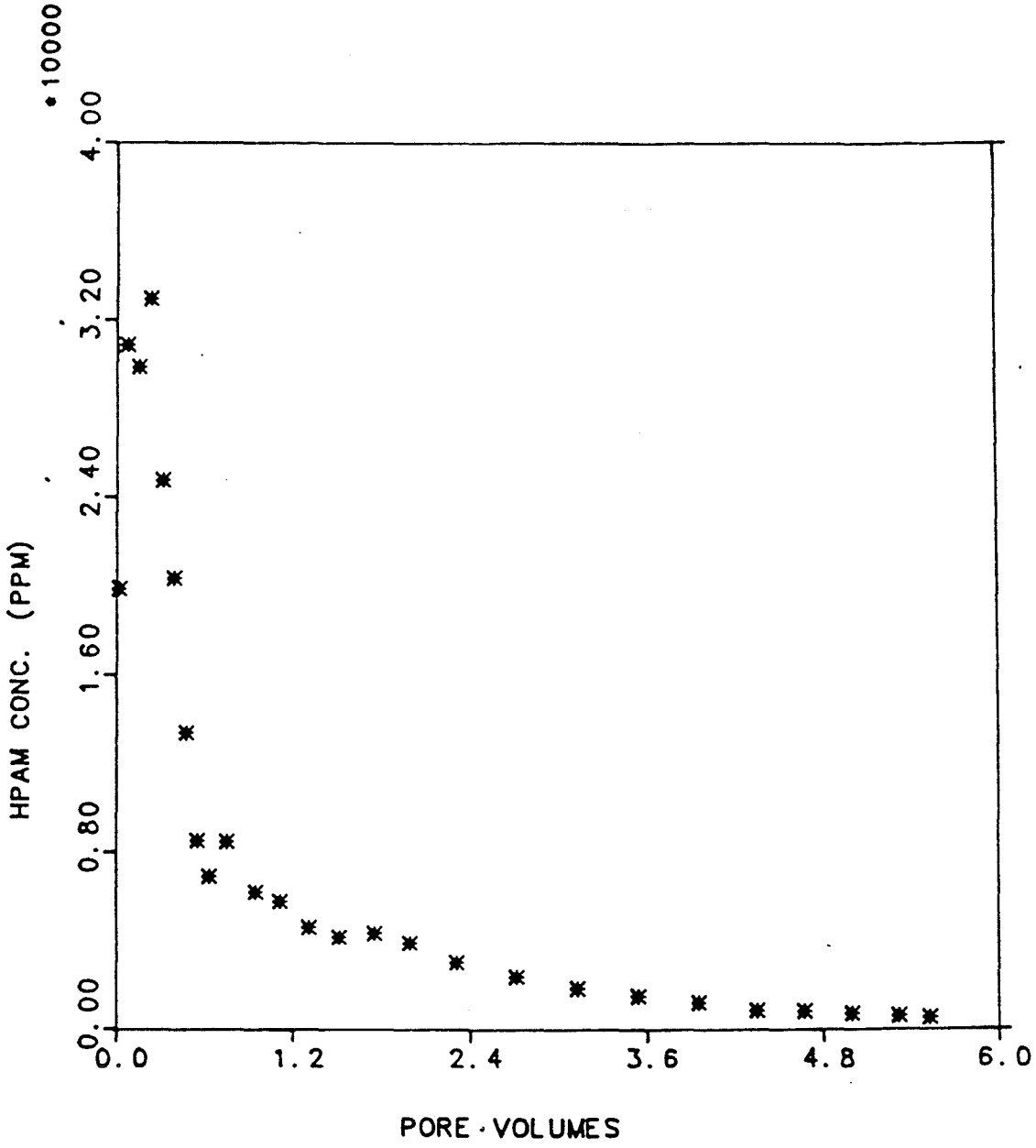


Figure 4.7: EXP-7 HPAM postflush concentration

provided by the manufacturer controls the operation of the whole system.

Three standards of 40, 20, and 10 ppm were used to establish the calibration curve and the effluent samples were diluted to within the calibrated range prior to the measurement. The chromium analysis was performed at the wavelength of 286.257 nm and the results were converted to the desired concentration unit by the computer. Typical examples of the results of the measurements of the chromium concentration in the effluent and postflush samples are shown in Figure 4.8 and Figure 4.9.

## 4.6 Yield Stress Measurements

Yield stress is an important property of a fully developed gel which determines the pressure gradient the gel can sustain without being displaced by the injecting fluid. In this study, the yield stress of a gel is defined as the minimum stress required to initiate the displacement. Assuming the gel moves as a plug after the yield point is reached [10], the yield stress of a gel can be determined from the pressure gradient required to initiate the flow in a tube according to the following equation:

$$\tau_w = \frac{D\Delta P}{4L} \tag{4.4}$$

where $\tau_w$ is the yield stress at the wall of the tube, $D$ is the inside diameter of the tube, $L$ is the length of the tube, and $\Delta P$ is the measured pressure gradient.

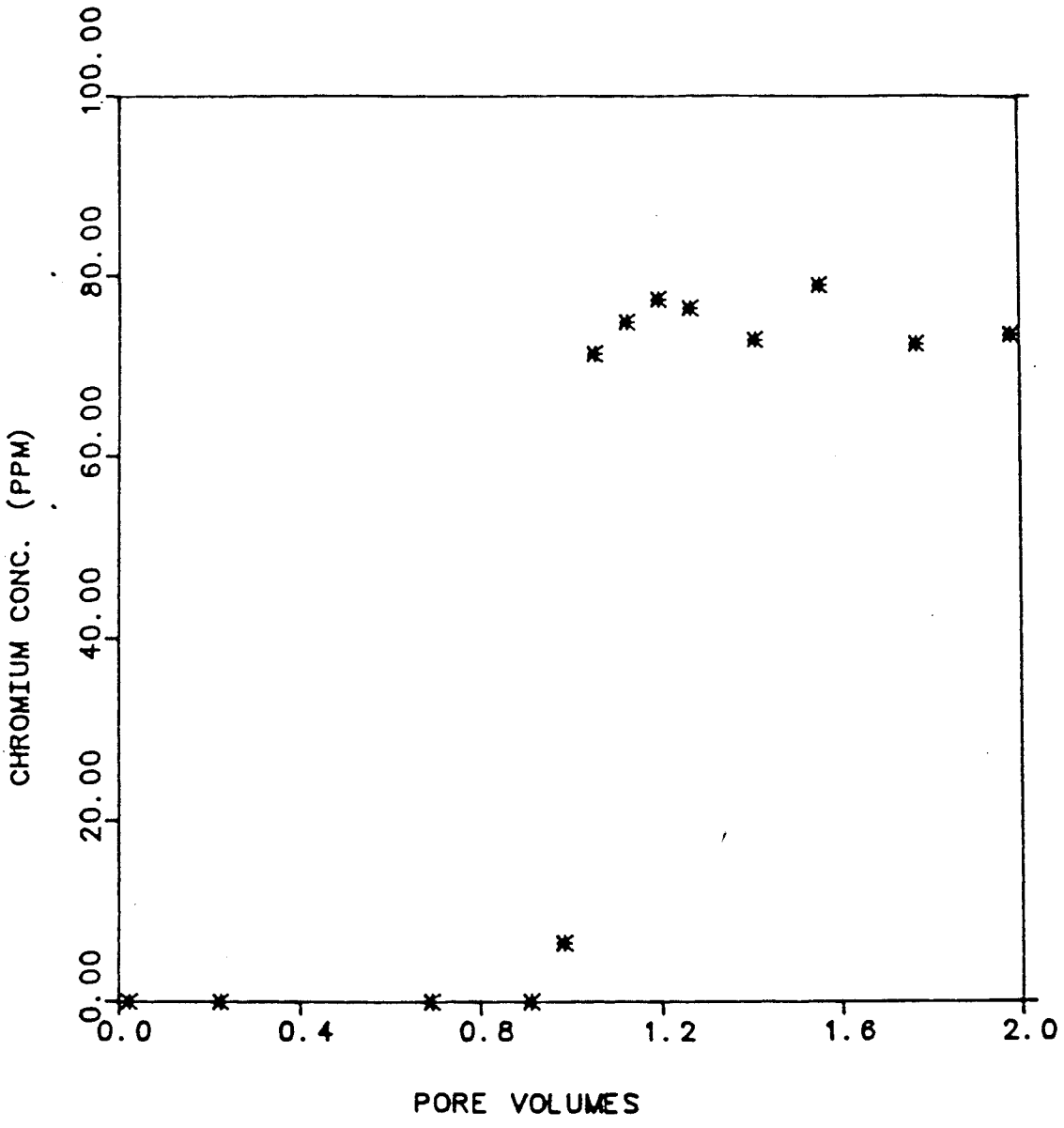


Figure 4.8: EXP-7 chromium effluent concentration

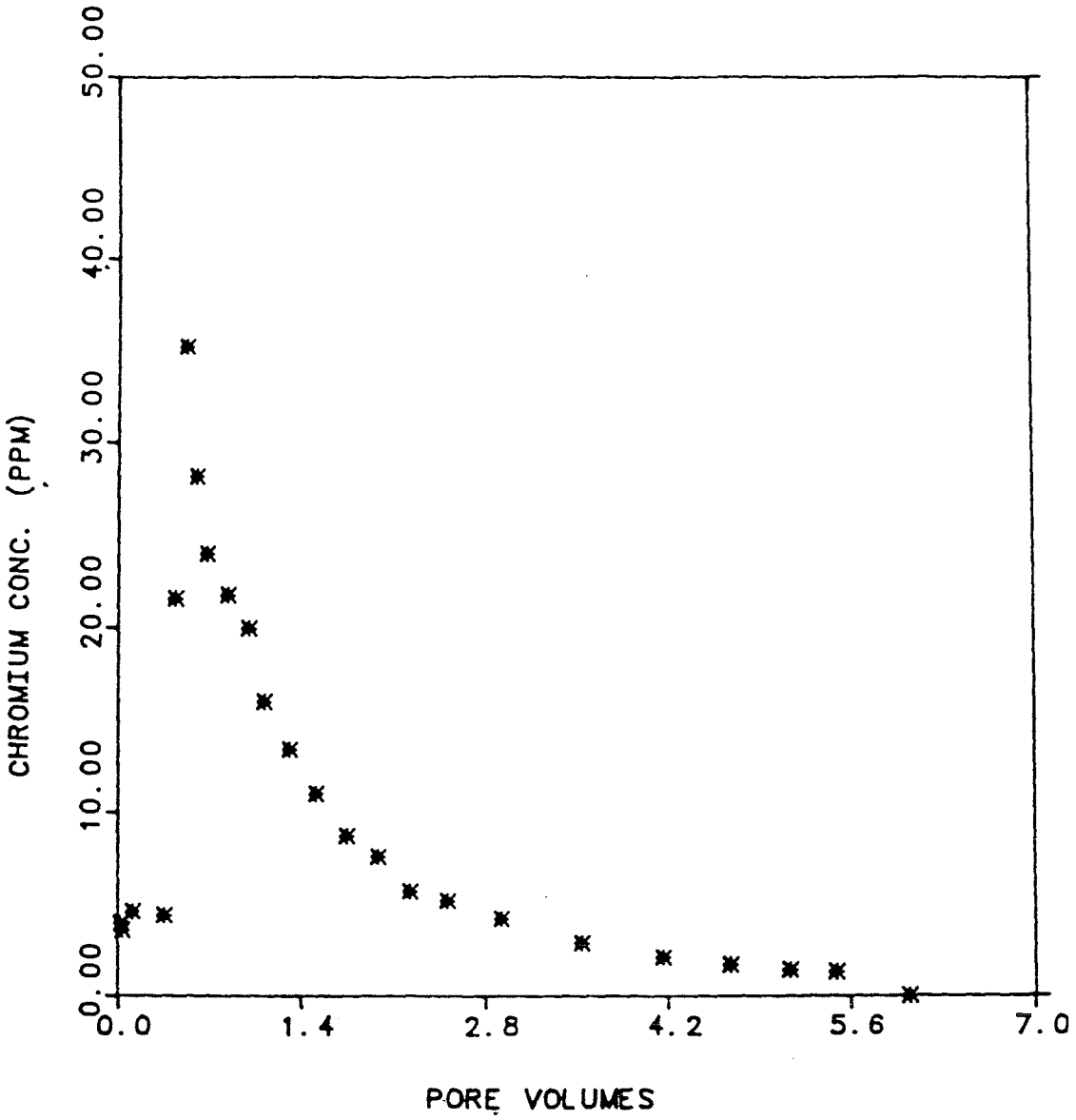


Figure 4.9: EXP-7 chromium postflush concentration

The tests were conducted in a 10-in long stainless steel tubing with an inner diameter of 0.05 in. The pressure gradient was monitored by a precision Heise pressure gauge. The whole set-up was placed in a temperature controlled air bath and the temperature was maintained at $50°C$ throughout the test period.

The gelling solution was first prepared according to the procedure described in Section 3.1.2 and then transferred into the stainless steel tubing. The tube loaded with gelling solution was allowed to rest in the air bath for the same amount of time as the shut-in period employed in the sandpack flood experiment before the test was conducted. Compressed nitrogen was employed to provide the necessary pressure gradient during the test period. The pressure was increased systematically in increments of 1 psi with an elapsed time of 30 sec between each increment to allow the system to attain equilibrium. A sudden pressure drop signifies the displacement of the gel in the tube. The pressure level at which a sudden pressure drop occurred was recorded and the yield stress of the gel was calculated using equation (4.4). The results of the yield stress measurements of different gelling solutions are presented in Table 4.6.

In order to estimate the actual pressure gradient needed to initiate the flow of a gel in the porous medium, a simple capillary tube model is employed. In this model, cylindrical pores of uniform cross section running from one end of the pore to another is assumed to constitute the porous medium. The average pore size of the porous medium is estimated from the following equation:

Table 4.6: Summary of the results of the yield stress measurements

| Gel System | HPAM | S.D. (ppm) | Reducing Agent (ppm) | $\Delta P$ (psig) | $\tau_w$ $(dyne/cm^2)$ |
|---|---|---|---|---|---|
| GS-3 | 3.3% | 400 | S.T.: 500 | 9.0 | 775.8 |
| GS-4 | 3.3% | 500 | S.T.: 625 | 11.5 | 991.3 |
| GS-5 | 3.3% | 600 | S.T.: 750 | 24.0 | 2068.8 |
| GS-7 | 3.3% | 750 | T.: 750 | 31.5 | 2715.3 |
| GS-8 | 3.3% | 1000 | T.: 1000 | 33.0 | 2844.6 |

HPAM: Partially Hydrolyzed Polyacrylamide

S.D.: Sodium Dichromate

S.T.: Sodium Thiosulfate

T. : Thiourea

$$k = \frac{\phi r^2}{8\tau} \tag{4.5}$$

where $k$ is the permeability, $\phi$ is the porosity, $r$ is the radius of the pore, and $\tau$, the tortuosity, is the squared ratio of the capillary tube length to the length of the porous medium. The tortuosity is assumed to be three in this study. The actual pressure gradient needed to initiate the flow of a gel in a sandpack can then be calculated by using equation (4.4).

# Chapter 5

# Discussion of Results

## 5.1 Effect of Reducing Agents on Gelation Time and Gel Strength

Three different reducing agents, sodium bisulfite, sodium thiosulfate, and thiourea were tested in this study. Table 5.1 is the summary of the gelation time and gel strength of the gelling solutions involved. The results reveal that with the comparable concentration combination the gelation times of the gelling solutions using sodium bisulfite, sodium thiosulfate and thiourea increased in the respective order. The greater than 6000 $dyne/cm^2$ gel strength found in Table 5.1 indicates that the gel strength of the corresponding gel exceeds the maximum scale of the rheometer used. Since the less than ten minute gelation time of the gelling solutions using sodium bisulfite as reducing agent was too short for our purpose, no further tests were conducted on these gelling solutions.

It is obvious from the results listed in Table 5.1 that the final gel strength($G'$) of a gelling solution using thiourea as reducing agent is generally stronger than a comparable gelling solution using sodium thiosulfate as reducing agent. Since the polyacrylamide polymer used in this study is in the partially hydrolyzed form having anionic carboxyl groups scattered along

the main chain, the repulsion between polymer molecules and segments of the same molecule as the result of the presence of the negatively charged anionic carboxyl groups accounts for the higher viscosity of the partially hydrolyzed polymacrylamide polymer (HPAM)[45]. The same inter- and intra-molecular repulsion forces prevent the polymer molecules from moving freely in the solution, which in turn limit the number of available crosslinking sites to trivalent chromium cations. Olatunji et al.[51] studied the redox reaction between thiourea and . They discovered that thiourea molecules were first oxidized to dimers by reacting with dichromate, and the dimers then formed different complexes with trivalent chromium cations and water molecules. The additional ionic shielding provided by these complex ions reduces the repulsion between polymer molecules. Consequently, the crosslinking density of gelling solutions using thiourea as reducing agent may be higher than the comparable gelling solutions using sodium thiosulfate as reducing agent.

The results summarized in Table 5.1 also reveal that while using the same kind of reducing agent, higher redox concentration results in stronger gel strength and shorter gelation time. Hence, the control of gel strength and gelation time combination of a gelling solution can be accomplished by carefully selecting the type and concentration of the redox system involved.

The result of curve fitting shown in Figure 5.1 indicates that the gel strength of a gelling solution using sodium thiosulfate as reducing agent is linearly proportional to the logarithm of the corresponding sodium dichromate concentration with a correlation coefficient $R = 0.98$. This indicates that, within the concentration range studied, the increase of redox concentration of a gelling solution using sodium thiosulfate as reducing agent has a more

Table 5.1: Compositions of the gelling solutions and summary of the results of the gelation studies of these gelling solutions

| Gel System | HPAM | S.D. (ppm) | Reducing Agent (ppm) | Gelation Time (hr.) | $G'$ $(dyne/cm^2)$ |
|---|---|---|---|---|---|
| GS-1 | 3.3% | 300 | S.T.: 400 | 55.0 | 18.99 |
| GS-3 | 3.3% | 400 | S.T.: 500 | 30.0 | 194.80 |
| GS-4 | 3.3% | 500 | S.T.: 625 | 17.0 | 236.80 |
| GS-5 | 3.3% | 600 | S.T.: 750 | 12.0 | 314.20 |
| GS-6 | 3.3% | 600 | T.: 600 | 79.0 | 1128.00 |
| GS-7 | 3.3% | 750 | T.: 750 | 56.0 | $> 6000$ |
| GS-8 | 3.3% | 1000 | T.: 1000 | 32.0 | $> 6000$ |
| GS-9 | 3.3% | 1500 | S.B.: 1500 | $< 0.2$ | NA |
| GS-10 | 2.0% | 1500 | S.B.: 1500 | $< 0.2$ | NA |

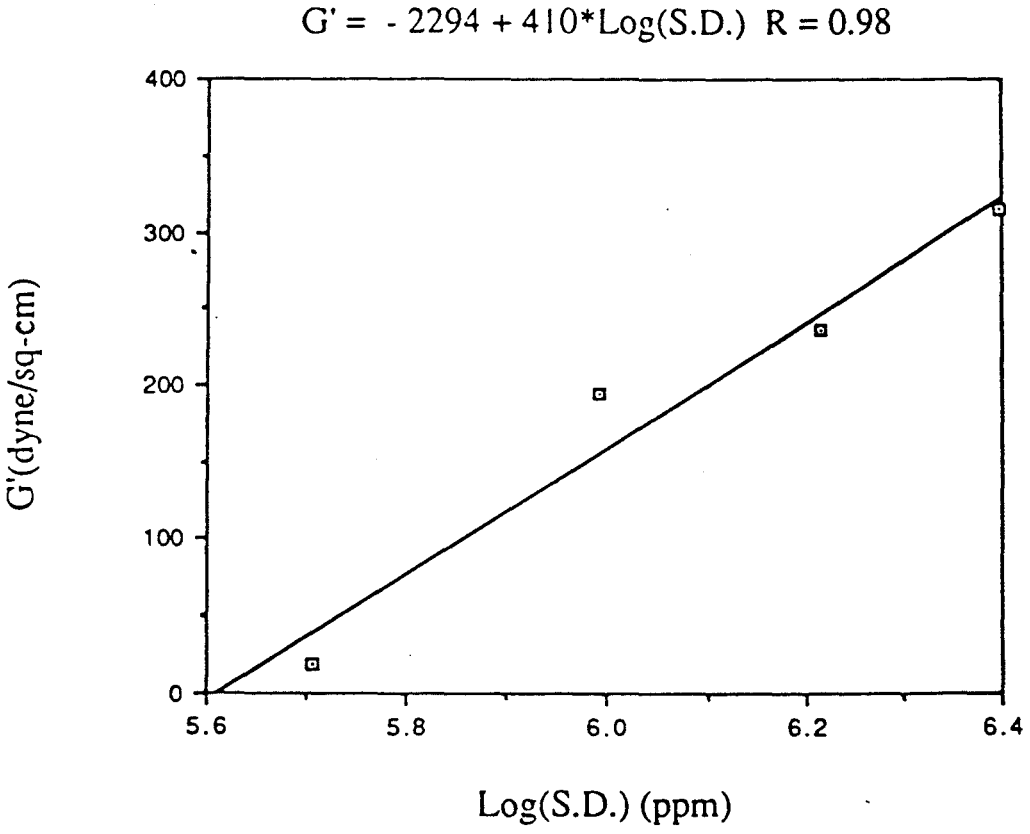


Figure 5.1: Functional relationship between gel strength and redox concentration of gel systems using sodium thiosulfate as reducing agent

profound effect on its final gel strength at the lower end of the concentration range than at the higher end of the concentration range.

## 5.2 Effect of Gel Strength on Permeability Reduction

In order to study the correlation between gel strength of a gelling solution and its permeability reduction characteristic, gelling solutions with a wide range of gel strength were tested in sandpacks having approximately the same average permeabilities.

Table 5.2 presents a summary of the extent of permeability reduction and the gel strength of the gelling solutions involved in the in-situ gelation studies. The results indicate that the residual resistance factor, which is a measure of the degree of permeability reduction after treatment, increased with increasing gel strength. Up to this point, no quantitative correlation between gel strength and permeability reduction can be identified.

However, the results indicate that for weak gels having gel strength less than 200 $dyne/cm^2$, the extent of permeability reduction remains low and the increase of $R_{RF}$ is slow with increasing gel strength. For strong gels having gel strength greater than 1000 $dyne/cm^2$, complete plugging of the sandpacks was observed. A pressure buildup on the order of a hundred $psi$ was detected by the analog pressure gauge on the pump before the weak gel started to flow. The pump output pressure then decreased and eventually leveled off when the steady state was reached. The actual pressure gradients needed to initiate the flow of gel were not recorded. Table 5.3 presents the pressure gradients needed

Table 5.2: Summary of the resulting $R_{RF}$ of in-situ gelation experiments and the gel strength of the corresponding gels

| Exp. No. | Gel System | Shut-in Time (hr.) | $G'$ $(dyne/cm^2)$ | $R_{RF}$ |
|---|---|---|---|---|
| EXP-7 | GS-1 | 100 | 18.99 | 1.21 |
| EXP-9 | GS-3 | 100 | 194.80 | 1.38 |
| EXP-11 | GS-6 | 200 | 1128.00 | $\sim \infty$ |
| EXP-10 | GS-7 | 100 | $> 6000$ | $\sim \infty$ |
| EXP-5 | GS-8 | 100 | $> 6000$ | $\sim \infty$ |

to start the flow of the gel in sandpacks of the gelling solutions involved in the in-situ gelation studies. These values are calculated from the yield stress of each individual gelling solution according to the procedure described in Section 4.6. Since the maximum output pressure of the pump was set at the limit of the experimental set-up of 800 *psi*, it is clear that the complete plugging of the sandpacks by the gelling solutions having strong gel strength can be attributed to the maximum pump output pressure being smaller than the pressure gradients needed to start the flow of the gels. Consequently, in order to penetrate deep into the reservoir and seal off the high permeability thief zones, a gelling solution using thiourea as reducing agent is preferred due to its long gelation time and strong yield strength. However, a gelling solution using sodium thiosulfate as reducing agent is recommended when shorter treatment distance and partial plugging of target zones are desired.

## 5.3 Effect of Initial Sandpack Permeability on Permeability Reduction

In order to study the effect of initial permeability of porous medium on the permeability reduction characteristic of a gelling solution, in-situ gelation experiments using the same gelling solution were performed on sandpacks having different initial permeabilities. Table 5.4 is a summary of the extent of permeability reduction of sandpacks having different initial permeabilities after treated with the same gelling solution. The gelling solution consisted of 3.3% HPAM, 2% NaCl, 400ppm sodium dichromate, and 500ppm sodium thiosulfate. The results are inconclusive with no obvious correlation between initial permeability and the extent of Permeability reduction.

Table 5.3: Summary of the pressure gradients needed to initiate the flow of the gels involved in sandpack flood experiments

| Exp. No. | Gel System | $\Delta P(psig)$ | $R_{RF}$ |
|---|---|---|---|
| EXP-9 | GS-3 | 330 | 1.38 |
| EXP-12 | GS-3 | 410 | 1.22 |
| EXP-15 | GS-3 | 590 | 1.52 |
| EXP-10 | GS-7 | 1140 | $\sim \infty$ |
| EXP-5 | GS-8 | 1050 | $\sim \infty$ |

Table 5.4: Summary of the resulting $R_{RF}$ on sandpacks having different permeability before treatment

| Exp. No. | Gel System | Shut-in Time (hr.) | $k_i$ (Darcy) | $R_{RF}$ |
|---|---|---|---|---|
| EXP-9 | GS-3 | 100 | 5.2 | 1.38 |
| EXP-12 | GS-3 | 100 | 3.34 | 1.22 |
| EXP-15 | GS-3 | 100 | 1.42 | 1.52 |

## 5.4 Behavior of Gelling Solution during Injection Period

The sandpack holder used in this study has five equally spaced pressure taps and the pressure drops across each section of the sandpack were monitored continuously throughout the gelling solution injection period. The pressure drops across each section of the sandpack were plotted against the number of pore volumes of gelling solution injected and the results are shown in Figure 5.2 to Figure 5.5. Since the gelation process of the gelling solution was delayed by the redox reaction, the behavior of gelling solution during the injection period was similar to polymer flooding. The pressure drops across each section of the sandpack increased when the injection front was passing through and it leveled after the steady state was reached.

Huang et al. [26] reported that the shear force imposed on the gelling solution during the injection period of a sandpack flood experiment tends to accelerate the gelation process. Their results also reveal that due to the longer period of the gelling solution being exposed under shear the rate of gelation reaction increases with increasing distance from the entrance of the sandpack. The results shown in Figure 5.2 confirmed Huang's observation. The plot shows that the onset of gelation, indicated by the sharp increase of pressure drop, at section four occurred earlier than those sections closer to the entrance. However, for gelling solutions having longer gelation time, the acceleration of the gelation process due to the shear effect could not be observed during the relatively short injection period. This explains why this phenomenon was not observed in other in-situ gelation studies.

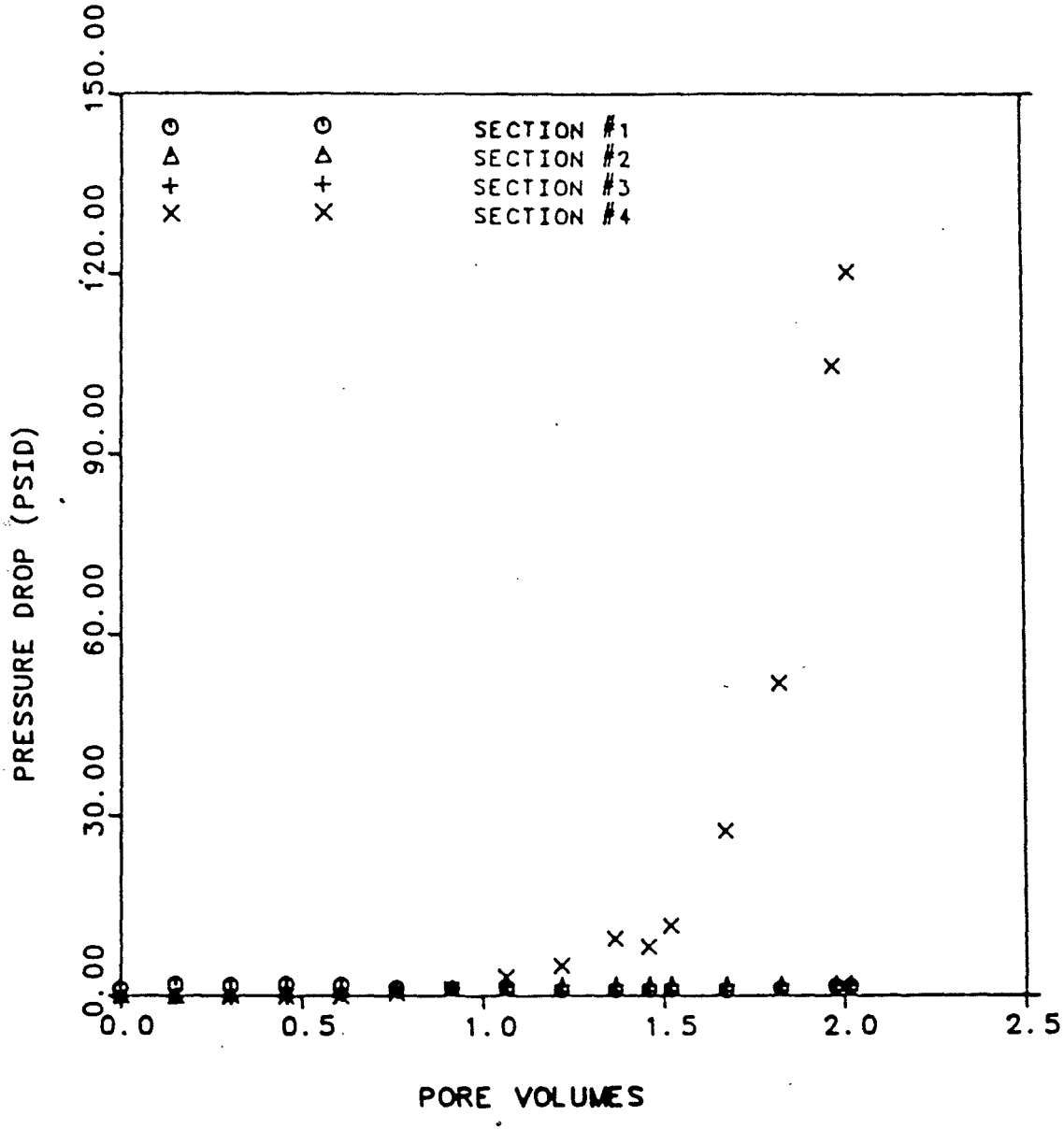


Figure 5.2: Pressure drop versus amount of gelling solution injected in pore volumes(EXP-5)

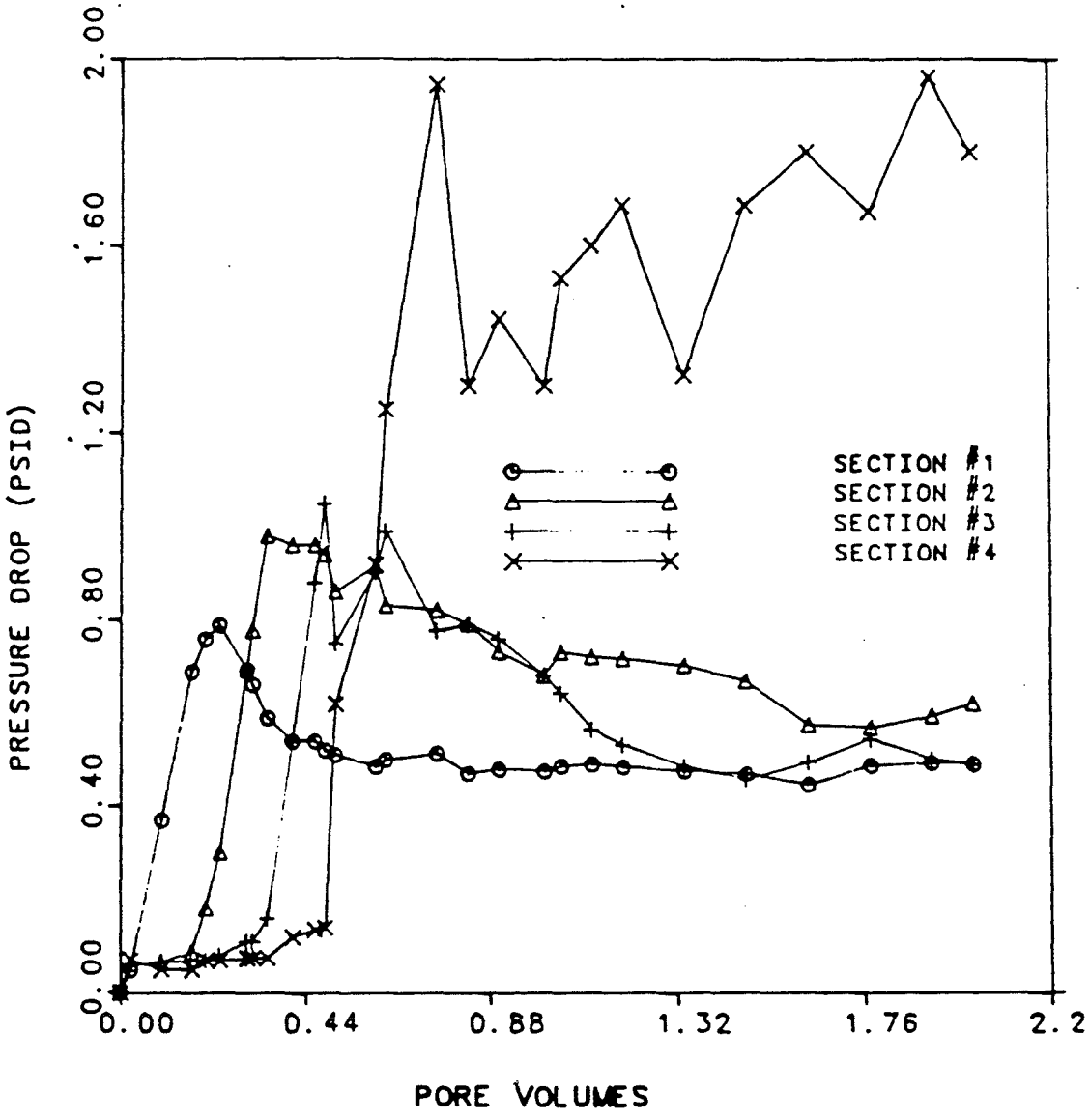


Figure 5.3: Pressure drop versus amount of gelling solution injected in pore volumes(EXP-7)

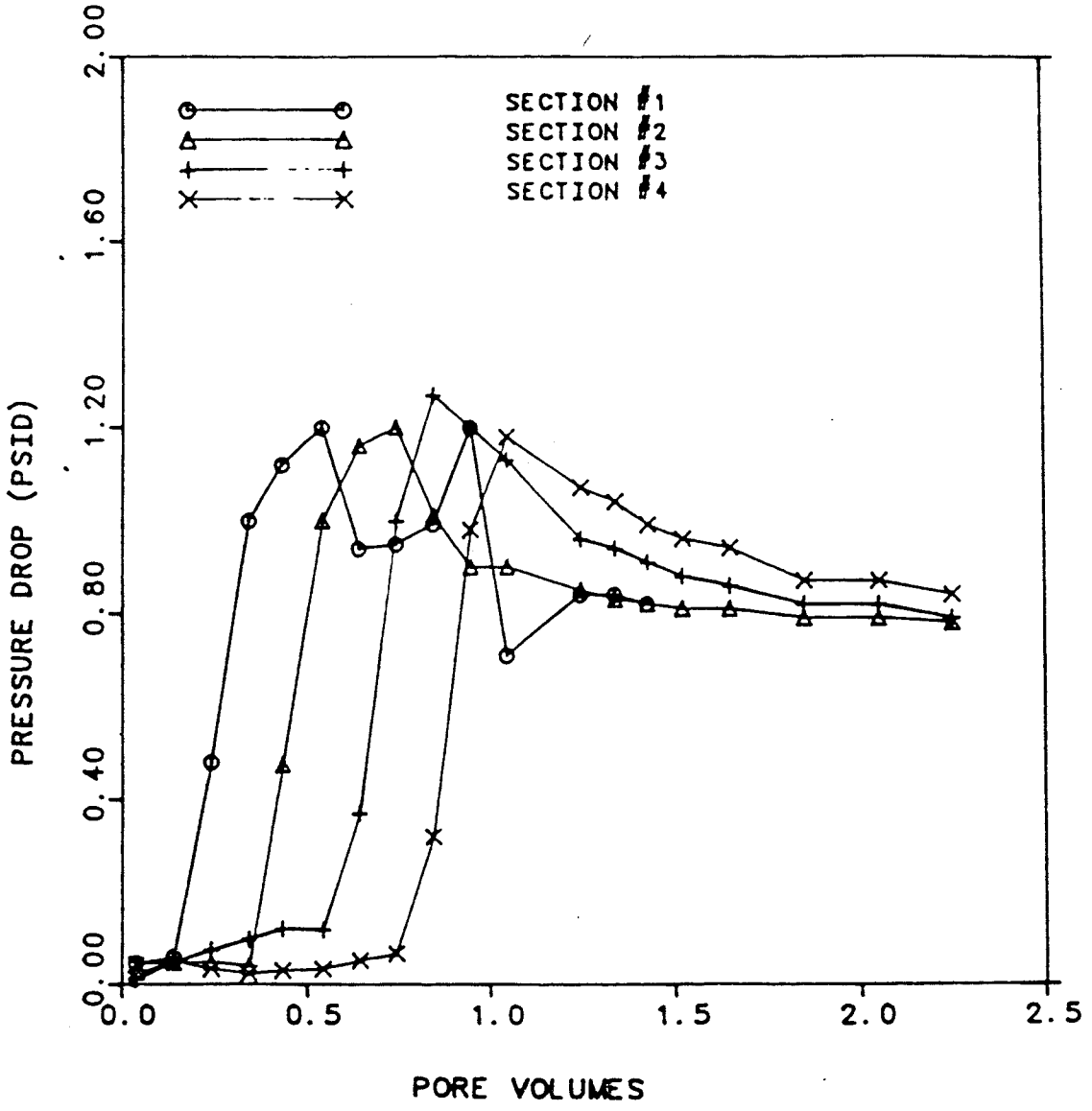


Figure 5.4: Pressure drop versus amount of gelling solution injected in pore volumes(EXP-12)

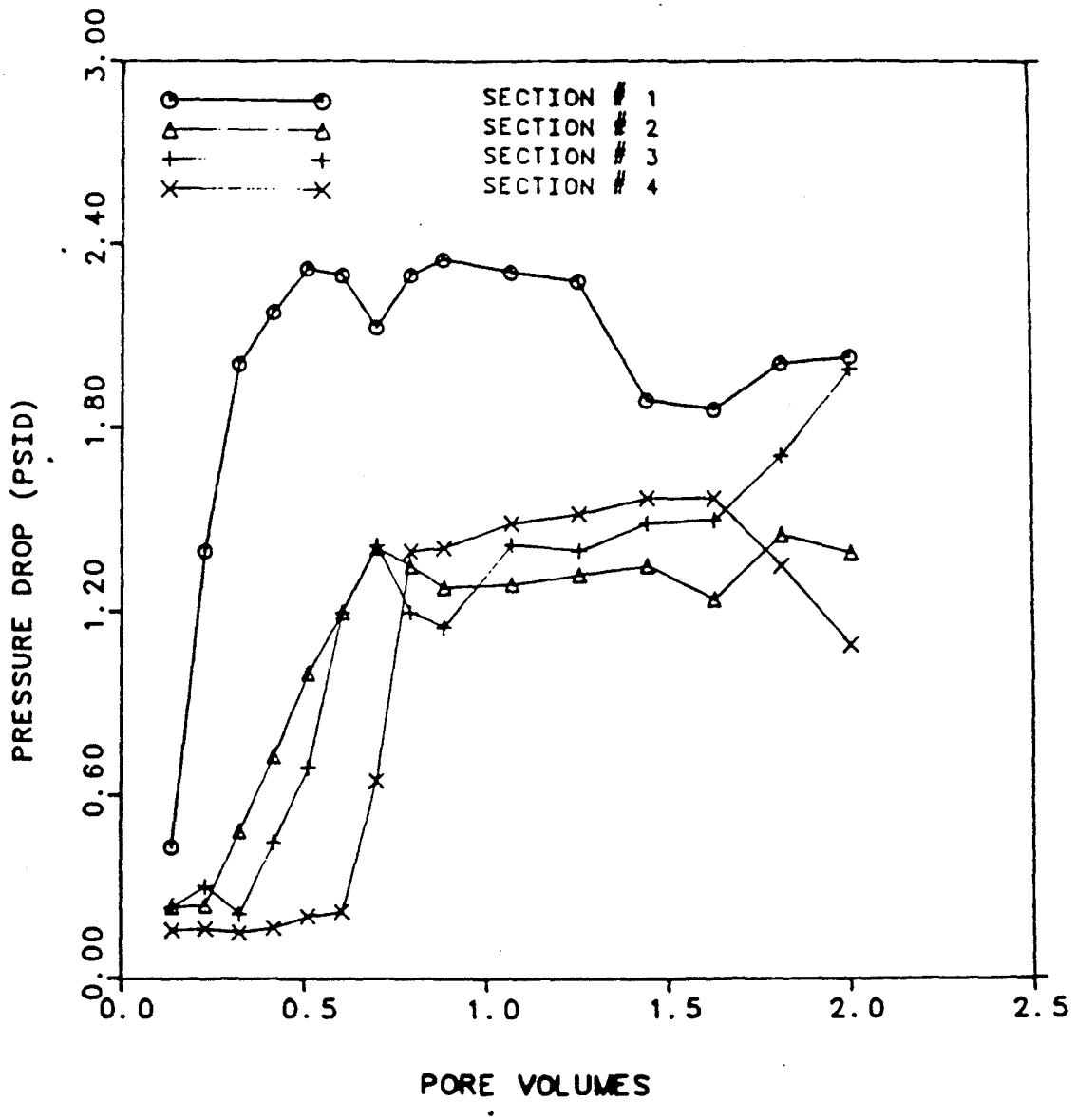


Figure 5.5: Pressure drop versus amount of gelling solution injected in pore volumes(EXP-15)

## 5.5 Polymer and Chromium Retention after Treatment

Table 5.5 presents the summary of the level of retention of polyacrylamide, chromium and the corresponding degree of permeability reduction after postflush. The results show that for the in-situ gelation studies using sandpacks having approximately the same average initial permeability, more polymer and chromium being retained results in higher level of permeability reduction and the ratio of the amount of polymer retained to the amount of chromium retained was found to be about 70 to 1 regardless of the degree of permeability reduction and the type of reducing agent used.

Since $Cr^{+3}$ has a coordination number of six, assuming that all the hexavalent chromium cations were reduced to the trivalent state and crosslinked only with carboxyl groups, the stoichiometry of the crosslinking reaction between the partially hydrolyzed polyacrylamide polymer and $Cr^{+3}$ is six moles of carboxyl group per mole $Cr^{+3}$. The theoretical weight ratio of the amount of polymer to the amount of $Cr^{+3}$ involved in the crosslinking process can be calculated from the reaction stoichiometry and the degree of hydrolysis of the polymer. The degree of hydrolysis of the polyacrylamide polymer employed in this study is 10%. The theoretical weight ratio calculated according to the reaction stoichiometry and the degree of hydrolysis of the polymer is 82 to 1. The ratios of the amount of polymer retained to the amount of chromium retained after the postflush stage of the in-situ gelation experiments being lower than the theoretical ratio can be attributed to less carboxyl groups being able to crosslink with $Cr^{+3}$.

The results also reveal that for the same gelling solution, lower initial permeability results in lower ratio of the retention of polymer to that of chromium. The results are inconclusive and no satisfactory explanations can be found for this behavior.

## 5.6 Effect of Redox Concentration on Rate of Gelation Reaction

From the theory of rubber elasticity modified by Graessley [53], the relationship between the gel strength, $G'$ and the crosslinking density, n, is given by

$$G' = gnKT + G_{en} \tag{5.1}$$

where $g$ is a constant [61], $K$ is the Boltzmann constant, $T$ is the absolute temperature, and $G_{en}$ is the contribution of temporary chain entanglement to the storage modulus.

Since $G_{en}$ is very small in dilute polymer, the time rate of change of $G'$ is linearly proportional to the time rate of change of crosslinking density.

$$\frac{dG'}{dt} = gKT\frac{dn}{dt} \tag{5.2}$$

This relationship provides a way of determining the rate of buildup of a three dimensional gel structure from the time rate of change of $G'$.

Prud'homme et al. [32] studied the effect of polymer and redox concentration on the rate of buildup of gel structure by plotting the maximum rate of gelation against the polymer and redox concentration logarithmically.

The same scheme used by Prud'homme et al. [32] was employed in this study to analyze the effect of redox concentration on the rate of gel structure buildup. For the gelling solutions using sodium thiosulfate and thiourea as reducing agents, plots of the maximum rate of change of storage modulus versus the concentration of sodium dichromate on a logarithm scale are shown in Figure 5.6 and Figure 5.7. The plot shown in Figure 5.6 suggests that within the concentration range studied, the effect of redox concentration of the gelling solution using sodium thiosulfate as reducing agent on the rate of gel structure buildup is different at the low redox concentration range from that at the high redox concentration range. The slope from Figure 5.6 suggests that while holding the polymer concentration constant, the kinetic expression of the gelling solution using sodium thiosulfate as reducing agent having redox concentration higher than 400 ppm is given by

$$\left(\frac{dn}{dt}\right)^{\cdot}_{max} = kC^{0.8}_{S.D.}. \tag{5.3}$$

For gelling solutions having redox concentration lower 400 ppm, the slope from Figure 5.6 indicates that the kinetic rate expression is given by

$$\left(\frac{dn}{dt}\right)_{max} = kC_{S.D.}^{8.4}. \tag{5.4}$$

Figure 5.7 reveals that the effect of changing of redox concentration of the gelling solution using thiourea as reducing agent on the rate of gel structure buildup is given by

$$\left(\frac{dn}{dt}\right)_{max} = kC_{S.D.}^{5.6}. \tag{5.5}$$

The results of the kinetic studies performed by Prud'homme et al. [32] suggest that the initial rate of gel formation for the gel consisting of an anionic polyacrylamide, sodium dichromate as the source of $Cr^{+6}$, and sodium bisulfite as reducing agent is second order in both polymer and chromium concentration.

Southard et al. [29] studied the reaction kinetics of the redox reaction between dichromate and thiourea in the presence of polyacrylamide by monitoring the solution color change during the reduction of $Cr^{+6}$ into $Cr^{+3}$. Their results suggest that the kinetics of the redox reaction in the presence of polyacrylamide polymer is first order in dichromate, thiourea, and hydrogen ions.

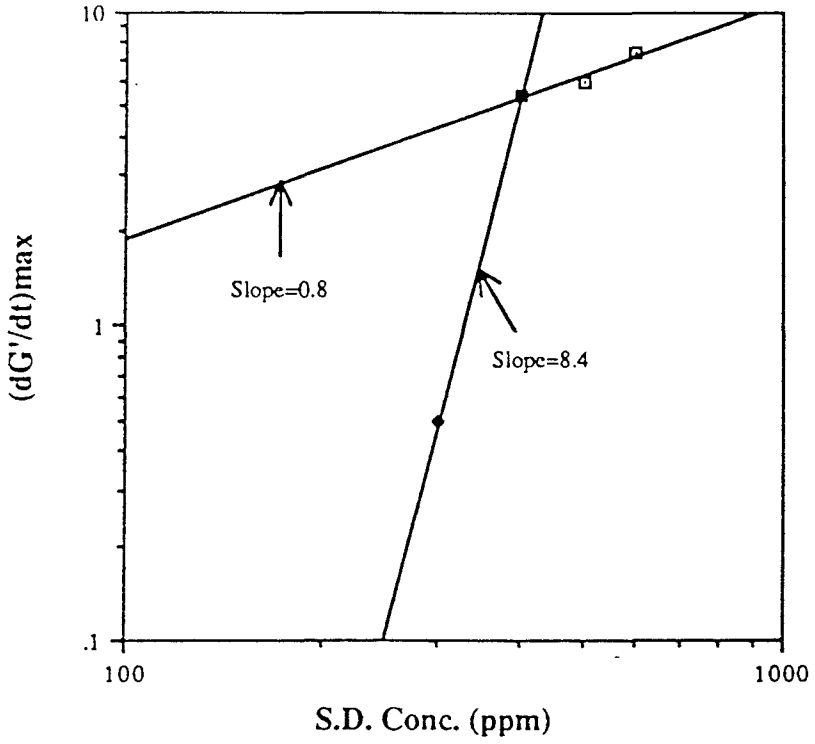


Figure 5.6: The rate of change of storage modulus vs. redox concentration on the logarithm scale of gel systems using sodium thiosulfate as reducing agent

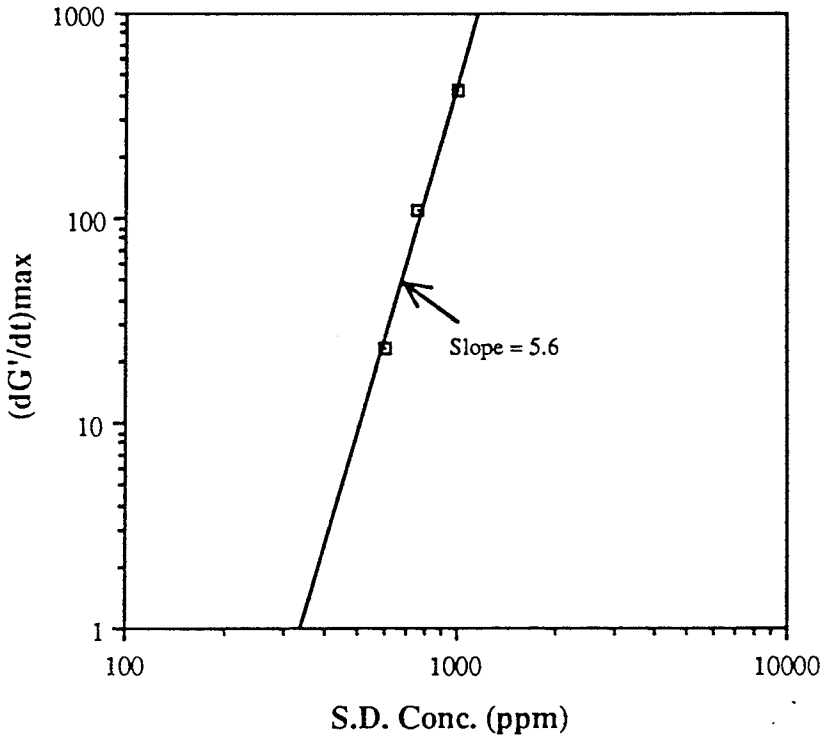


Figure 5.7: The rate of change of storage modulus vs. redox concentration on the logarithm scale of gel systems using thiourea as reducing agent

Table 5.5: Summary of the $R_{RF}$ and the resulting HPAM and Chromium retention

| Exp. No. | $R_{RF}$ | Amt. Retnd.($\mu$g/g) HPAM | Amt. Retnd.($\mu$g/g) Chromium | Amt. Retnd.(HPAM)/ Amt. Rtnd.(Chromium) |
|---|---|---|---|---|
| EXP-7 | 1.21 | 1029.9 | 15.36 | 67.05 |
| EXP-9 | 1.38 | 1309.8 | 17.12 | 76.49 |
| EXP-10 | $> 6000$ | 4225.3 | 58.37 | 72.39 |
| EXP-12 | 1.22 | 341.6 | 17.12 | 19.95 |
| EXP-15 | 1.52 | 299.6 | 17.07 | 17.55 |

# Chapter 6

# Conclusions and Recommendations

## 6.1 Conclusions

The following conclusions are drawn from the results of gelation and rheological studies of the polyacrylamide/chromium gel system employed in this project.

1. The gelation time of a gelling solution decreases with increasing polymer, chromium and reducing agent concentration.

2. With a comparable concentration combination, the gelation times of the gelling solutions using sodium bisulfite, sodium thiosulfate, and thiourea as reducing agents increases in the respective order.

3. The dynamic oscillatory testing technique is found to be an effective tool in studying the buildup of three dimensional gel structure.

4. The gel strength of a gelling solution using thiourea as reducing agent is stronger than a comparable gelling solution using sodium thiosulfate as reducing agent.

5. For gelling solutions using the same kind of reducing agent, higher chromium concentration results in stronger gel strength and shorter gelation time.

6. The gelation time and gel strength combination of a gelling solution can be controlled by carefully selecting the type and concentration of the redox system employed.

7. The gel strength of a gelling solution using sodium thiosulfate as reducing agent is linearly proportional to the logarithm of the corresponding sodium dichromate concentration.

8. The effect of changing of chromium concentration of the gelling solution using sodium thiosulfate as reducing agent on the rate of gel structure buildup is different at the low chromium concentration range from that at the high chromium concentration range.

The following conclusions are drawn from the results of in-situ gelation studies of the polyacrylamide/chromium gelling solution system employed in this project.

1. The extent of permeability reduction after treatment increases with increasing gel strengths of the gelling solution system involved.

2. For weak gel systems having gel strength less than 200 $dyne/cm^2$, the extent of permeability reduction was low and increased slowly with increasing gel strength.

3. For stronger gel systems having gel strength greater than 1000 $dyne/cm^2$, complete plugging of the porous media was observed.

4. The complete plugging of the sandpacks by gel systems having gel strength greater than 1000 $dyne/cm^2$ can be attributed to the stress

applied to the gel during the postflush stage being smaller than the yield stress of the gel.

5. A gelling solution system using thiourea as reducing agent is recommended when longer treatment distance and complete plugging of high permeability thief zones are desired.

6. A gelling solution system using sodium thiosulfate as reducing agent is recommended when shorter treatment distance and partial plugging of the target zones are desired.

7. The extent of permeability reduction increases with increasing polymer and chromium retention.

8. The ratio of the amount of polymer being retained to the amount of chromium being retained was found to be close for sandpack systems having approximately the same initial permeability regardless of the extent of permeability reduction and the reducing agent involved.

9. For the same gelling solution system, lower ratios of the amount of polymer being retained to that of chromium were observed for sandpacks having lower initial permeabilities.

## 6.2 Recommendations

Results of our studies indicate that the detailed mechanism behind the gelation reaction and the permeability reduction characteristics of a gelling solution system is very complicated. In order to develop a comprehensive

model for polymer gel treatment design and optimization, the following recommendations are suggested:

1. More rheological studies need to be performed to better understand the kinetics of gelation reaction.

2. The effect of temperature on gel strength of a gelling solution needs to be investigated.

3. The detailed mechanisms of polymer and chromium retention in the porous medium need to be examined.

4. The effect of shear and shear history on the permeability reduction characteristics of a gelling solution system need to be investigated.

# BIBLIOGRAPHY

[1] Downs, S. L. and Gohel, M. K. :"Injection Profile Corrections—A Review of Workover Techniques—Willard Unit," Journal of Petroleum Technology, Vol. 26, May 1974, p. 557.

[2] Felsenthal, Martin and Gangle, Francis J. :"A Case Study of Thief Zones in a California Waterflood," Journal of Petroleum Technology, Vol. 27, Nov. 1975, p. 1385.

[3] Froning, S. P. and Birdwell, B. F. :"Here's How Getty Controls Injectivity Profile in Ventura," Oil and Gas Journal, Feb. 10, 1975, p. 60.

[4] Peacock, Robert A. :"What Can Be Done to Improve Waterflooding," paper SPE 4903 presented at SPE-AIME 44th California Meeting, San Francisco, April 1974.

[5] Thomeer, J. H. and Abrams, A. :"A Shallow Plugging—Selective Re-entry Technique for Profile Correction," Journal of Petroleum Technology, Vol. 29, May 1977, p. 571.

[6] Rogers, E. B., Jr. :"Successful Well Stimulation Program Has Revitalized a California Oil Field," Journal of Petroleum Technology, Vol. 18, Dec. 1976, p. 1420.

[7] Ellenberger, C. W. and Aseltine, R. J. :"Selective Acid Stimulation to Improve Vertical Efficiency in Injection Wells," Journal of Petroleum Technology, Vol. 29, Jan. 1977, p. 25.

[8] Ford, W. O., Jr. and Kelldorf, W. F. N. :"Field Results of a Short-Setting-Time Polymer Placement Technique," Journal of Petroleum Technology, July 1976, p. 749.

[9] Sorbie, K. S., Roberts, L. J., and Clifford, P. J. :" Calculations on the Behaviour of Time-Setting Polymer Gels in Porous Media," prenented at AIChE National Spring Meeting, Houston, Texas, March 1985.

[10] Batycky, J. P.,Maini, B. B., and Milosz, G. :"A Study of the Application of Polymeric Gels in Porous Media," paper SPE 10620 presented at 6th International Symposium on Oilfield and Geothermal Chemistry, Dallas, Texas, Jan. 1982.

[11] Navratil, M.,Sovak, M. and Mitchell, M. S. :"Diverting Agents for Sweep Improvements in Flooding Operations—Laboratory Studies," paper SPE 10621 presented at 6th International Symposium on Oilfield and Geothermal Chemistry, Dallas, Texas, Jan. 1982.

[12] Hessert, J. E. and Fleming, P. D. :"Gelled Polymer Technology for Control of Water in Injection and Production Wells," presented at 3rd Tertiary Oil Recovery Conference, Wichita, Kansas, April 1979.

[13] Fitch, J. P. and Canfield, C. M. :"Field Performance Evaluation of Crosslinked Polymers to Increase Oil Recovery in the Wilmington Field, California," paper SPE 5366 presented at the 45th Annual California Regional Meeting of the SPE, Ventura, April 1975.

[14] Needham, R. B., Threlkeld, C. B., and Gall, J. W. :"Control of Water Mobility Using Polymers and Multivalent Cations," paper SPE

4747 presented at SPE-AIME Improved Oil Recovery Symposium, Tulsa, Oklahoma, April 1974.

[15] Abdo, M. K., Chung, H. S., Phelps, C. H. and Klaric, T. M. :"Field Experience with Floodwater Diversion by Complexed Biopolymers, " paper SPE 12642 presented at SPE/DOE 4th Symposium on Enhanced Oil Recovery, Tulsa, Oklahoma, April 1984.

[16] Conway, M. K., Almond, S. W. , Briscoe, J. E. , and Harris, L. E. :"Chemical Model for the Rheological Behaviour of Crosslinked Fluid Systems," Journal of Petroleum Technology, p. 315, Feb. 1983.

[17] Silva, Luis F. and Farouq Ali, A. M. :"Waterflood Performance in the Presence of Stratification and Formation Plugging," paper SPE 3556 presented at SPE-AIME 46th Annual Fall Meeting, New Orleans, Louisiana, Oct. 1971.

[18] Tsau, J. S. :"Modeling of Permeability Reducing Vertical Conformance Treatments," M. S. Thesis, The University of Texas at Austin, Dec. 1985.

[19] Sandiford, B. B. and Graham, G. A. :"Injection of Polymer Solutions in Producing Wells," AIChE Symposium Series, Vol. 69, No. 127, p. 38, 1973.

[20] Sloat, Ben:"Increasing Oil Recovery by Chemical Control of Producing Water-Oil Ratios," paper SPE 5341 presented at SPE-AIME Rocky Mountain Regional Meeting, Denver, April 1975.

[21] Domingnez, J. G. and Willhite, G. P. :"Retention and Flow Characteristics of Polymer Solutions in Porous Media," Society of

Petroleum Engineers Journal, April, 1977, p. 111.

[22] Gogarty, W. B. :"Mobility Control with Polymer Solutions," Society of Petroleum Engineers Journal, June 1967, p. 161.

[23] Sparlin, Derry D. :"An Evaluation of Polyacrylamides for Reducing Water Production," Journal of Petroleum Technology, Vol. 28, Aug. 1976, p. 906.

[24] Kukin, V. V., Pik, I. D., and Solyakov, Yu. V. :"Influence of Rheological Properties of Polyacrylamide Solutions on Development of Resistance Factors in Formations with Inhomogeneous Permeability," *Neftpromuishvoe Delo*, No. 2, 1978, p. 13.

[25] Sandiford, B. B. :"Laboratory and Field Studies of Water Floods Using Polymer Solution to Increase Oil Recovery," Journal of Petroleum Technology, Aug. 1964, p. 917.

[26] Huang, Chyi-Gang, Green, D. W., and Willhite, G. P. :" Experimental Study of the In-Situ Gelation of Chromium(+3)- Polyacrylamide Polymer in Porous Media," paper SPE/DOE 12638 presented at 4th Symposium on Enhanced Oil Recovery, Tulsa, Oklahoma, 1984.

[27] Thurston, G. B., Pope, G. A. :"Viscoelastic Properties and Rheology of Fluids in EOR," project report, Center for Enhanced Oil and Gas Recovery Research, The University of Texas at Austin, 1988.

[28] Terry, R. E., Huang, C., Green, D. W., Michnick, M. J., and Willhite, G. P. :"Correlation of Gelation Times for Polymer Solutions

Used as Mobility Control Agents," Society of Petroleum Engineers Journal, April 1981.

[29] Southard, M. Z., Green, D. W., and Willhite, G. P. :" Kinetics of the Chromium(VI)/Thiourea Reaction in the Presence of Polyacrylamide," paper SPE/DOE 12715 presented at the SPE/DOE 4th Symposium on Enhanced Oil Recovery, Tulsa, Oklahoma, April 1984.

[30] Prud'homme, R. K. and Uhl, J. T. :"Kinetics of Polymer/Metal-Ion Gelation," paper SPE/DOE 12640 presented at the SPE/DOE 4th Symposium on Enhanced Oil Recovery, Tulsa, Oklahoma, April 1984.

[31] Jordan, D. S., Green, D. W., Terry, R. E., and Willhite, G. P. :"The Effect of Temperature in Gelation Time for Polyacrylamide-Chromium(III) Systems," paper SPE 10059 presented at the 56th Annual Fall Conference of SPE, San Antonio, Texas, October 1981.

[32] Prud'homme, R. K., Uhl, J. T., Poinsatte, J. P., and Halverson, F. :"Rheological Monitoring of the Formation of Polyacrylamide/Cr(+3) Gels," Society of Petroleum Engineers Journal, Oct. 1983, p. 804.

[33] Thurston, G. B., Pope, G. A. :"Viscoelastic Properties and Rheology Fluids in EOR," project report, Center for Enhanced Oil and Gas Recovery Research, The University of Texas at Austin, 1987.

[34] Aslam, S., Vossoughi, S., and Willhite, G. P. :"Viscometric Measurement of Chromium(III)-Polyacrylamide Gels by Weissennberg Rheogoniometer," paper SPE/DOE 12639 presented at

the SPE/DOE 4th symposium on Enhanced Oil Recovery, Tulsa, Oklahoma, April 1984.

[35] Sorbie, K. S., Parker, A., and Clifford, P. J. :" Experimental and Theoretical Study of Polymer Flow in Porous Media," paper SPE 14231 presented at 60th Annual Fall Conference of SPE, Las Vegas, Sep. 1985.

[36] Hortes, E. :"Development of A Reservoir Model For Polymer-Gel Treatment," CEOGRR roport 87-3, 1987.

[37] McLaughlin, H. C., Jewell, R. L., and Colombo, G. R. :" A Low Viscosity Solution for Injectivity Profile Change," paper No. 851-41-I presented at the Spring Meeting for the Mid-Continent District Division of Production of the API, Oklahoma City, Oklahoma, March 1967.

[38] Thomas, C. P. :"The Mechanism of Reduction of Water Mobility by Polymers in Glass Capillary Arrays," Society of Petroleum Engineers Journal, June 1976, p. 130.

[39] Ghazali, H. A. and Willhite, G. P. :"Permeability Modification Using Aluminum Citrate/Polymer Treatments: Mechanisms of Permeability Reduction in Sandpacks," paper SPE 13583 presented at the International Symposium in Oilfield and Geothermal Chemistry, Phoenix, Arizona, April 1985.

[40] Parmeswar, R. and Willhite, G. P. :"A Study of the Reduction of Brine Permeability in Berea Sandstone Using the Aluminum Citrate Process," paper SPE 13582 presented at the International

Symposium in Oilfield and Geothermal Chemistry, Phoenix, Arizona, April 1985.

[41] Mumallah, N. A. :"Chrimium (III) Propionate: A Crosslinking Agent for Water Soluble Polymers in Real Oilfield Waters," paper SPE 15906 presented at the SPE International Symposium on Oilfield Chemistry, San Antonio, Texas, Feb. 1987.

[42] Routson, W. G., Neale, M., and Penton, J. R. :"A New Blocking Agent for Waterflood Channeling," paper SPE 3992 presented at the 47th Annual Fall Meeting of the SPE-AIME, San Antonio, Texas, Oct. 1972.

[43] Dovan, H. T. and Hutchins, R. D. :"Development of a New Aluminum-Polymer Gel System for Permeability Adjustment," paper SPE/DOE 12641 presented at the SPE/DOE 4th Symposium on Enhanced Oil Recovery, Tulsa, Oklahoma, April 1984.

[44] Burkholder, L. :"Xanthan Gel System Effective for Profile Modification," reprint, Oil and Gas Journal, April 1985.

[45] Martin, F. D. and Sherwood, N. S. :"The Effect of Hydrolysis of Polyacrylamide on Solution Viscosity, Polymer Retention and Flow Resistance Properties," paper SPE 5339 presented at the Rocky Mountain Regional Meeting of the SPE, Denver, Colorado, April 1975.

[46] Mungan, N. :"Rheology and Adsorption of Aqueous Polymer Solutions," Journal of Petroleum Technology, Vol. 18, 1966, p. 1143.

[47] Nouri, H. H. and Root, P. J. :"A Study of Polymer Solution Rheology, Flow Behavior and Oil Displacement Processes," paper SPE

3523 presented at the 46th Annual Fall Meeting of the SPE, New Orleans, Louisiana, Oct. 1971.

[48] Hirasaki, G. H. and Pope, G. A. :"Analysis of Factors Influencing the Mobility and Adsorption in Flow of Polymer Solutions through Porous Media," Society of Petroleum Engineers Journal, Vol. 14, 1974, p. 337.

[49] Chauveteau, G. and Kohler, N. :"Polymer Flooding: The Essential Elements for Laboratory Evaluation," paper SPE 4745 presented at the Symposium on Improved Oil Recovery, Tulsa, Oklahoma, April 1974.

[50] Smith, F. W. :"The Behavior of Partially Hydrolyzed Polyacrylamide Solutions in Porous Media," Journal of Petroleum Technology, Vol. 22, 1970, p. 148.

[51] Olatunji, M. A. and McAuley, A. :"Metal-ion Oxidations. Part XII. Oxidation of Thiourea and NN' –Ethylenethiourea by Chromium(VI) in Perchlorate Media," Journal of Chem. Soc. , Dalton Transactions, 1975, p. 682.

[52] Clampitt, R. L. and Hessert, J. E. :"Method for Controlling Formation Permeability," U.S. Patent No. 3,785,437(1974).

[53] Pearson, D. S. and Graessley, W. W. :"Elastic Properties of Well-Characterized Ethylene-Propylene Copolymer Networks," Macromolecules Vol. 13, 1980, p. 1001.

[54] Flory, P. J. : *Proc.*, Series A, Royal Society, London (1976) 351, 351.

[55] Rosen, S. L. : *Fundamental Principles of Polymeric Materials*, John Wiley & Sons Inc., New York City (1982) 15, 199.

[56] Thurston, G. B., Ozon, P. M., and Pope, G. A. :"The Viscoelasticity and Gelation of Some Polyacrylamide and Xanthan Gum Solution," project report, Center for Enhanced Oil and Gas Recovery Research, The University of Texas at Austin, 1985.

[57] Billheimer, J. S., and Parrette, R. :"Apparatus for Automatic Determination of Gelation Time," Anal. Chem. Vol. 28, 1956, p. 272.

[58] Marrs, W. M., and Wood, P. D. :"The Gelation and Rupture Properties of Gelatin Gels," Photographic Gelatin, 1976, p. 101.

[59] Perkins, T. K., and Johnston, O. C. :"A Review of Diffusion and Dispersion in Porous Media," Society of Petroleum Engineers Journal, March 1963, p. 70.

[60] Foshee, W. C., Jennings, R. R., and West, T. J. :"Preparation and Testing of Partially Hydrolyzed Polyacrylamide Solutions," paper presented at the 51st Annual Fall Technical Conference and Exhibition of the Society of Petroleum Engineers of AIME, New Orleans, Louisiana, Oct. 1976.

[61] Gottleib M., Macosko C. W., Benjamin G. S., Meyers K. O., and Merrill E. W. :"Equilibrium Modulus of Model Poly(dimethylsiloxane) Networks," Macromolecules, Vol. 14, 1981, p. 1039.

# Appendix A

# Results of Dispersion Tests

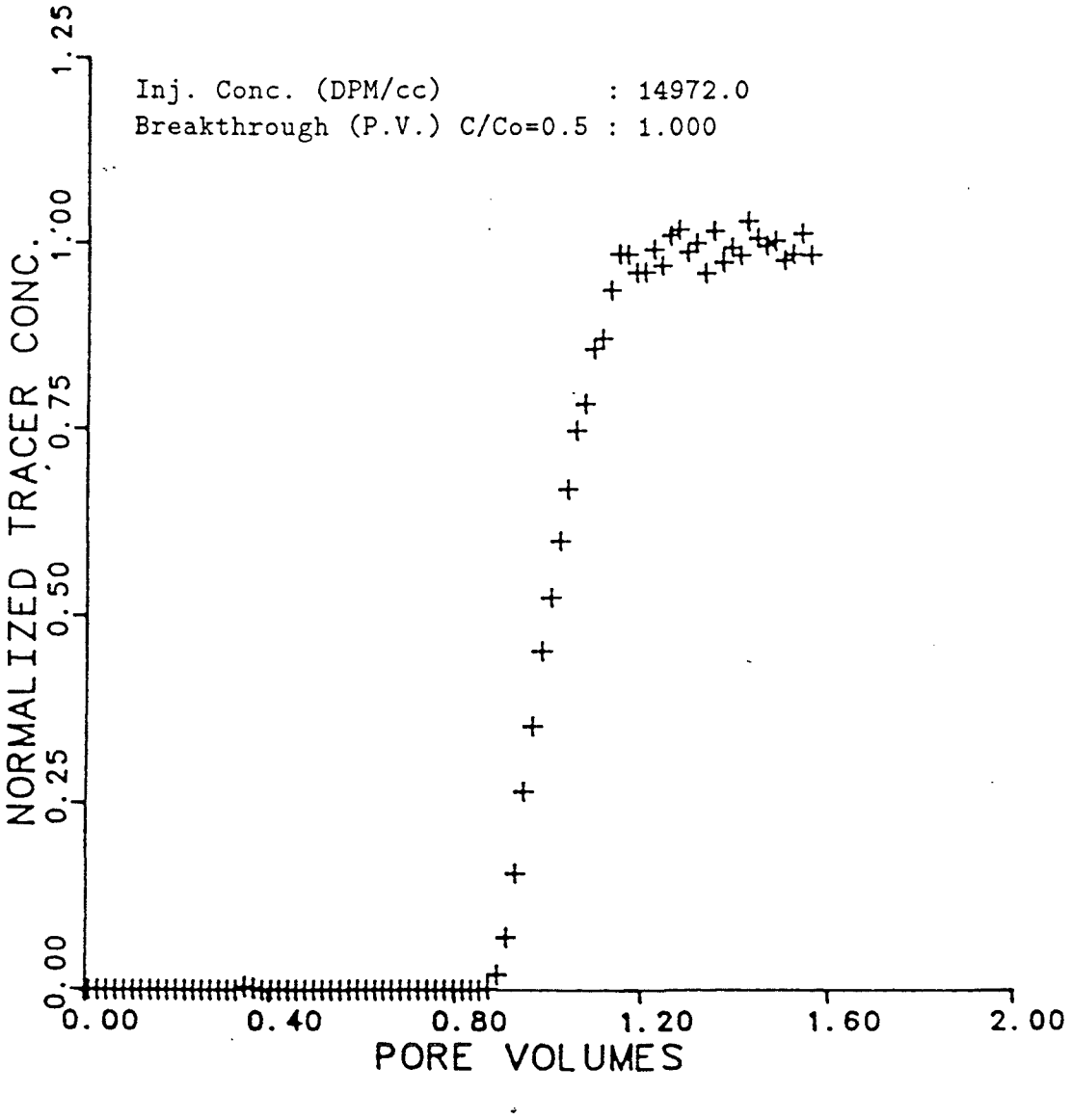


Figure A.1: Tracer breakthrough curve of the sandpack used in EXP-7

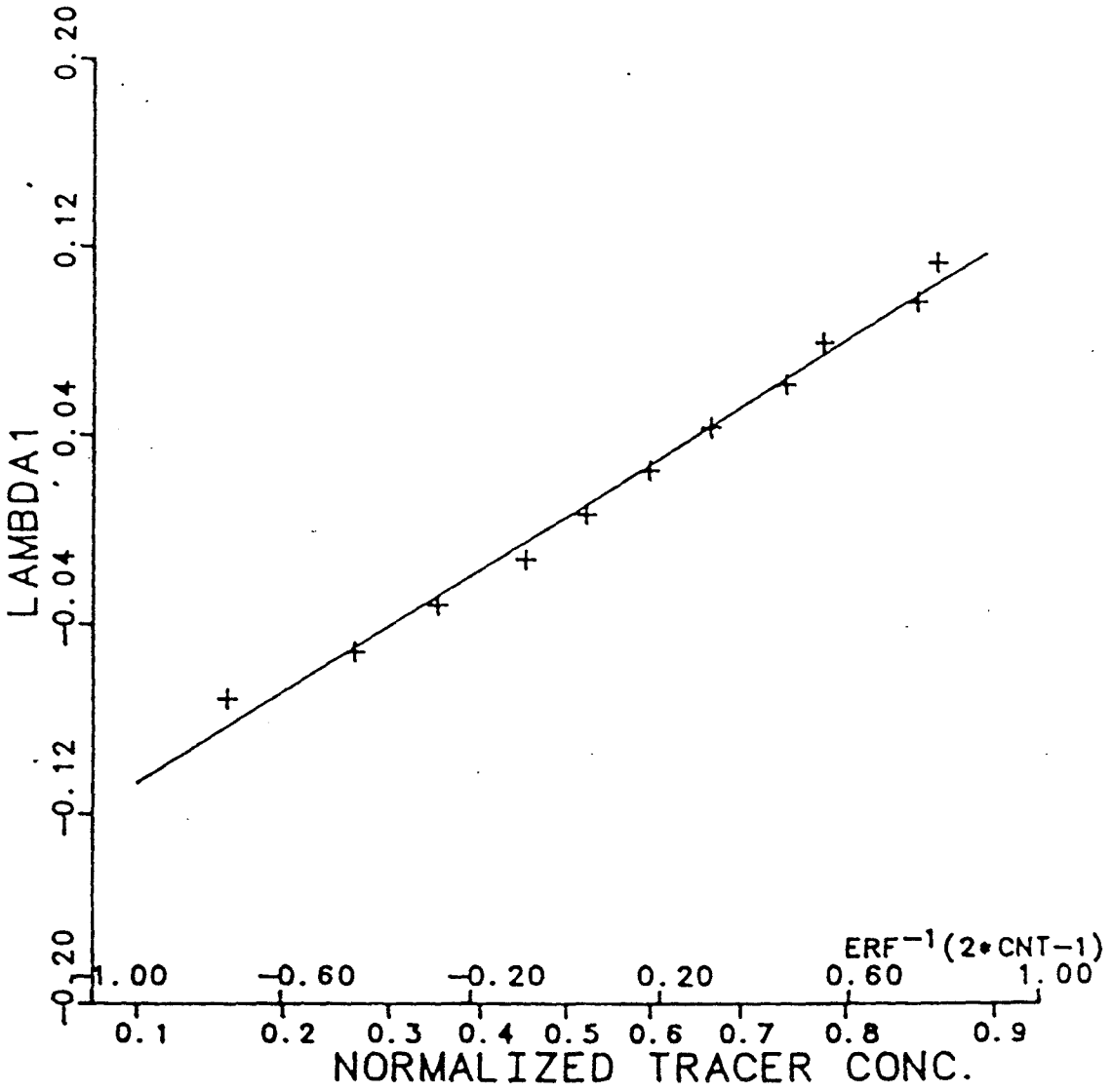


Figure A.2: $\lambda$ vs. normalized tracer concentration plot of the sandpack used in EXP-7

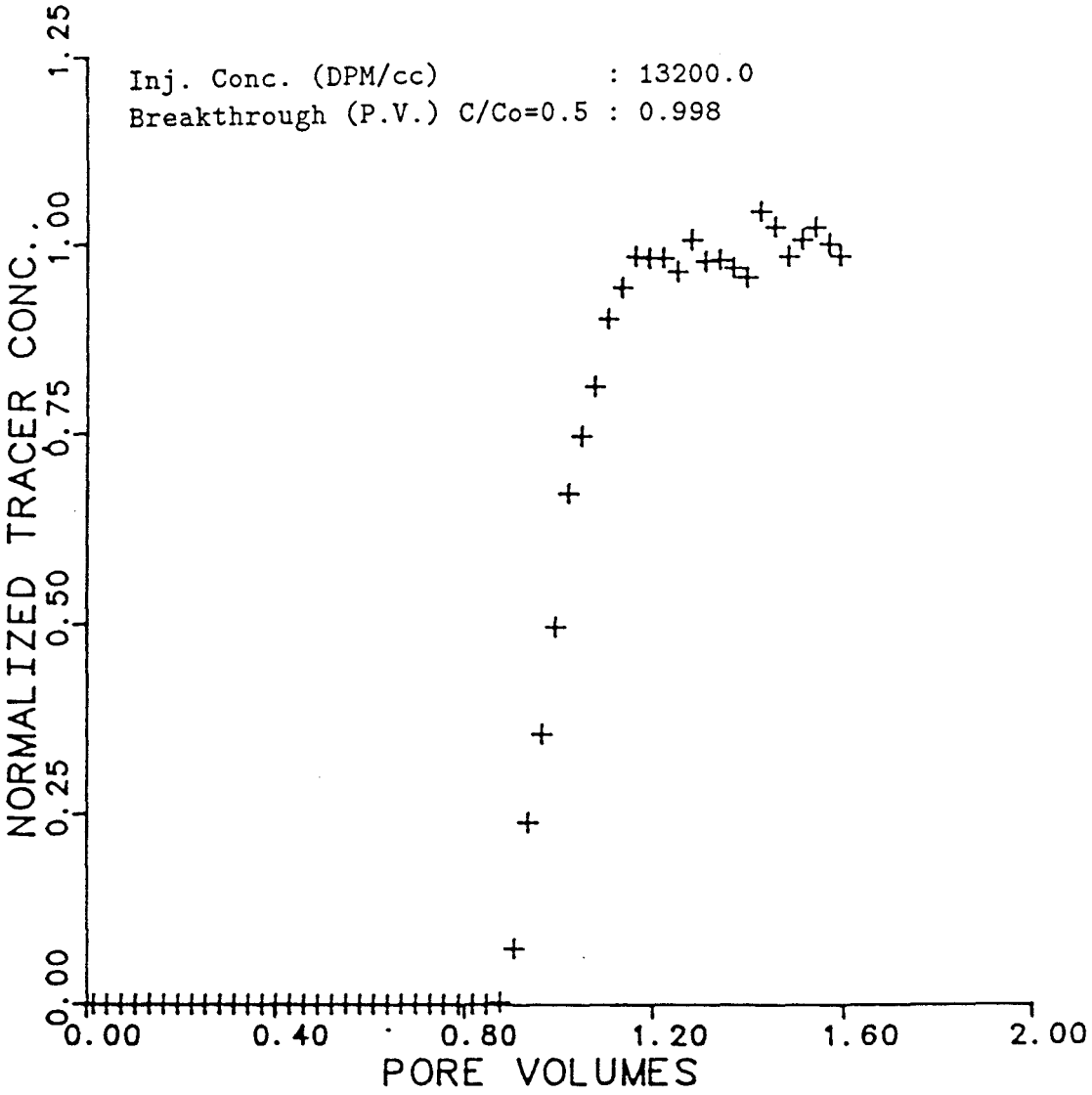


Figure A.3: Tracer breakthrough curve of the sandpack used in EXP-9

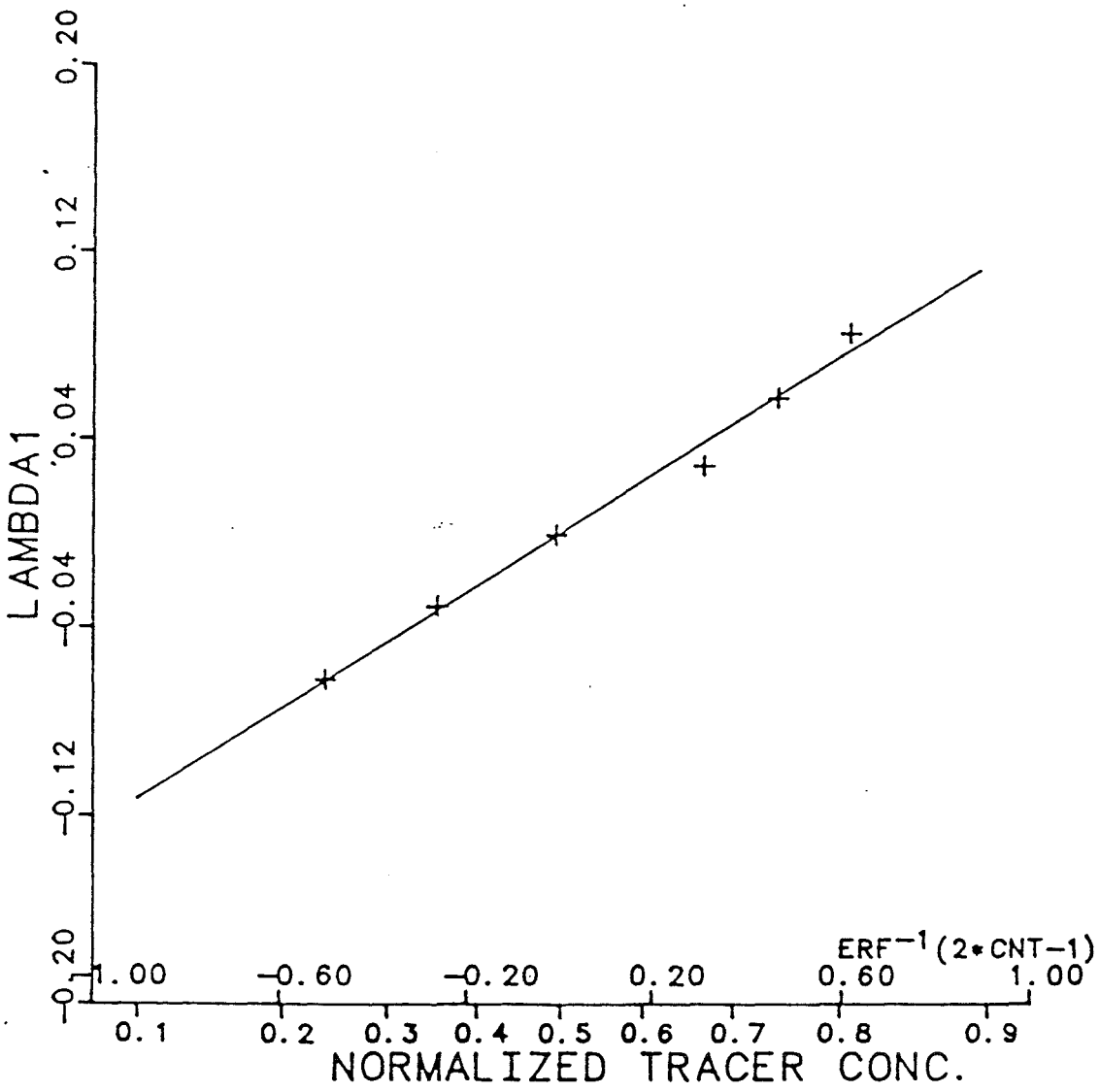


Figure A.4: $\lambda$ vs. normalized tracer concentration plot of the sandpack used in EXP-9

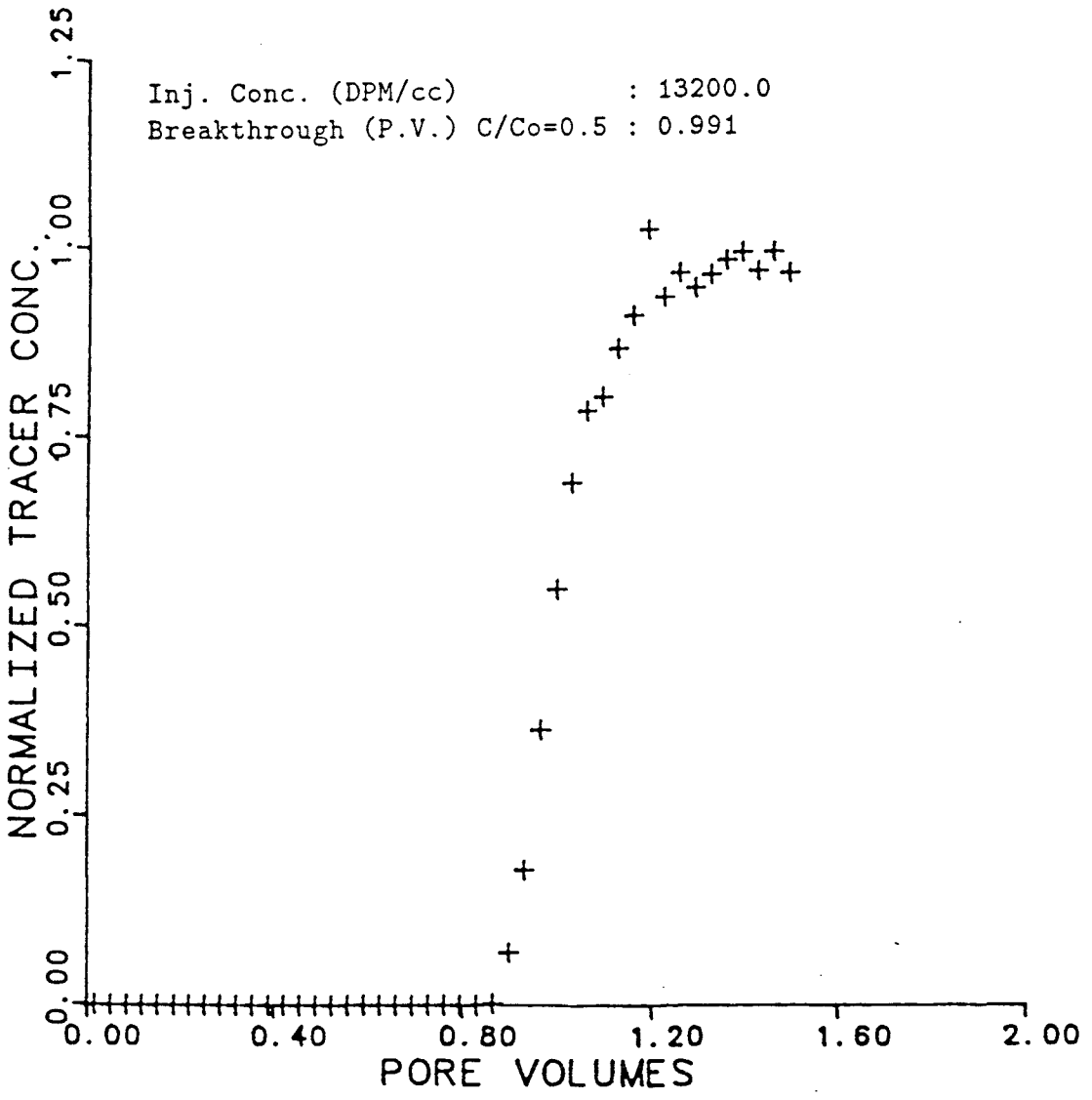


Figure A.5: Tracer breakthrough curve of the sandpack used in EXP-10

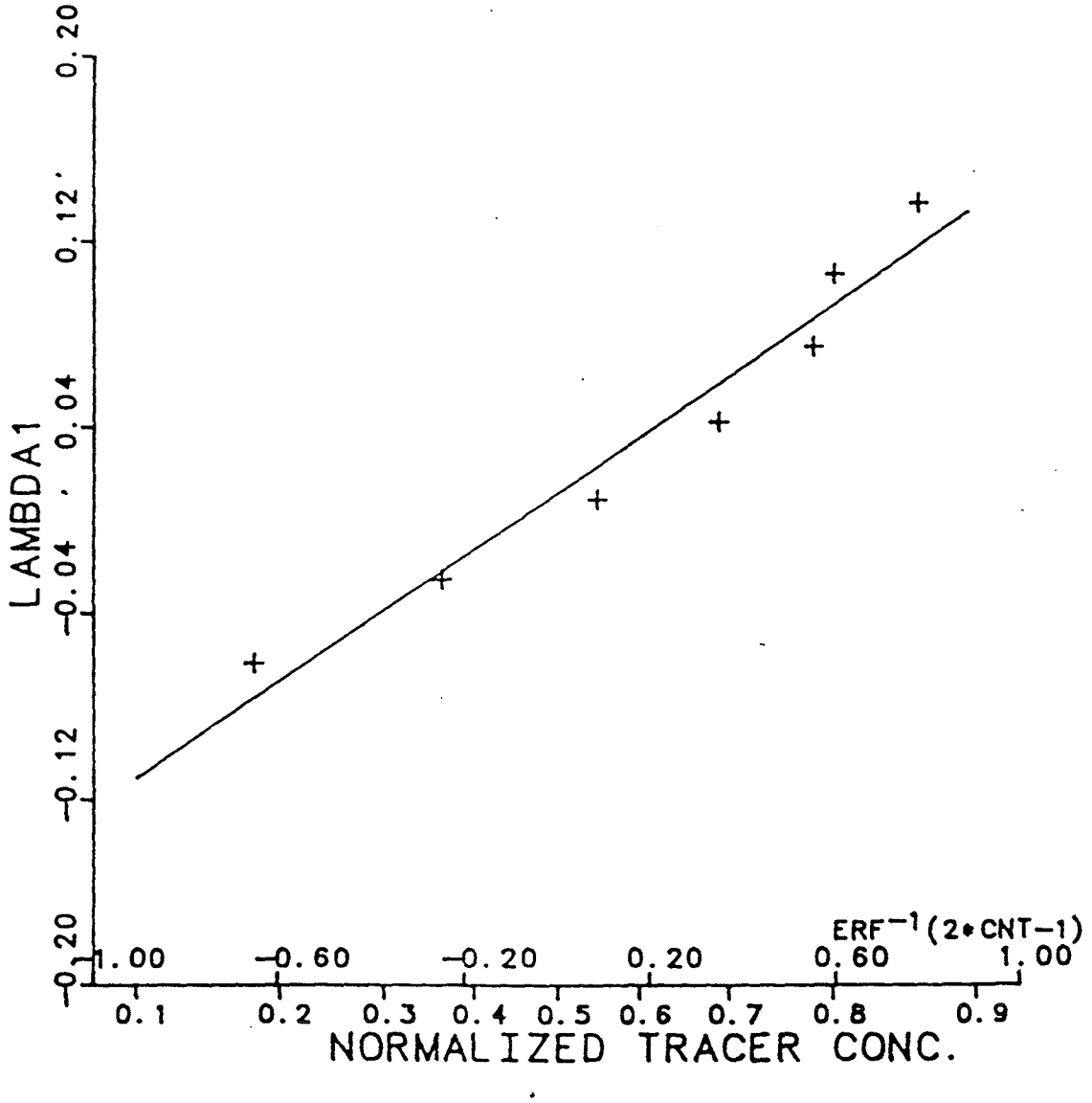


Figure A.6: $\lambda$ vs. normalized tracer concentration plot of the sandpack used in EXP-10

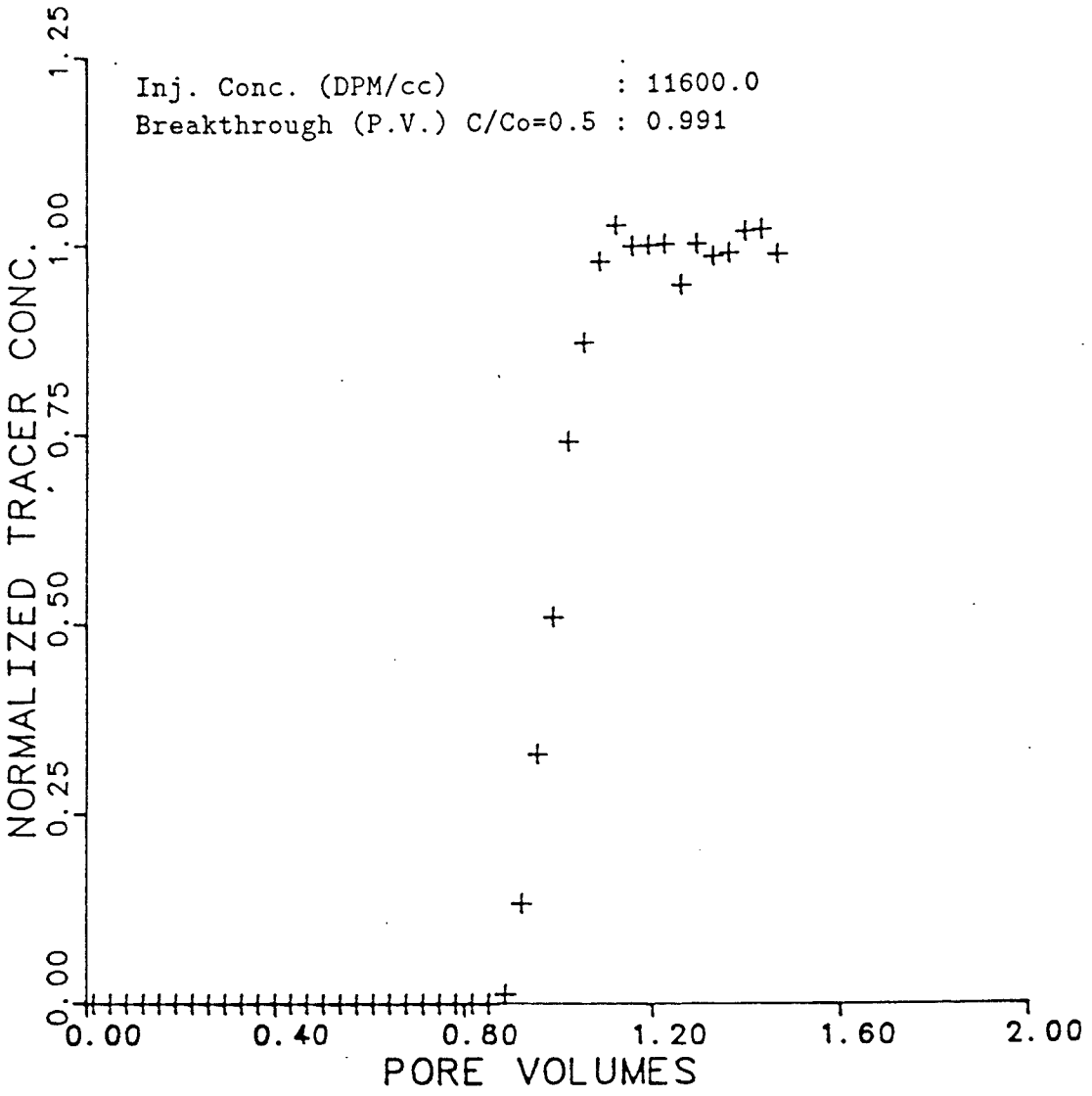


Figure A.7: Tracer breakthrough curve of the sandpack used in EXP-11

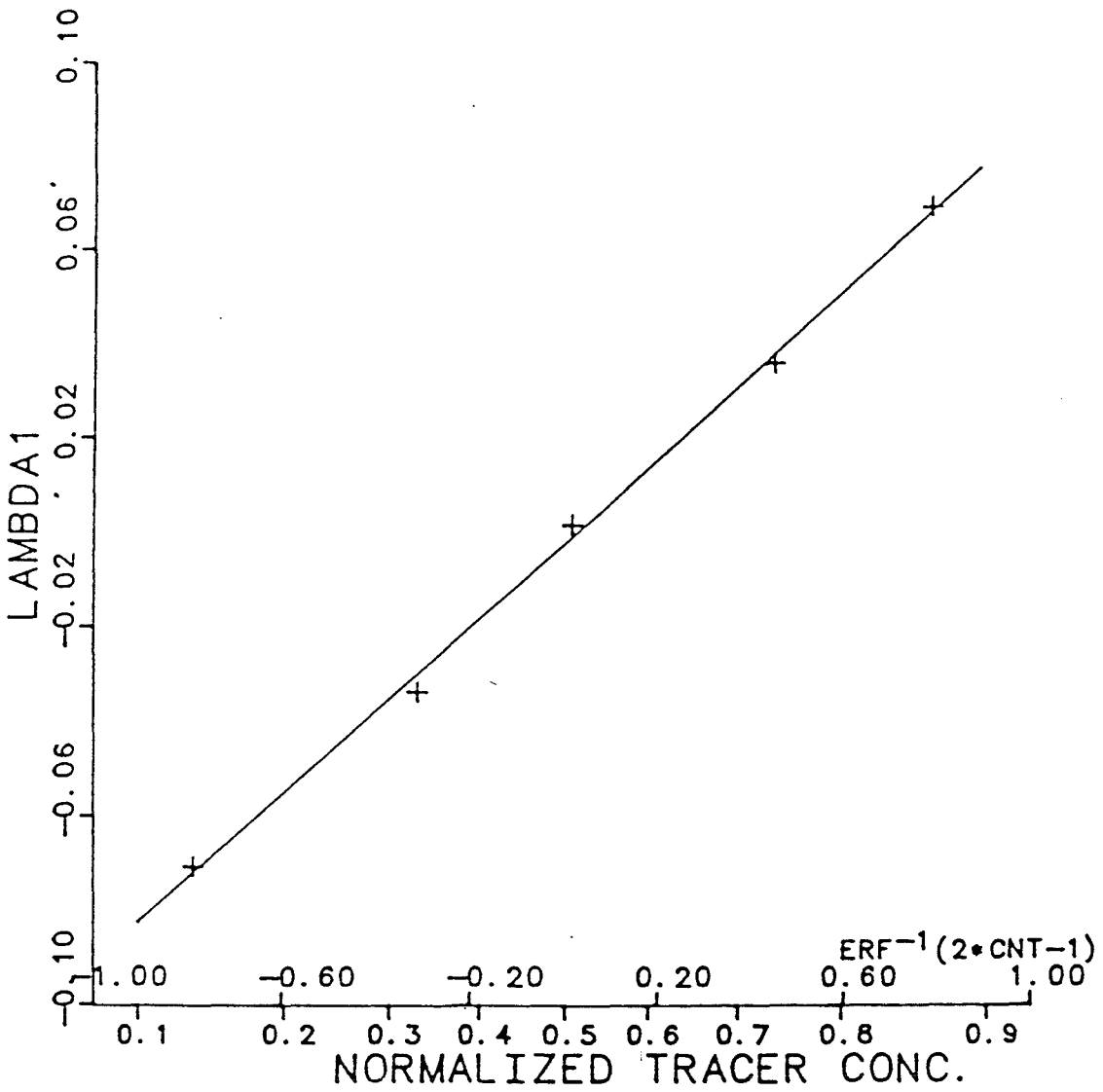


Figure A.8: $\lambda$ vs. normalized tracer concentration plot of the sandpack used in EXP-11

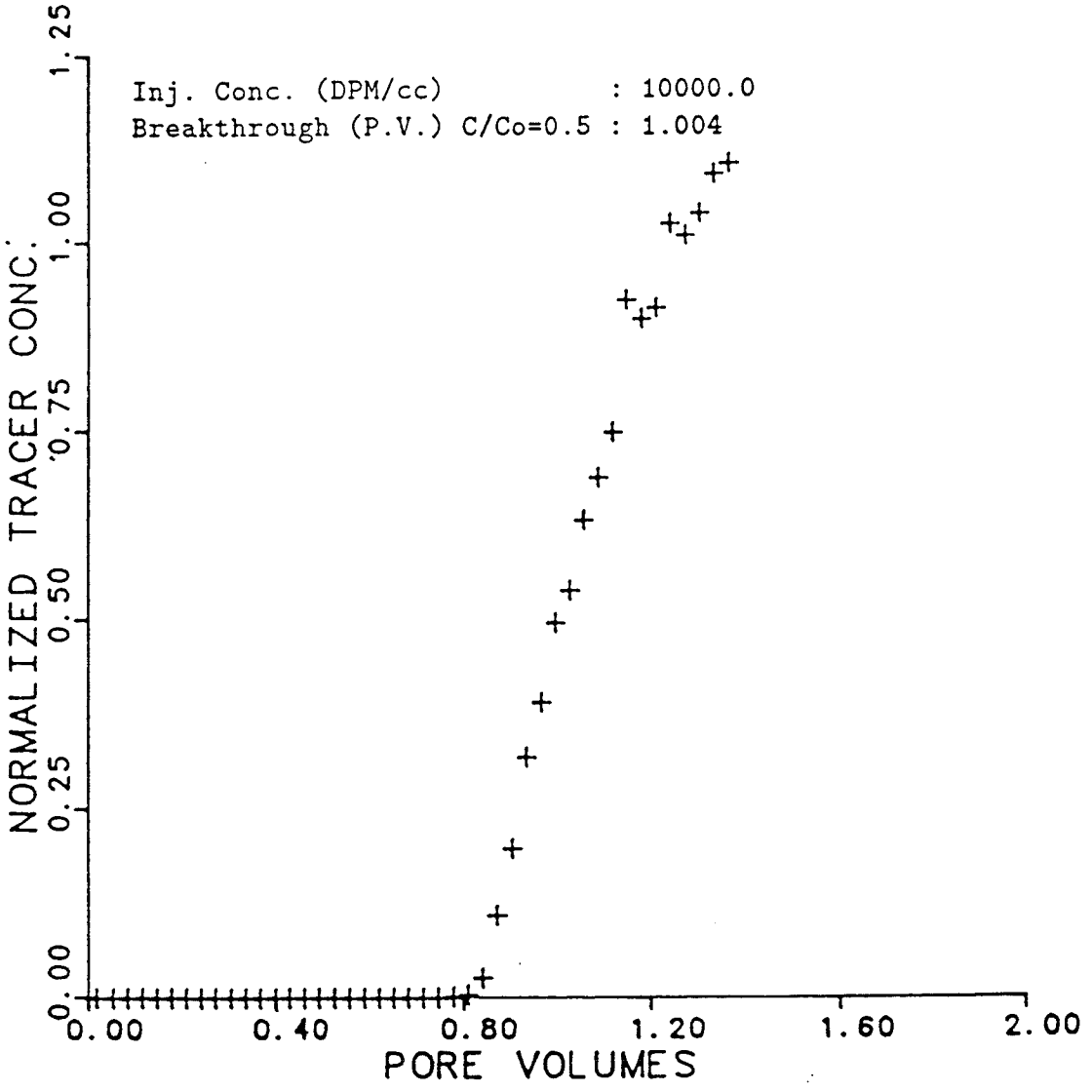


Figure A.9: Tracer breakthrough curve of the sandpack used in EXP-12

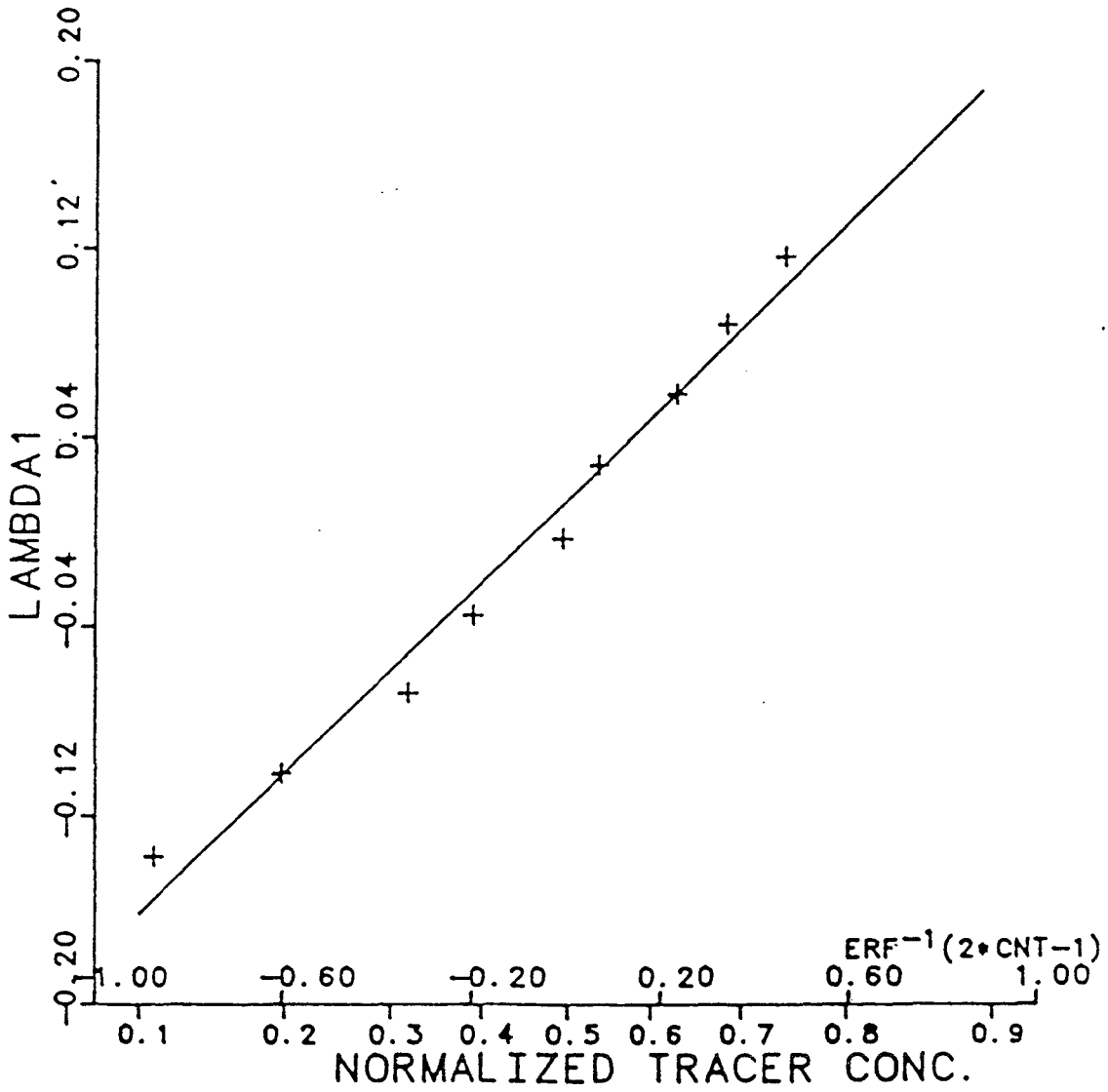


Figure A.10: $\lambda$ vs. normalized tracer concentration plot of the sandpack used in EXP-12

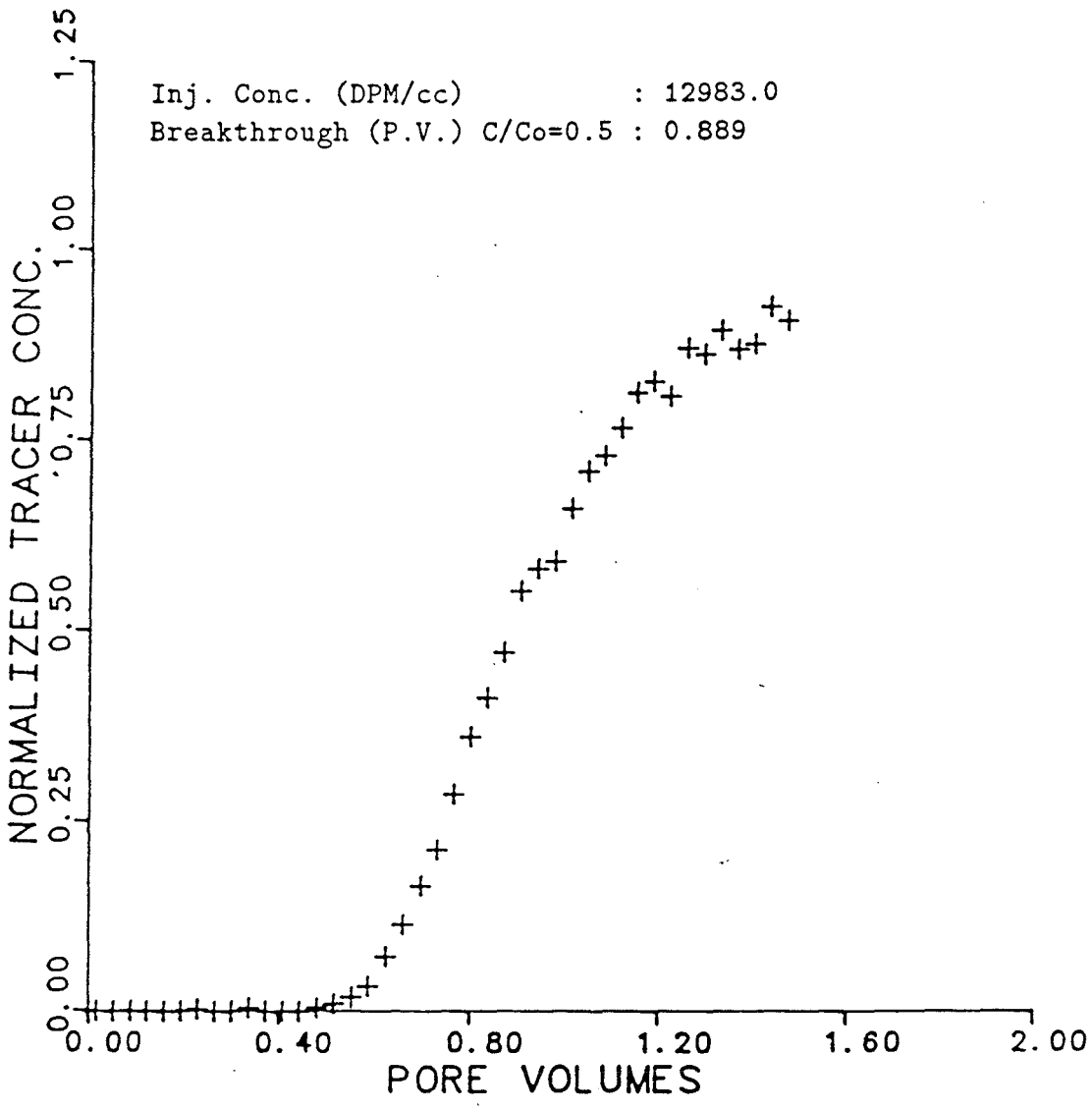


Figure A.11: Tracer breakthrough curve of the sandpack used in EXP-15

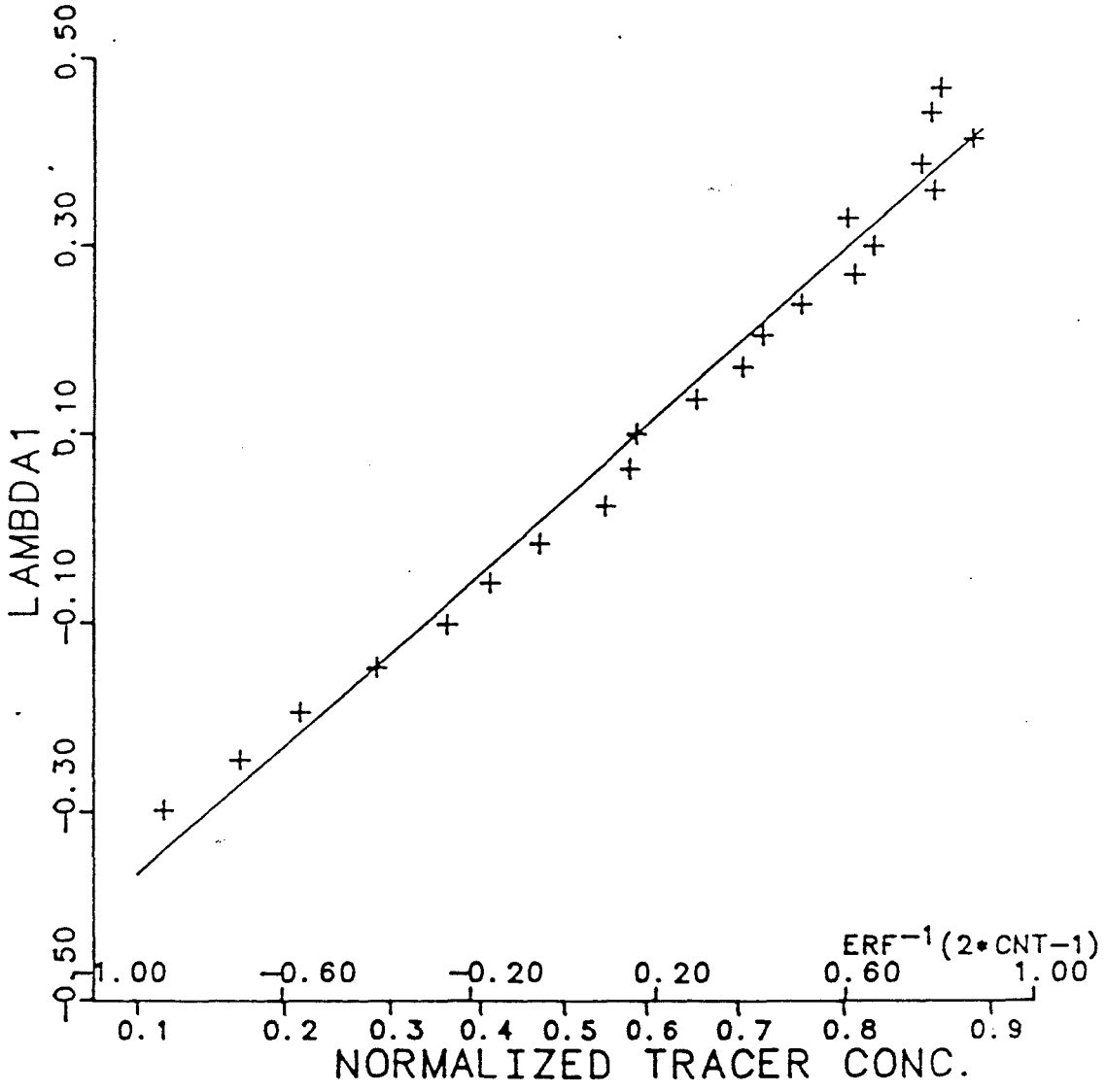


Figure A.12: $\lambda$ vs. normalized tracer concentration plot of the sandpack used in EXP-15

Table A.1: Summary of the results of dispersion test(EXP-5)

| | |
|---|---|
| Exp. No. | : Tracer Test(EXP-5) |
| Pore Volume(cc) | : 407.2 |
| Fractional Flow | : 100% Brine(2% NaCl) |
| Tracer | : Tritium |
| Max. Conc. (DPM/cc) | : 14911.0 |
| Inj. Conc. (DPM/cc) | : 14911.0 |
| Breakthrough (P.V.) C/Co=0.5 | : 0.982 |
| Flow Rate (cc/min) | : 1.93 |
| Lambda1 (10) | : -0.08 |
| Lambda1 (90) | : 0.08 |
| Dispersivity (cm) | : 0.110 |

Table A.2: Summary of the results of dispersion test(EXP-7)

| | |
|---|---|
| Exp. No. | : Tracer Test(EXP-7) |
| Pore Volume(cc) | : 411.14 |
| Fractional Flow | : 100% Brine(2% NaCl) |
| Tracer | : Tritium |
| Max. Conc. (DPM/cc) | : 14972.0 |
| Inj. Conc. (DPM/cc) | : 14972.0 |
| Breakthrough (P.V.) C/Co=0.5 | : 1.000 |
| Flow Rate (cc/min) | : 1.98 |
| Lambda1 (10) | : -0.11 |
| Lambda1 (90) | : 0.12 |
| Dispersivity (cm) | : 0.232 |

Table A.3: Summary of the results of dispersion test(EXP-9)

| | |
|---|---|
| Exp. No. | : Tracer Test(EXP-9) |
| Pore Volume(cc) | : 414.7 |
| Fractional Flow | : 100% Brine(2% NaCl) |
| Tracer | : Tritium |
| Max. Conc. (DPM/cc) | : 13200.0 |
| Inj. Conc. (DPM/cc) | : 13200.0 |
| Breakthrough (P.V.) C/Co=0.5 | : 0.998 |
| Flow Rate (cc/min) | : 2.00 |
| Lambda1 (10) | : -0.11 |
| Lambda1 (90) | : 0.11 |
| Dispersivity (cm) | : 0.234 |

Table A.4: Summary of the results of dispersion test(EXP-10)

| | |
|---|---|
| Exp. No. | : Tracer Test(EXP-10) |
| Pore Volume(cc) | : 432.9 |
| Fractional Flow | : 100% Brine(2% NaCl) |
| Tracer | : Tritium |
| Max. Conc. (DPM/cc) | : 13200.0 |
| Inj. Conc. (DPM/cc) | : 13200.0 |
| Breakthrough (P.V.) C/Co=0.5 | : 0.991 |
| Flow Rate (cc/min) | : 2.00 |
| Lambda1 (10) | : -0.11 |
| Lambda1 (90) | : 0.13 |
| Dispersivity (cm) | : 0.275 |

Table A.5: Summary of the results of dispersion test(EXP-11)

| | |
|---|---|
| Exp. No. | : Tracer Test(EXP-11) |
| Pore Volume(cc) | : 416.6 |
| Fractional Flow | : 100% Brine(2% NaCl) |
| Tracer | : Tritium |
| Max. Conc. (DPM/cc) | : 11600.0 |
| Inj. Conc. (DPM/cc) | : 11600.0 |
| Breakthrough (P.V.) C/Co=0.5 | : 0.991 |
| Flow Rate (cc/min) | : 2.0 |
| Lambda1 (10) | : -0.08 |
| Lambda1 (90) | : 0.08 |
| Dispersivity (cm) | : 0.119 |

Table A.6: Summary of the results of dispersion test(EXP-12)

| | |
|---|---|
| Exp. No. | : Tracer Test(EXP-12) |
| Pore Volume(cc) | : 405.2 |
| Fractional Flow | : 100% Brine(2% NaCl) |
| Tracer | : Tritium |
| Max. Conc. (DPM/cc) | : 10000.0 |
| Inj. Conc. (DPM/cc) | : 10000.0 |
| Breakthrough (P.V.) C/Co=0.5 | : 1.004 |
| Flow Rate (cc/min) | : 2.0 |
| Lambda1 (10) | : -0.16 |
| Lambda1 (90) | : 0.19 |
| Dispersivity (cm) | : 0.562 |

Table A.7: Summary of the results of dispersion test(EXP-15)

| | |
|---|---|
| Exp. No. | : Tracer Test(EXP-15) |
| Pore Volume(cc) | : 435.3 |
| Fractional Flow | : 100% Brine(2% NaCl) |
| Tracer | : Tritium |
| Max. Conc. (DPM/cc) | : 12983.0 |
| Inj. Conc. (DPM/cc) | : 12983.0 |
| Breakthrough (P.V.) C/Co=0.5 | : 0.889 |
| Flow Rate (cc/min) | : 2.08 |
| Lambda1 (10) | : -0.37 |
| Lambda1 (90) | : 0.42 |
| Dispersivity (cm) | : 2.901 |

# Appendix B

# Properties of Sandpacks

Table B.1: Properties of sandpack used in EXP-5

| | | |
|---|---|---|
| Exp. No. | : | EXP-5 |
| Mesh Size Range | : | 80-115 |
| Pore Volume (cc) | : | 407.2 |
| Dispersivity (cm) | : | 0.110 |
| Porosity (%) | : | 30.7 |
| Length of Sandpack (cm) | | |
| Section #1 | : | 15.5 |
| Section #2 | : | 15 |
| Section #3 | : | 15 |
| Section #4 | : | 15.5 |
| Inside Diameter (cm) | : | 5.08 |
| Permeabilities (Darcy) | | |
| At 100% Brine Saturation (Sw=1.0) | | |
| k1 | : | NA |
| k2 | : | 13.87 |
| k3 | : | 14.48 |
| k4 | : | NA |
| ktotal | : | NA |
| At Residual Oil Saturation (Sor=0.203) | | |
| k1 | : | NA |
| k2 | : | 5.23 |
| k3 | : | 5.84 |
| k4 | : | NA |
| ktotal | : | NA |
| After Postflush | | |
| k1 | : | 0.0 |
| k2 | : | 0.0 |
| k3 | : | 0.0 |
| k4 | : | 0.0 |
| ktotal | : | 0.0 |

Table B.2: Properties of sandpack used in EXP-7

| | | |
|---|---|---|
| Exp. No. | : | EXP-7 |
| Mesh Size Range | : | 80-115 |
| Pore Volume (cc) | : | 414.14 |
| Dispersivity (cm) | : | 0.232 |
| Porosity (%) | : | 30.8 |
| Length of Sandpack (cm) | | |
| Section #1 | : | 12.5 |
| Section #2 | : | 12.5 |
| Section #3 | : | 12.5 |
| Section #4 | : | 12.5 |
| Inside Diameter (cm) | : | 5.08 |
| Permeabilities (Darcy) | | |
| At 100% Brine Saturation (Sw=1.0) | | |
| k1 | : | 10.89 |
| k2 | : | 10.97 |
| k3 | : | 10.97 |
| k4 | : | 10.81 |
| ktotal | : | 10.91 |
| At Residual Oil Saturation (Sor=0.21) | | |
| k1 | : | 4.79 |
| k2 | : | 4.79 |
| k3 | : | 4.71 |
| k4 | : | 4.63 |
| ktotal | : | 4.73 |
| After Postflush (Sor=0.19) | | |
| k1 | : | 2.96 |
| k2 | : | 3.44 |
| k3 | : | 3.98 |
| k4 | : | 4.30 |
| ktotal | : | 3.90 |

Table B.3: Properties of sandpack used in EXP-9

| | | |
|---|---|---|
| Exp. No. | : | EXP-9 |
| Mesh Size Range | : | 80-115 |
| Pore Volume (cc) | : | 414.70 |
| Dispersivity (cm) | : | 0.234 |
| Porosity (%) | : | 31.2 |
| Length of Sandpack (cm) | | |
| Section #1 | : | 12.5 |
| Section #2 | : | 12.5 |
| Section #3 | : | 12.5 |
| Section #4 | : | 12.5 |
| Inside Diameter (cm) | : | 5.08 |
| Permeabilities (Darcy) | | |
| At 100% Brine Saturation (Sw=1.0) | | |
| k1 | : | 10.19 |
| k2 | : | 11.78 |
| k3 | : | 12.08 |
| k4 | : | 9.91 |
| ktotal | : | 10.91 |
| At Residual Oil Saturation (Sor=0.188) | | |
| k1 | : | 4.74 |
| k2 | : | 5.94 |
| k3 | : | 6.04 |
| k4 | : | 4.45 |
| ktotal | : | 5.20 |
| After Postflush (Sor=0.155) | | |
| k1 | : | 3.34 |
| k2 | : | 3.92 |
| k3 | : | 4.82 |
| k4 | : | 3.37 |
| ktotal | : | 3.78 |

Table B.4: Properties of sandpack used in EXP-10

| | | |
|---|---|---|
| Exp. No. | : | EXP-10 |
| Mesh Size Range | : | 80-115 |
| Pore Volume (cc) | : | 432.9 |
| Dispersivity (cm) | : | 0.275 |
| Porosity (%) | : | 32.2 |
| Length of Sandpack (cm) | | |
| Section #1 | : | 12.5 |
| Section #2 | : | 12.5 |
| Section #3 | : | 12.5 |
| Section #4 | : | 12.5 |
| Inside Diameter (cm) | : | 5.08 |
| Permeabilities (Darcy) | | |
| At 100% Brine Saturation (Sw=1.0) | | |
| k1 | : | 9.84 |
| k2 | : | 10.81 |
| k3 | : | 11.20 |
| k4 | : | 12.77 |
| ktotal | : | 11.06 |
| At Residual Oil Saturation (Sor=0.215) | | |
| k1 | : | 5.60 |
| k2 | : | 5.97 |
| k3 | : | 6.36 |
| k4 | : | 7.02 |
| ktotal | : | 6.19 |
| After Postflush (Sor=0.08) | | |
| k1 (md) | : | 20.9 |
| k2 (md) | : | 1.72 |
| k3 (md) | : | 6.28 |
| k4 (md) | : | 4.20 |
| ktotal (md) | : | 3.89 |

Table B.5: Properties of sandpack used in EXP-11

| | | |
|---|---|---|
| Exp. No. | : | EXP-11 |
| Mesh Size Range | : | 80-115 |
| Pore Volume (cc) | : | 416.6 |
| Dispersivity (cm) | : | 0.119 |
| Porosity (%) | : | 31.3 |
| Length of Sandpack (cm) | | |
| Section #1 | : | 12.5 |
| Section #2 | : | 12.5 |
| Section #3 | : | 12.5 |
| Section #4 | : | 12.5 |
| Inside Diameter (cm) | : | 5.08 |
| Permeabilities (Darcy) | | |
| At 100% Brine Saturation (Sw=1.0) | | |
| k1 | : | 11.66 |
| k2 | : | 10.97 |
| k3 | : | 12.13 |
| k4 | : | 13.44 |
| ktotal | : | 11.98 |
| At Residual Oil Saturation (Sor=0.204) | | |
| k1 | : | 5.08 |
| k2 | : | 5.38 |
| k3 | : | 5.80 |
| k4 | : | 5.96 |
| ktotal | : | 5.53 |
| After Postflush | | |
| k1 | : | 0.0 |
| k2 | : | 0.0 |
| k3 | : | 0.0 |
| k4 | : | 0.0 |
| ktotal | : | 0.0 |

Table B.6: Properties of sandpack used in EXP-12

| | | |
|---|---|---|
| Exp. No. | : | EXP-12 |
| Mesh Size Range | : | 60-200 |
| Pore Volume (cc) | : | 405.12 |
| Dispersivity (cm) | : | 0.562 |
| Porosity (%) | : | 32.1 |
| Length of Sandpack (cm) | | |
| Section #1 | : | 12.5 |
| Section #2 | : | 12.5 |
| Section #3 | : | 12.5 |
| Section #4 | : | 12.5 |
| Inside Diameter (cm) | : | 5.08 |
| Permeabilities (Darcy) | | |
| At 100% Brine Saturation (Sw=1.0) | | |
| k1 | : | 7.19 |
| k2 | : | 7.86 |
| k3 | : | 6.66 |
| k4 | : | 6.81 |
| ktotal | : | 7.10 |
| At Residual Oil Saturation (Sor=0.227) | | |
| k1 | : | 3.25 |
| k2 | : | 3.51 |
| k3 | : | 3.37 |
| k4 | : | 3.27 |
| ktotal | : | 3.34 |
| After Postflush (Sor=0.222) | | |
| k1 | : | 2.40 |
| k2 | : | 2.87 |
| k3 | : | 2.75 |
| k4 | : | 2.99 |
| ktotal | : | 2.73 |

Table B.7: Properties of sandpack used in EXP-15

| | | |
|---|---|---|
| Exp. No. | : | EXP-15 |
| Mesh Size Range | : | Oklahoma No.1 + 240 mesh Silica Flour(20 wt%) |
| Pore Volume (cc) | : | 435.3 |
| Dispersivity (cm) | : | 2.901 |
| Porosity (%) | : | 33.7 |
| Length of Sandpack (cm) | | |
| Section #1 | : | 12.5 |
| Section #2 | : | 12.5 |
| Section #3 | : | 12.5 |
| Section #4 | : | 12.5 |
| Inside Diameter (cm) | : | 5.08 |
| Permeabilities (Darcy) | | |
| At 100% Brine Saturation (Sw=1.0) | | |
| k1 | : | 3.38 |
| k2 | : | 3.86 |
| k3 | : | 3.37 |
| k4 | : | 3.63 |
| ktotal | : | 3.55 |
| At Residual Oil Saturation (Sor=0.207) | | |
| k1 | : | 1.03 |
| k2 | : | 1.76 |
| k3 | : | 1.53 |
| k4 | : | 1.62 |
| ktotal | : | 1.42 |
| After Postflush (Sor=0.200) | | |
| k1 | : | 0.657 |
| k2 | : | 1.133 |
| k3 | : | 1.062 |
| k4 | : | 1.077 |
| ktotal | : | 0.936 |

# Appendix C

# Results of Effluent Analysis

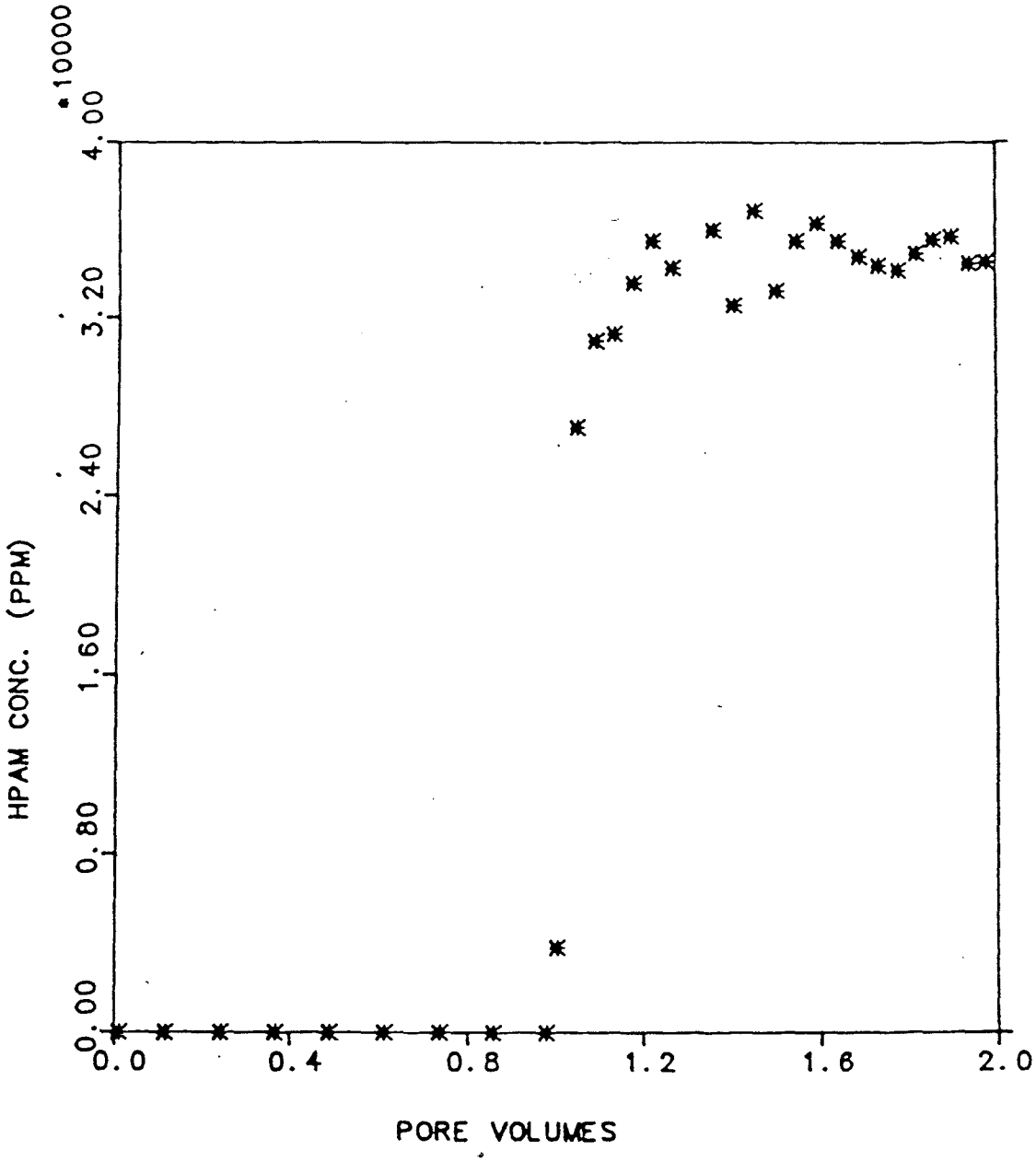


Figure C.1: EXP-5 HPAM effluent concentration

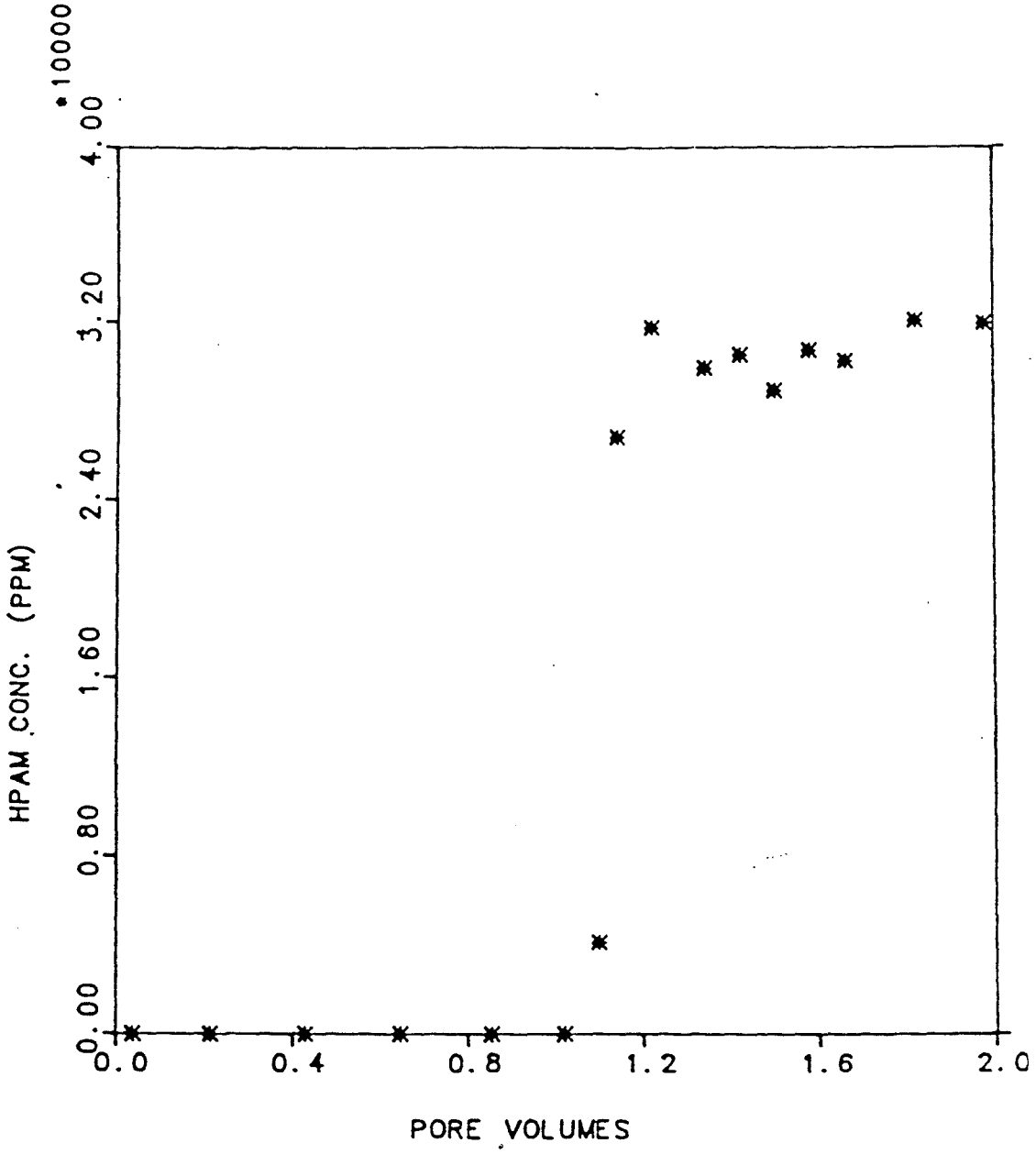


Figure C.2: EXP-9 HPAM effluent concentration

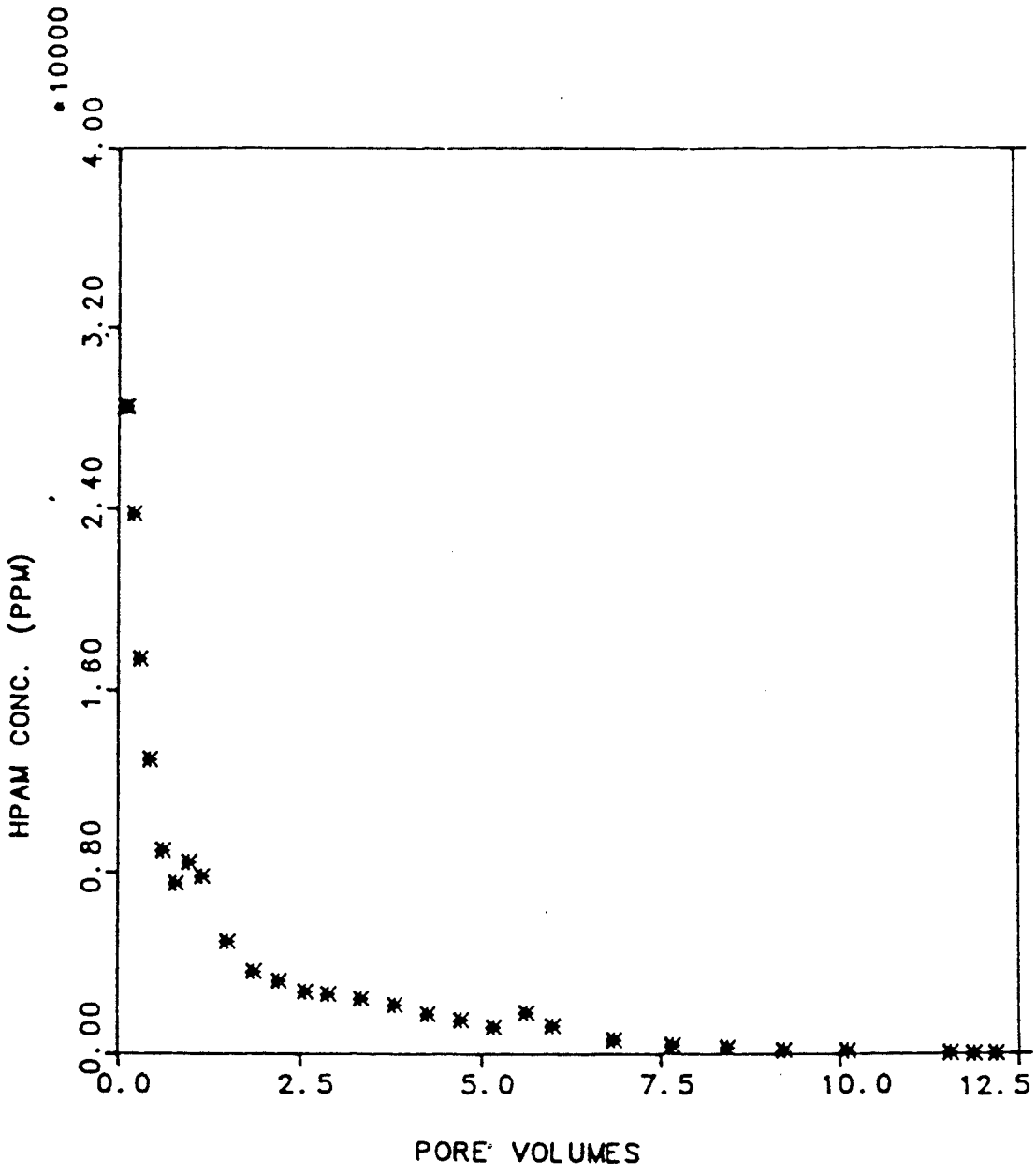


Figure C.3: EXP-9 HPAM postflush concentration

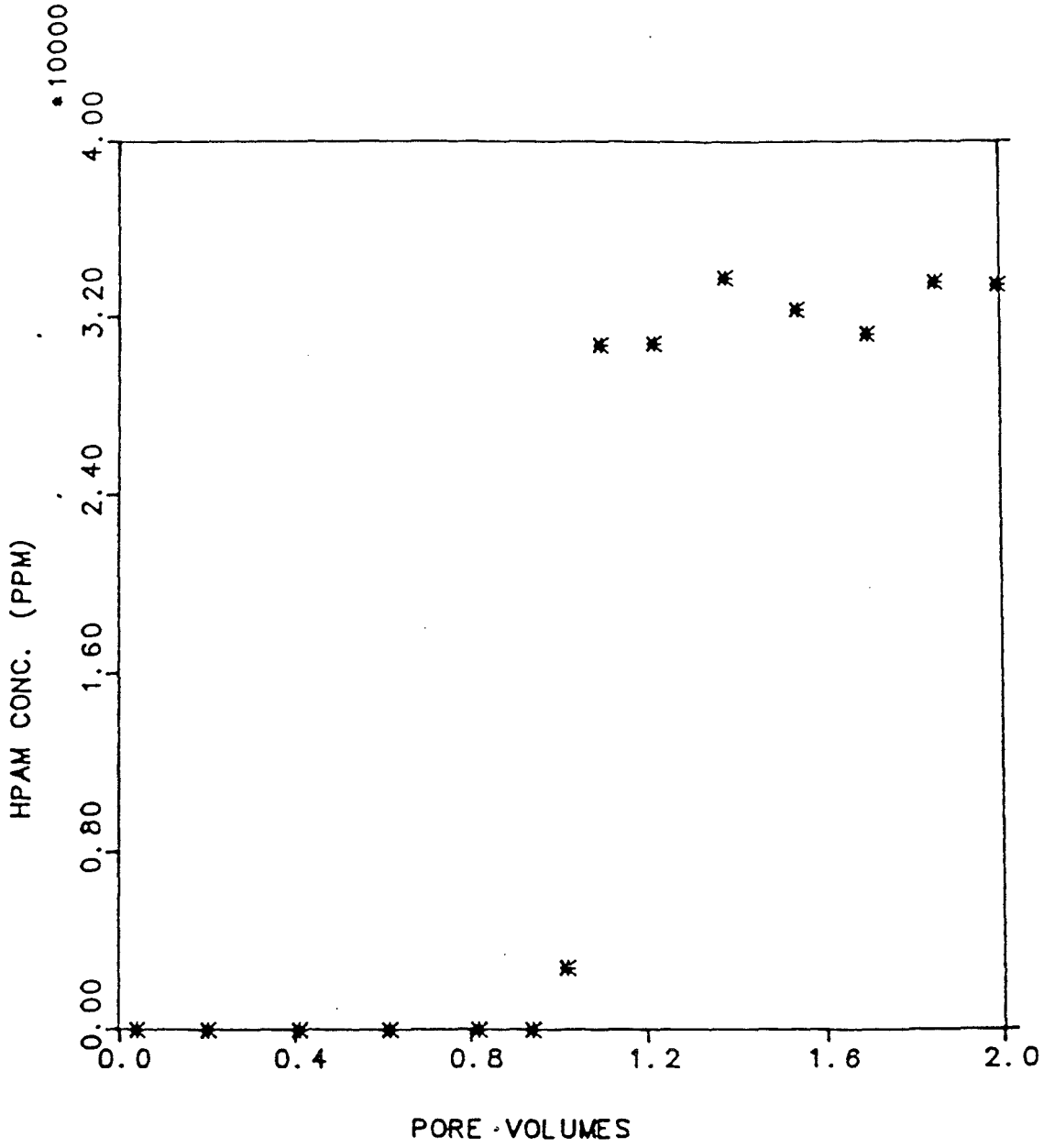


Figure C.4: EXP-10 HPAM effluent concentration

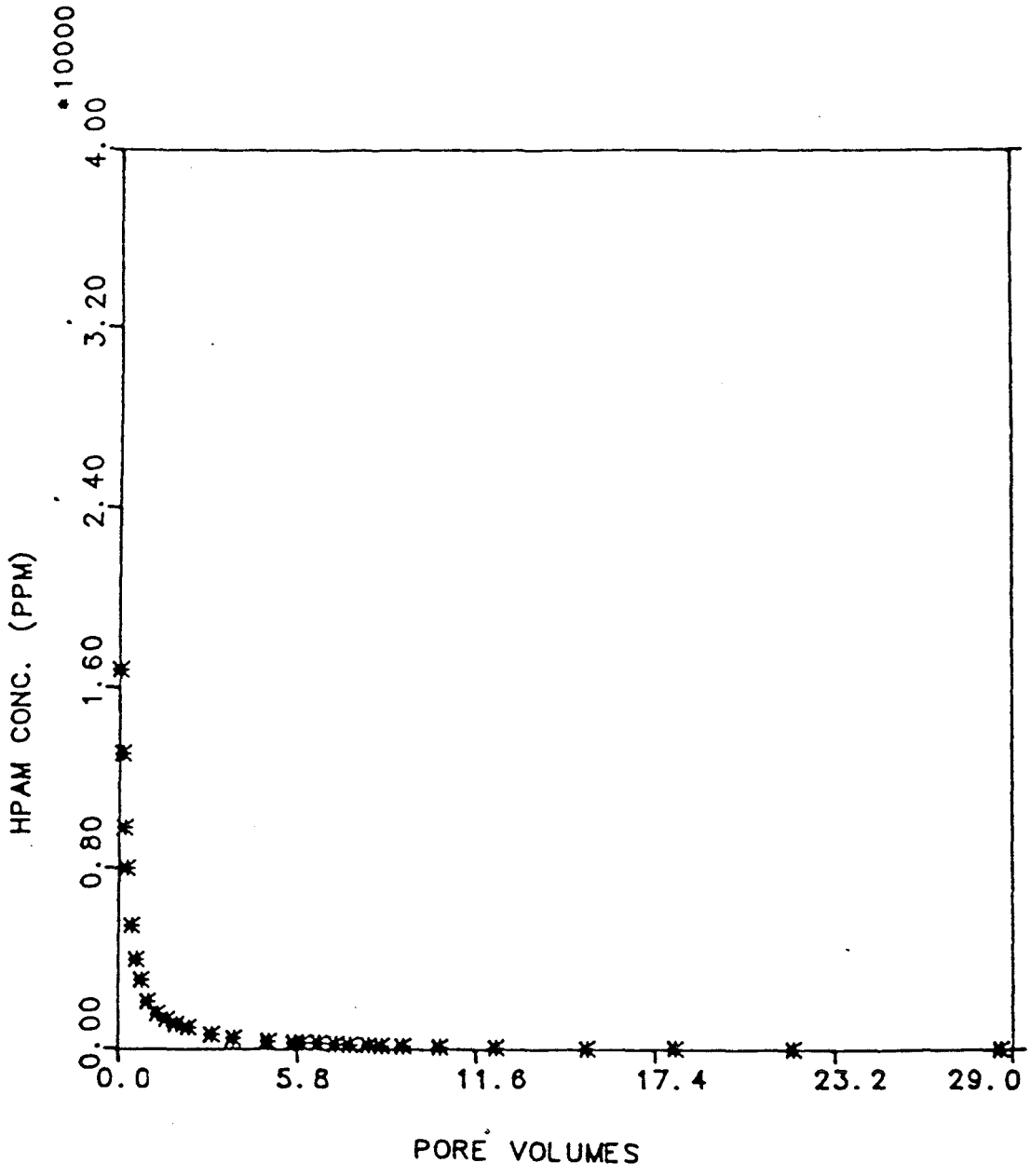


Figure C.5: EXP-10 HPAM postflush concentration

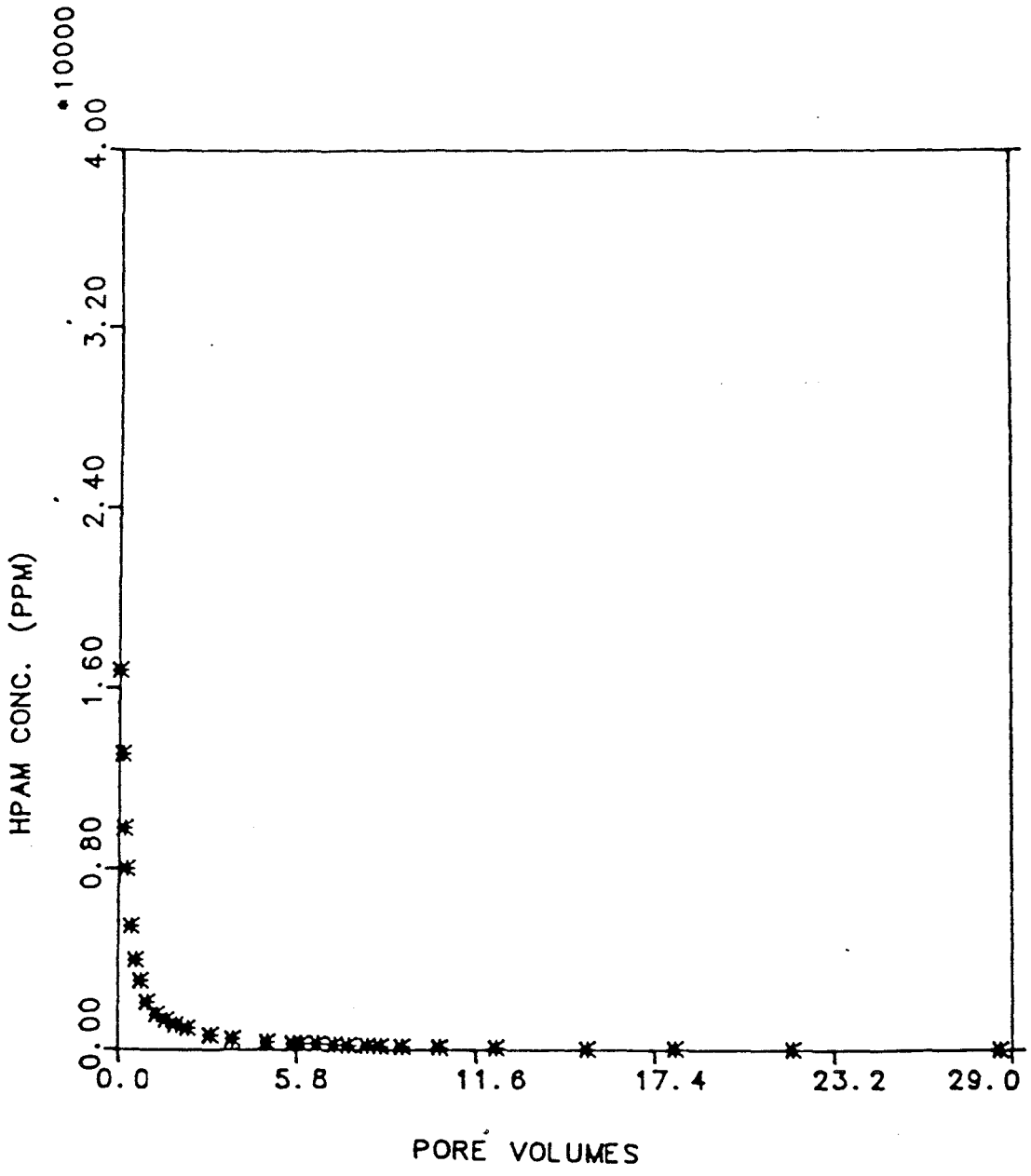


Figure C.5: EXP-10 HPAM postflush concentration

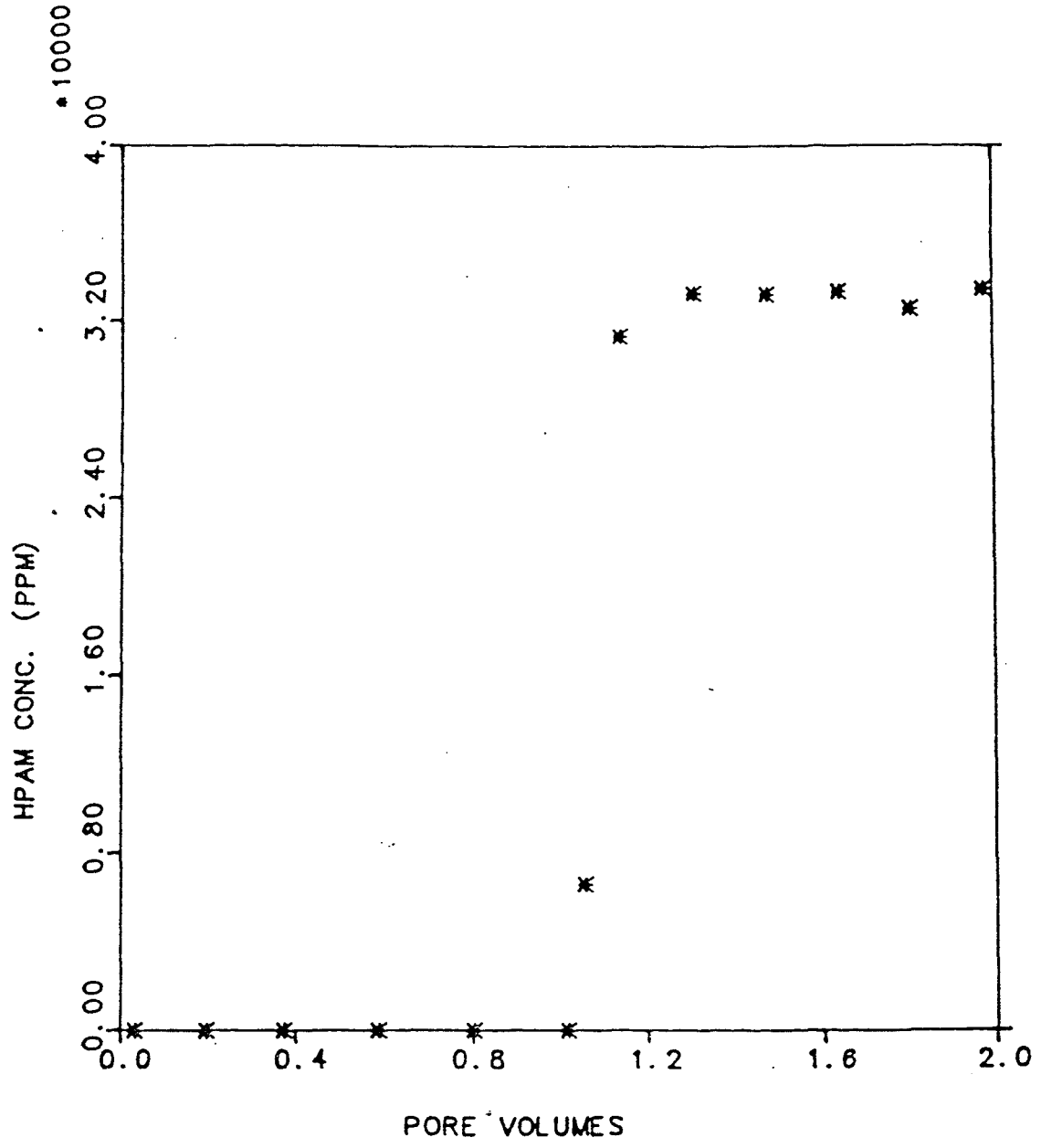


Figure C.6: EXP-12 HPAM effluent concentration

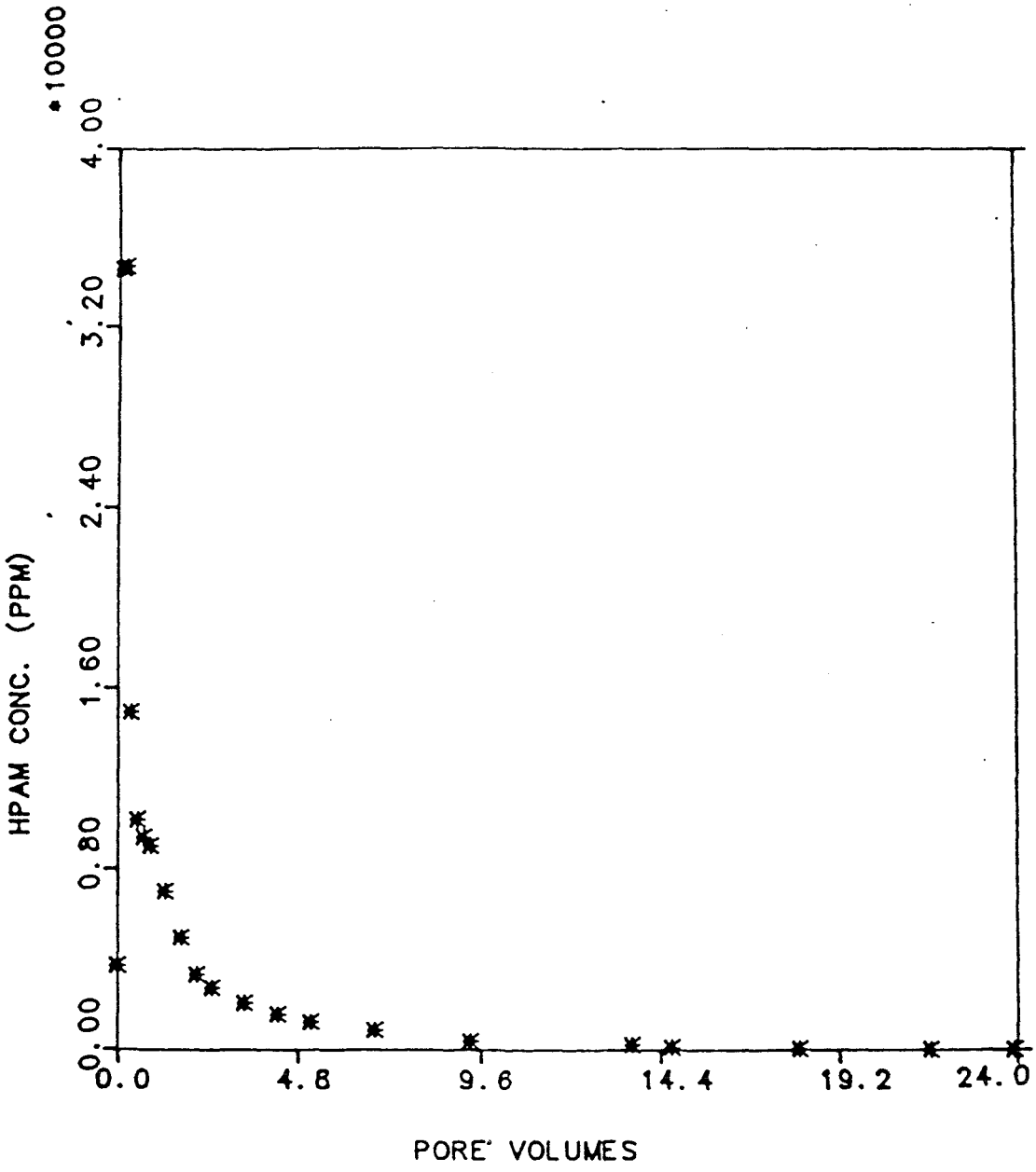


Figure C.7: EXP-12 HPAM postflush concentration

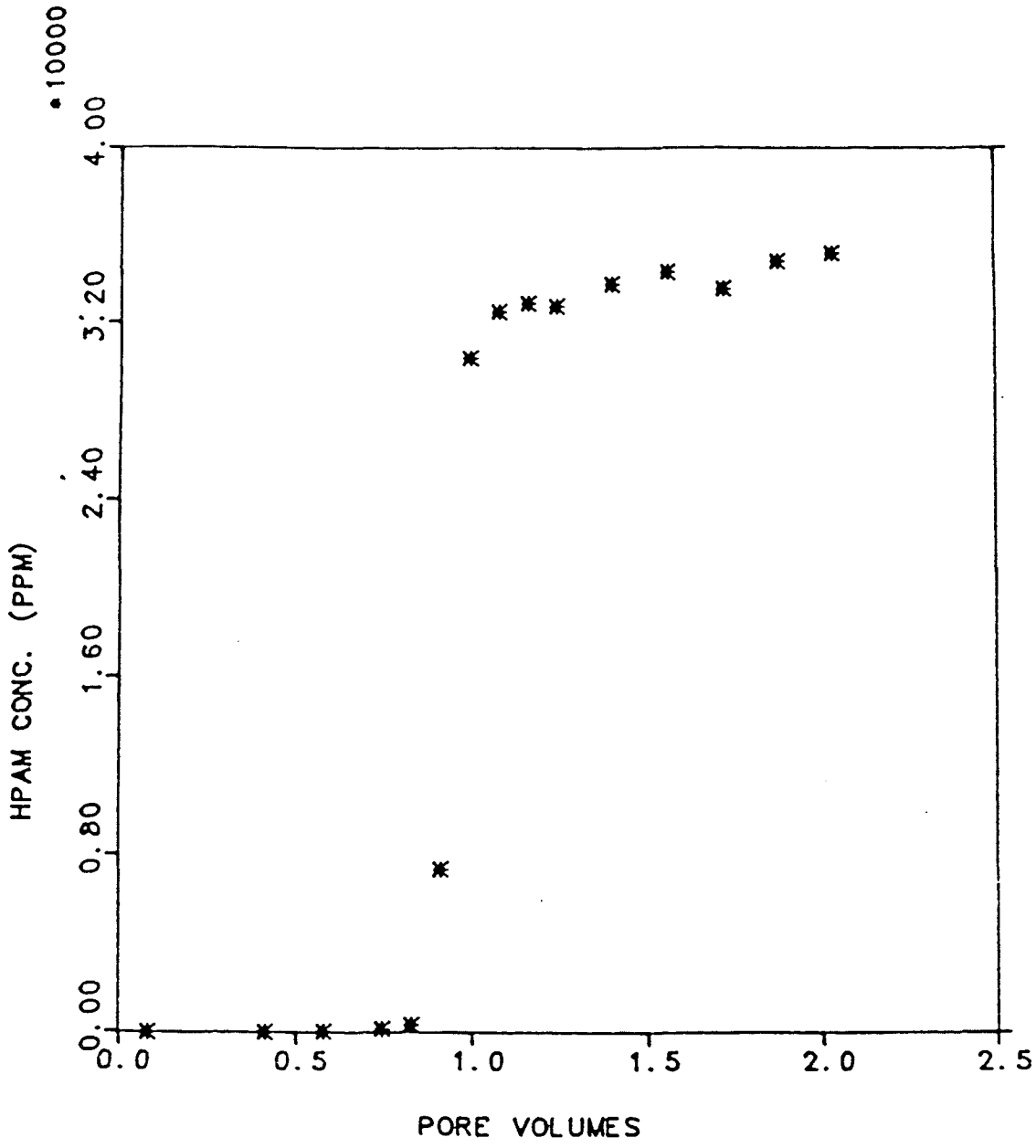


Figure C.8: EXP-15 HPAM effluent concentration

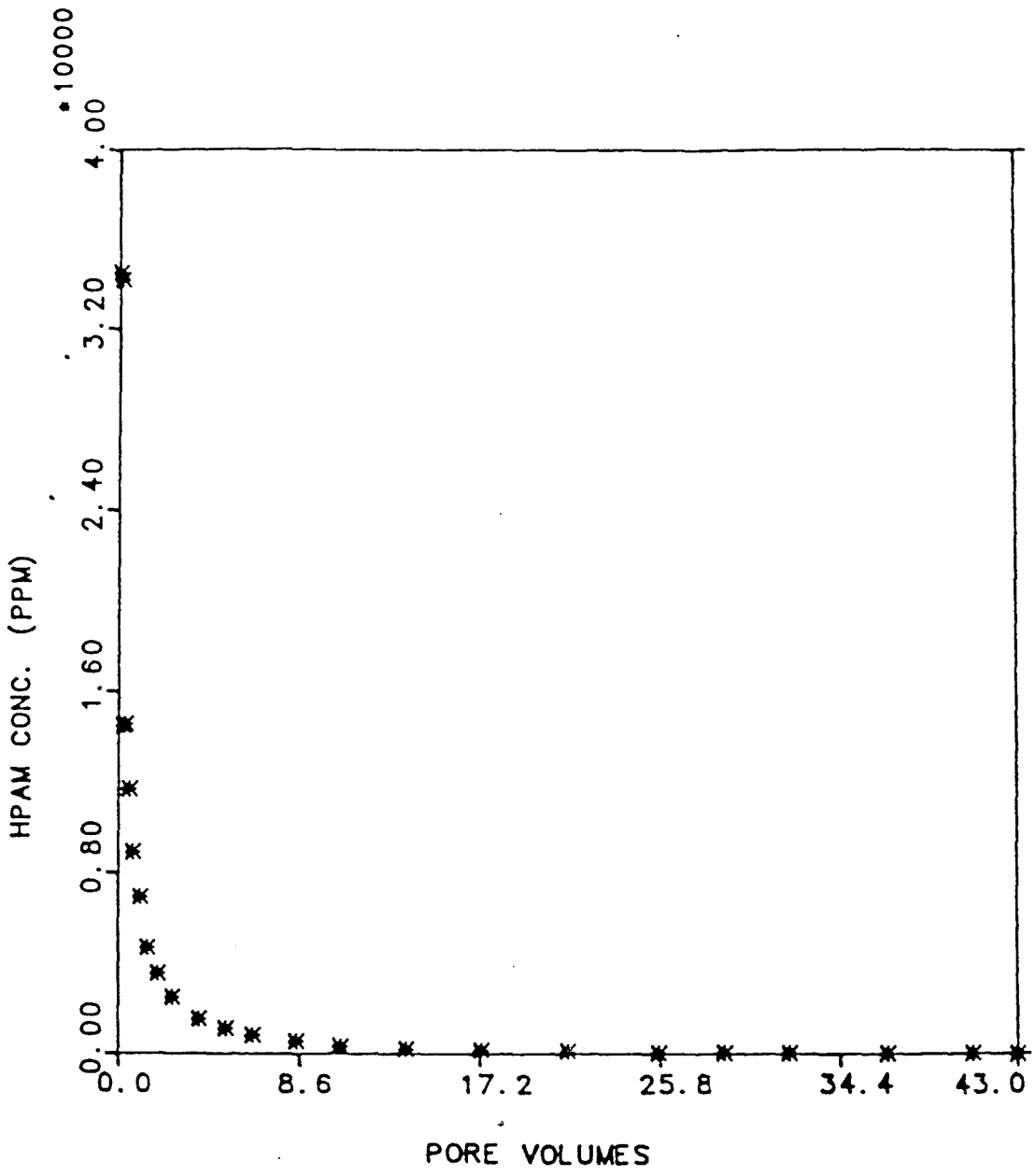


Figure C.9: EXP-15 HPAM postflush concentration

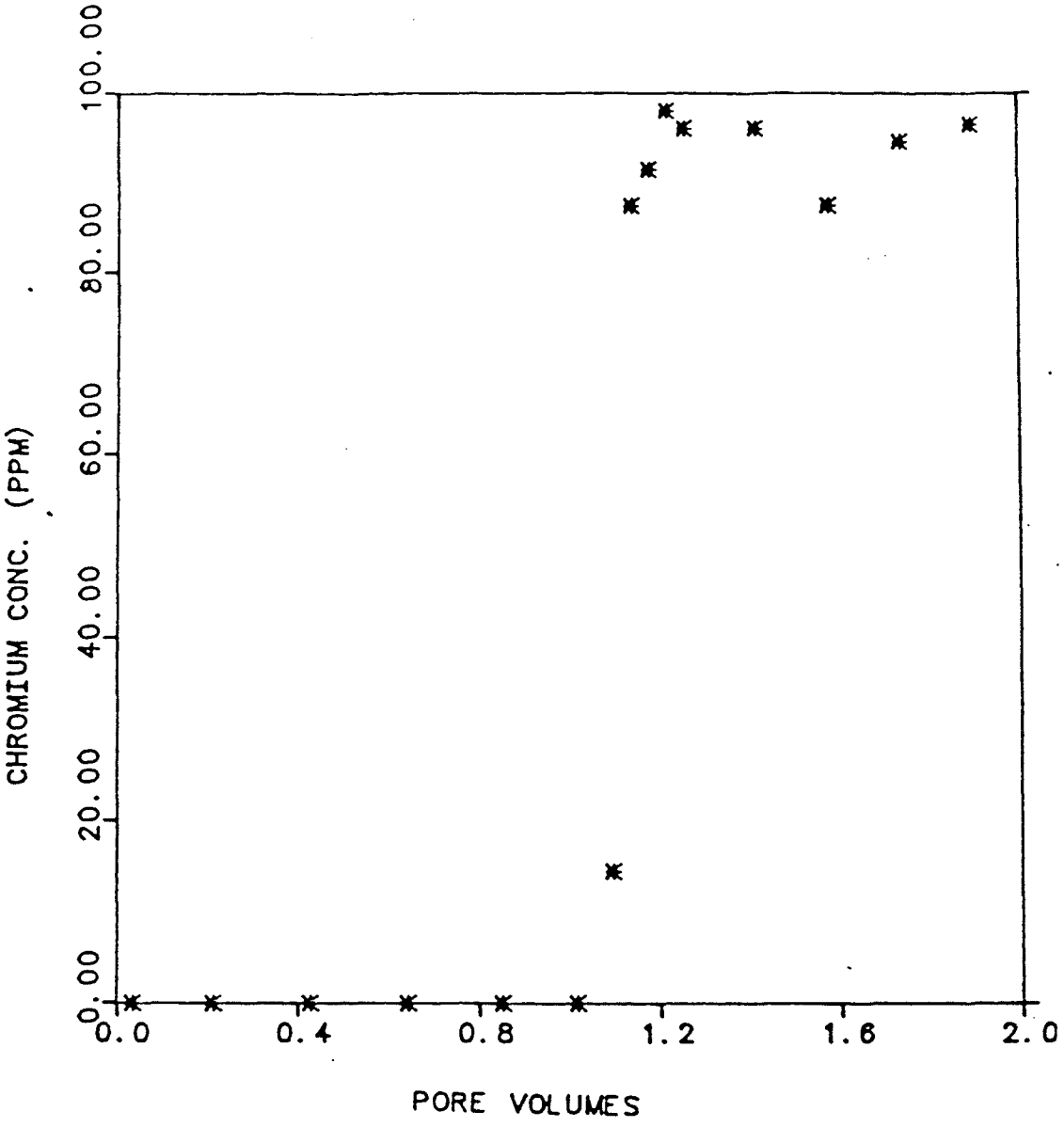


Figure C.10: EXP-9 chromium effluent concentration

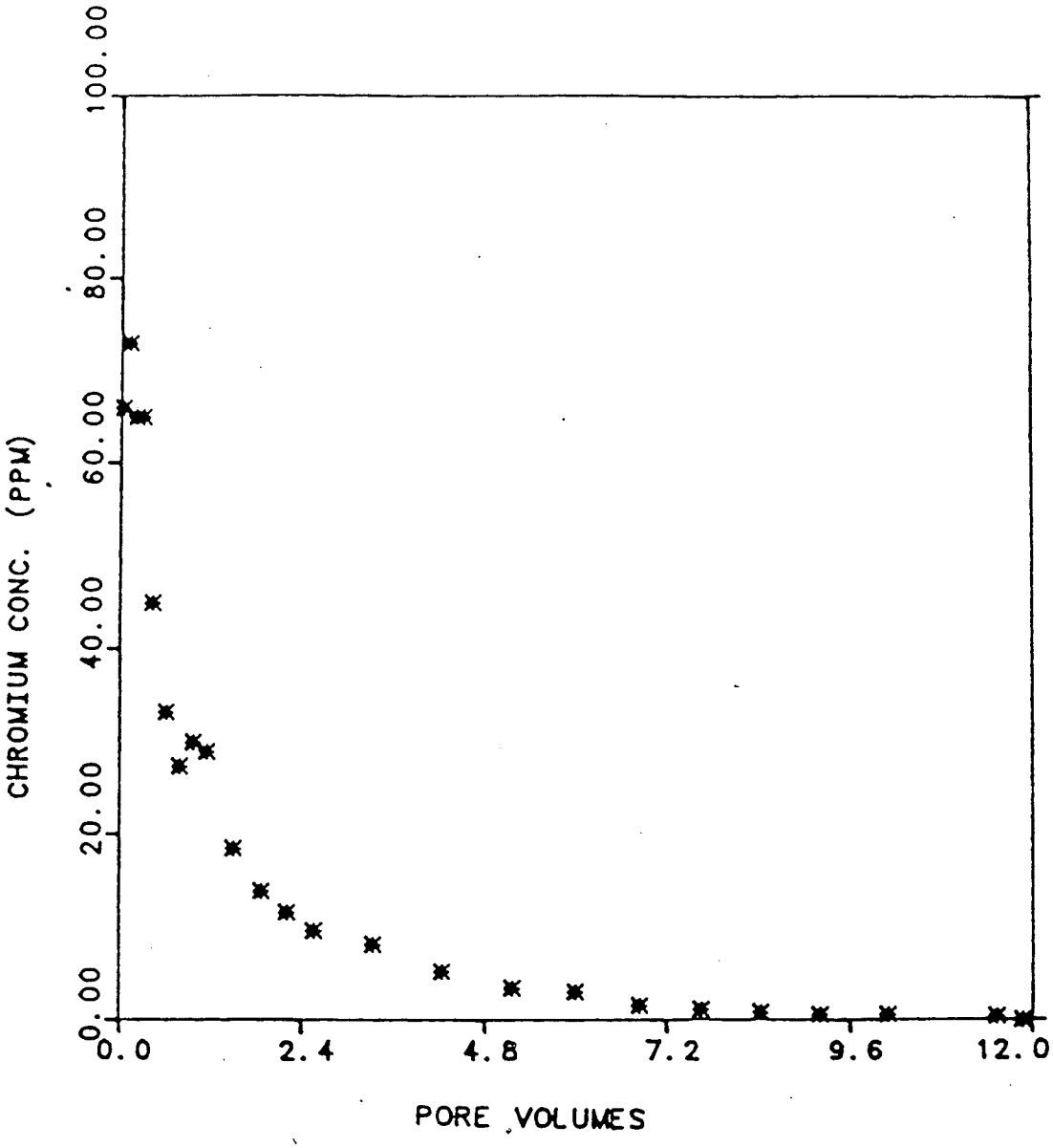


Figure C.11: EXP-9 chromium postflush concentration

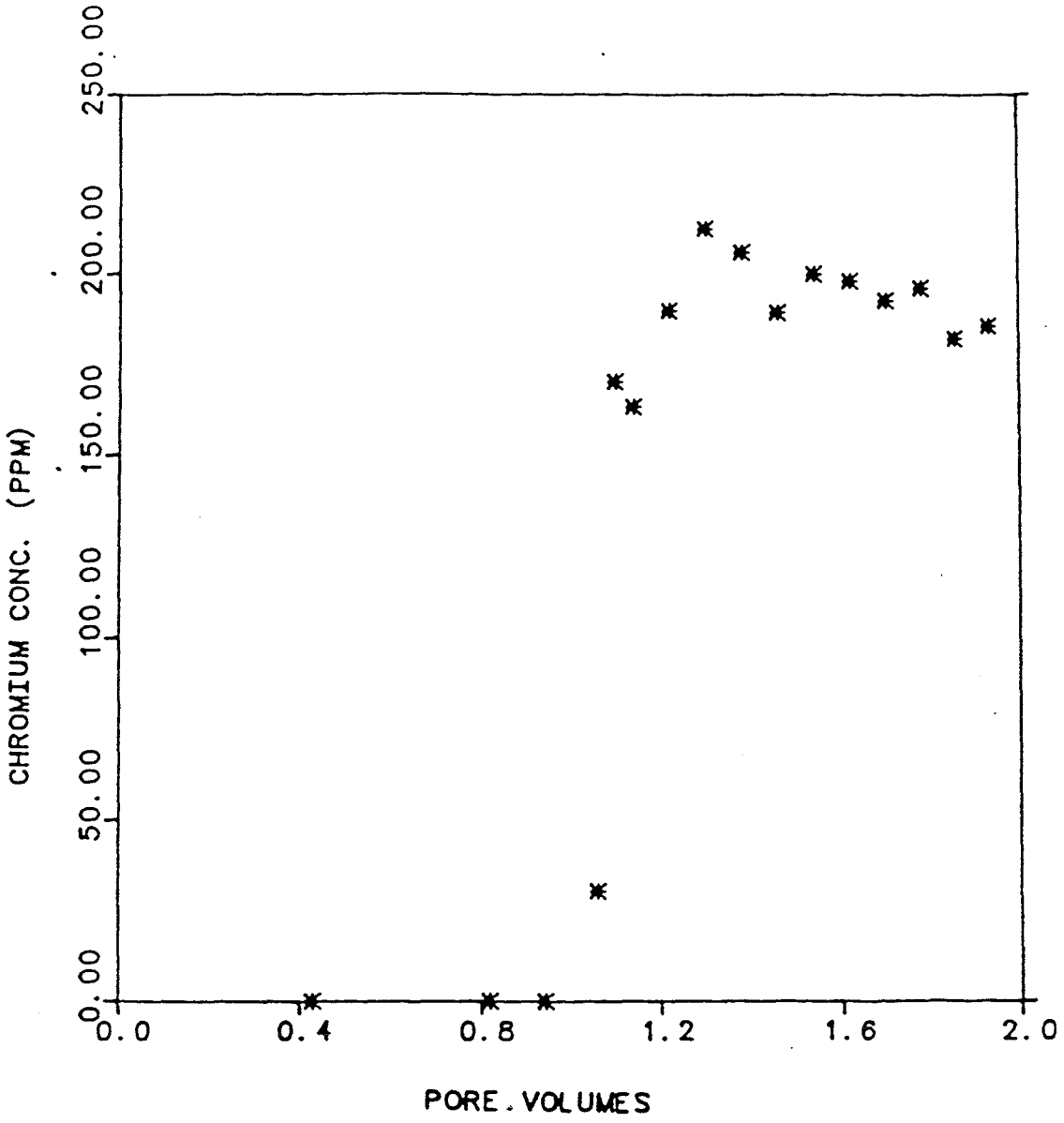


Figure C.12: EXP-10 chromium effluent concentration

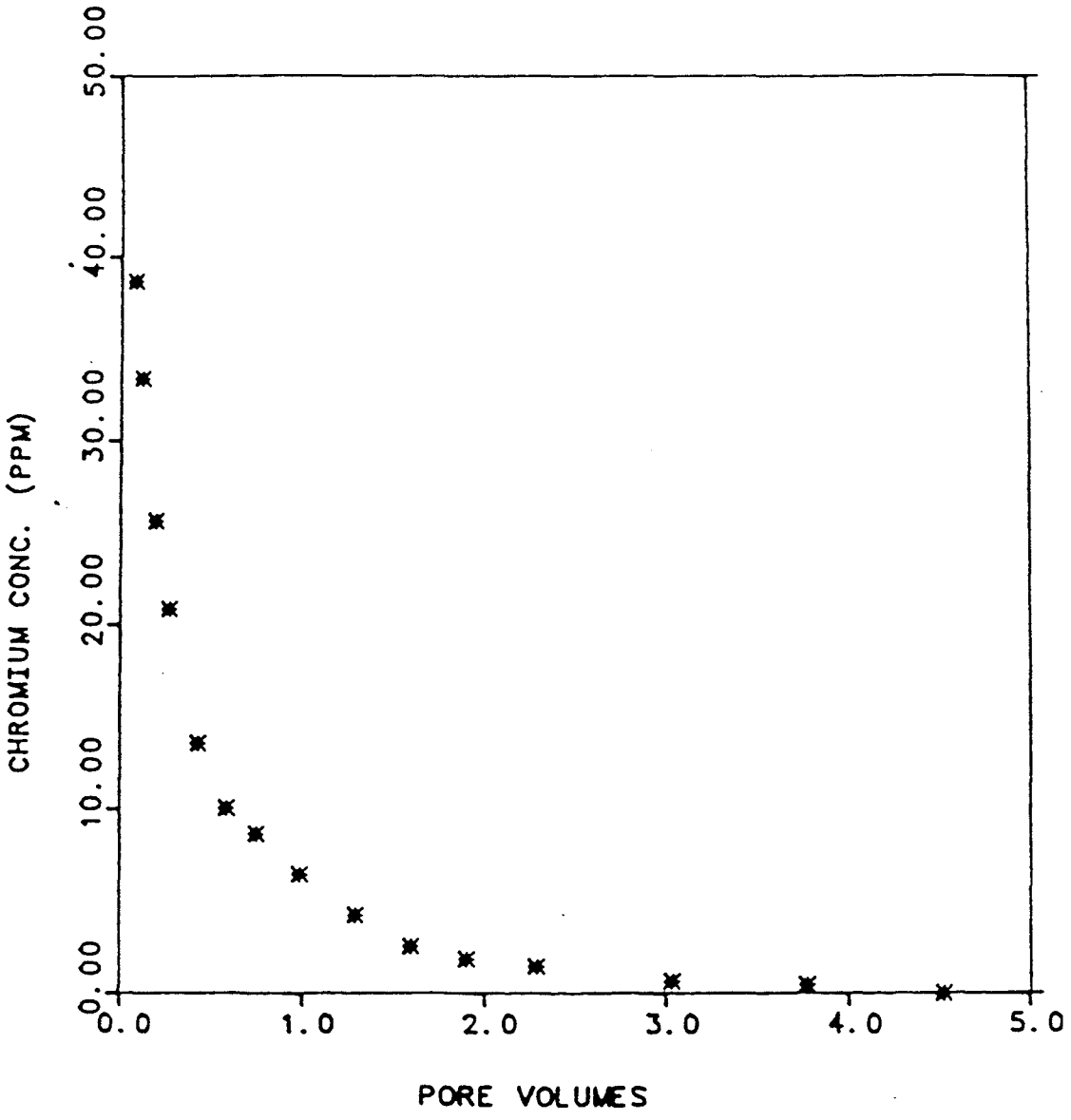


Figure C.13: EXP-10 chromium postflush concentration

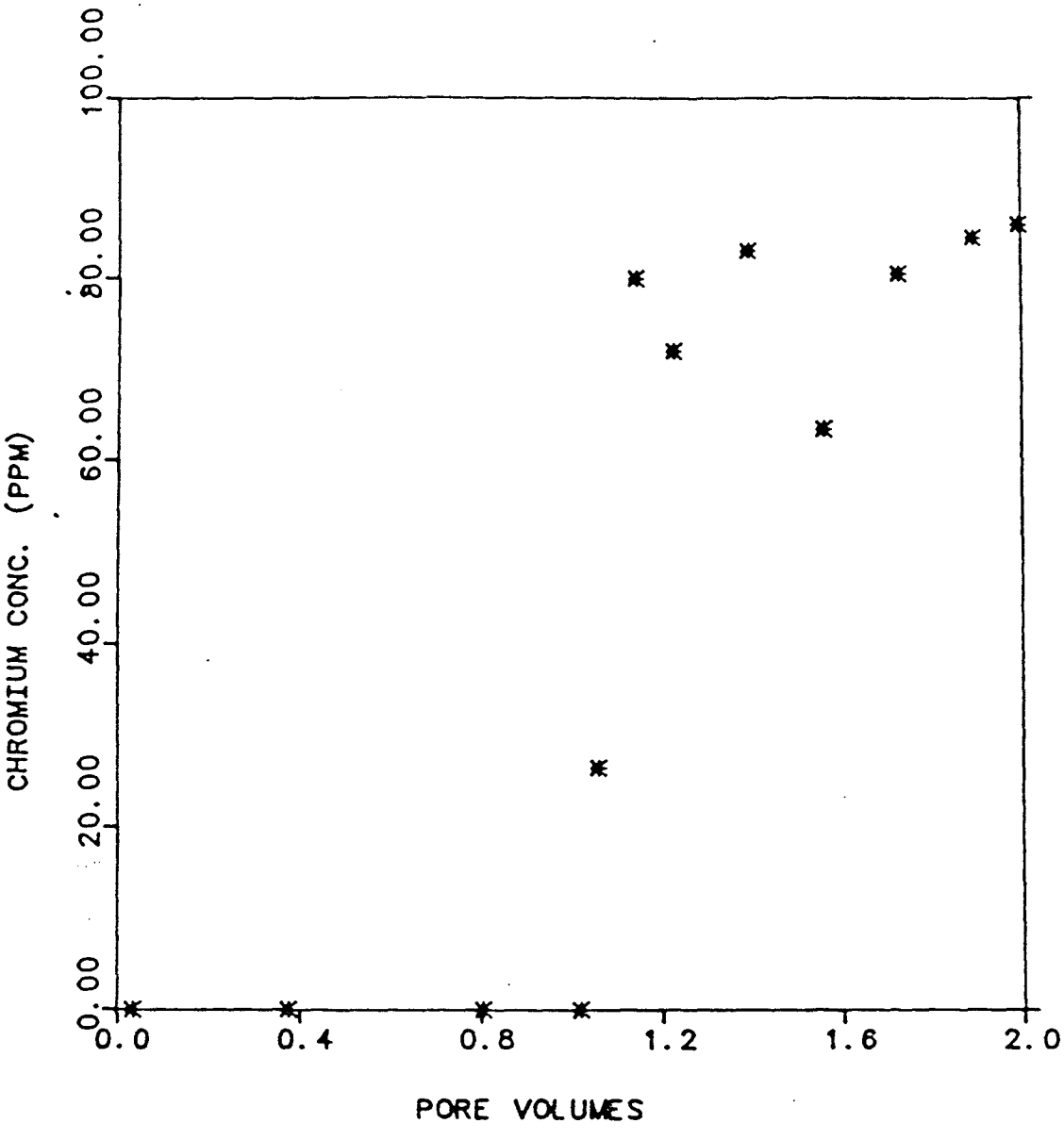


Figure C.14: EXP-12 chromium effluent concentration

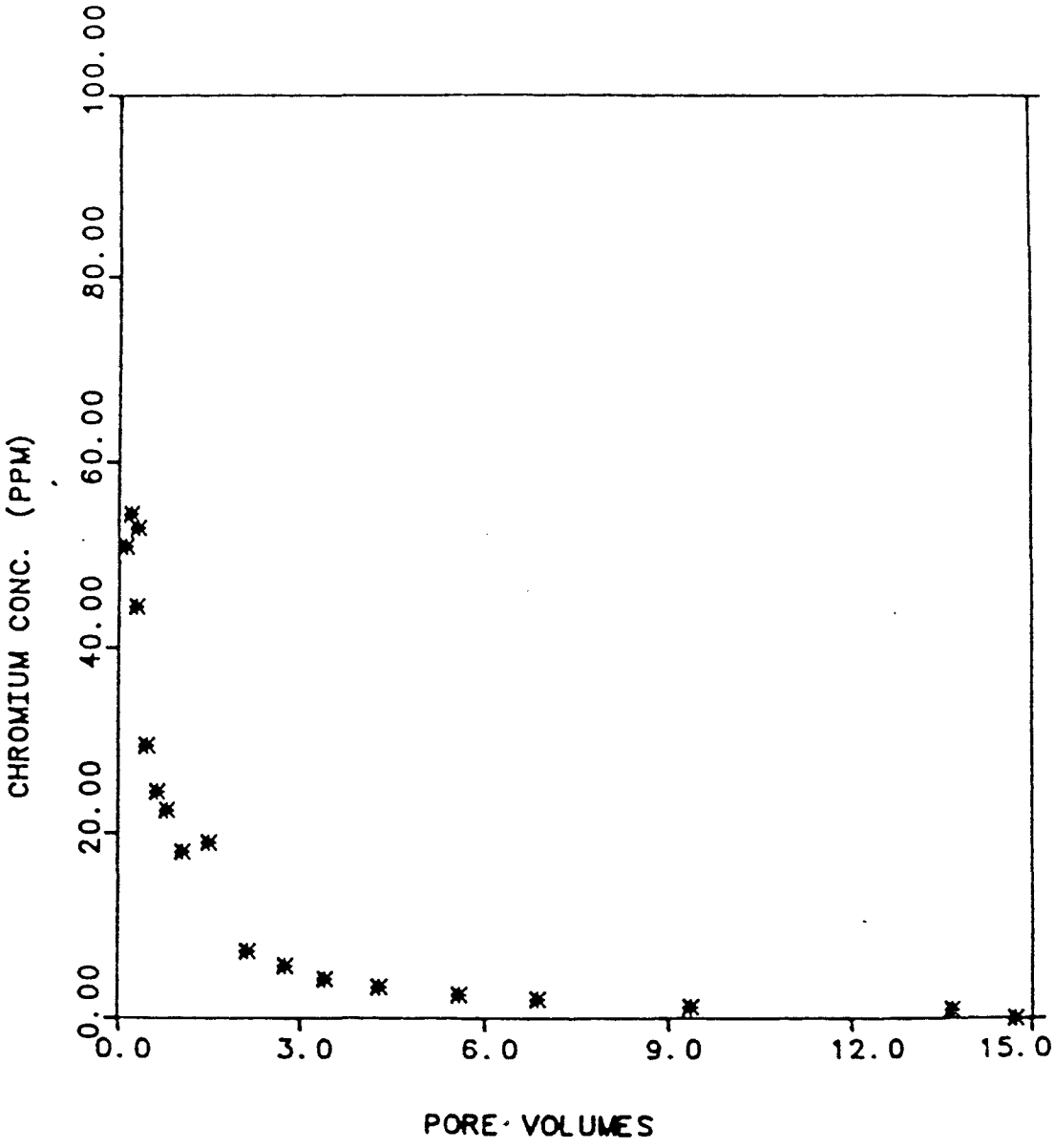


Figure C.15: EXP-12 chromium postflush concentration

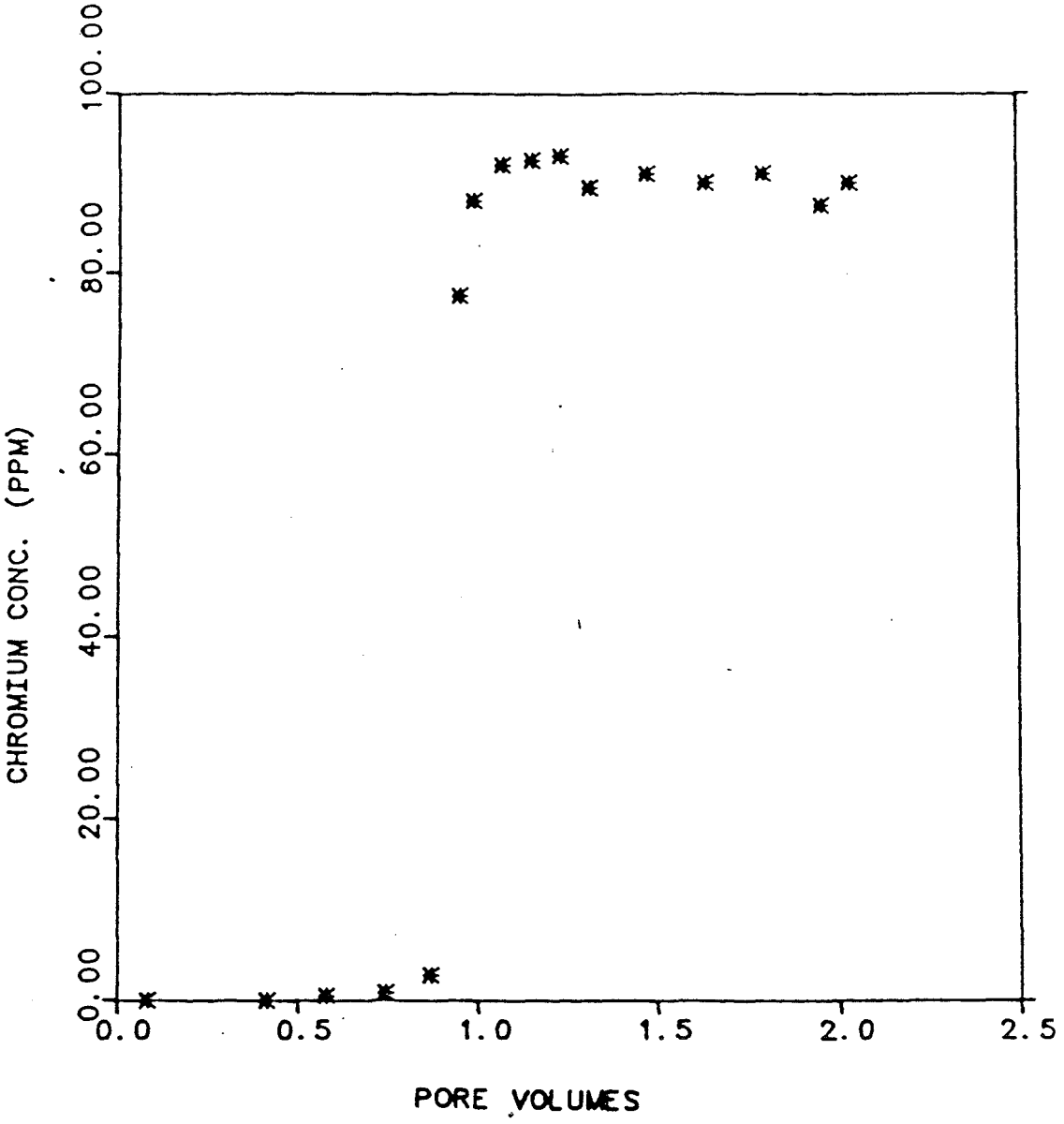


Figure C.16: EXP-15 chromium effluent concentration

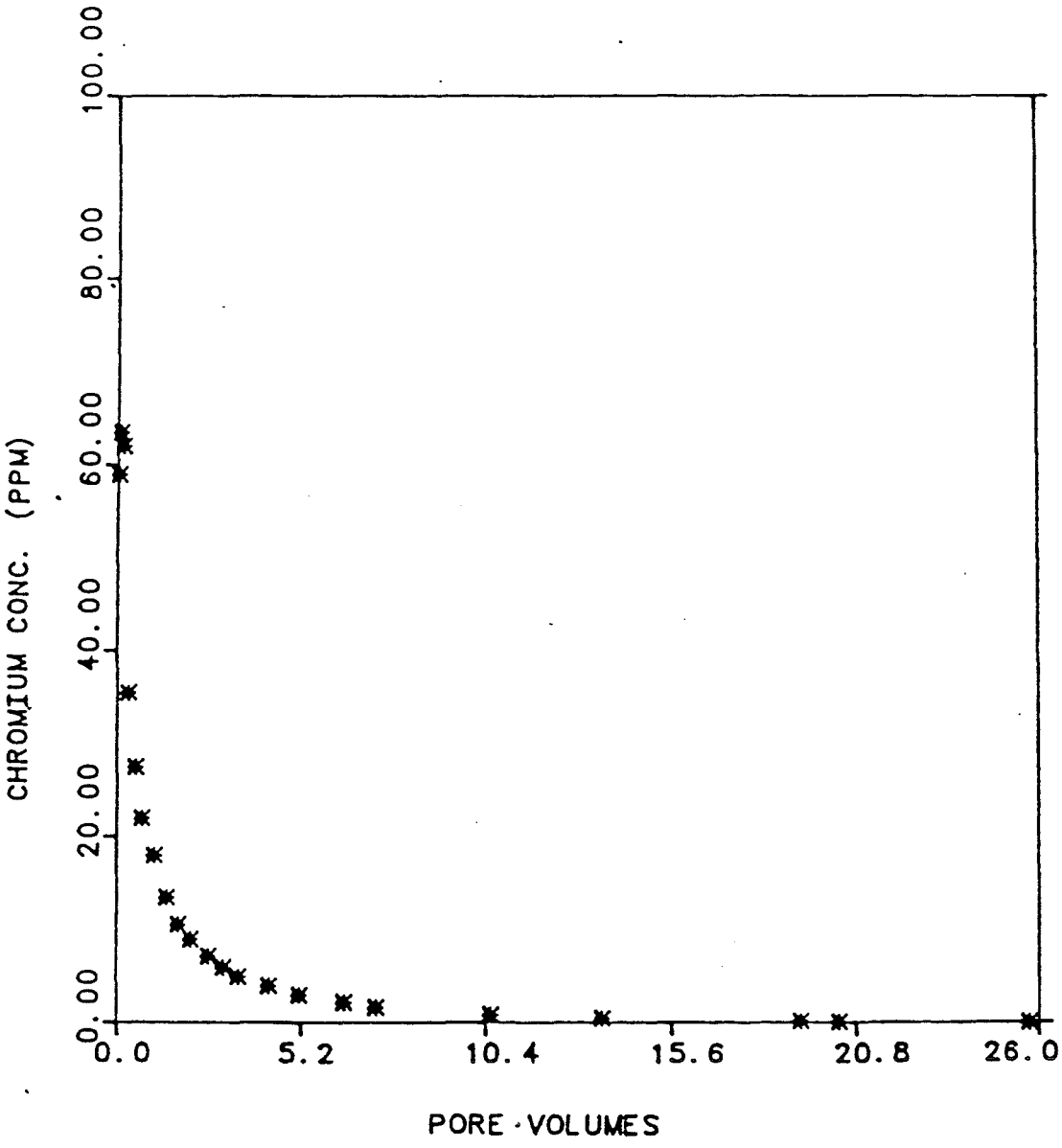


Figure C.17: EXP-15 chromium postflush concentration

# VITA

Jenn-Tai Liang was born in Tainan, Taiwan R.O.C. on July 16, 1957, the son of Shain-Lin Liang and Iong-Ching Chen. After receiving the degree of Bacherlor of Science with a major in Chemistry from Tamkang University, Taipei, Taiwan in June, 1979, he served as a second lieutenant in Chinese Army for two years. He married Hwa Chi Liang in June, 1981 after the completion of the military service. In July, 1981, he entered the graduate school of The University of Alabama and received the Master of Science degree in Petroleum Engineering in December, 1983. He attended the graduate school of The University of Texas at Austin to pursue the Ph.D. degree in September, 1983. His beloved daughter Carol Liang was born at Seton Medical Center Austin, Texas on September 11, 1987. The advent of Carol brought joy and happiness to the whole family.

Permanent address: 29 Lane 84 Jung Yu Street
Tainan, Taiwan
R.O.C.

This thesis was typeset[1] with LaTeX by the author.

[1] LaTeX document preparation system was developed by Leslie Lamport as a special version of Donald Knuth's TeX program for computer typesetting. TeX is a trademark of the American Mathematical Society. The LaTeX macro package for The University of Texas at Austin thesis format was written by Khe-Sing The.